Doctoral theses at NTNU, 2023:209

Muhammad Zohaib Sarwar

Vehicle-assisted bridge damage assessment using deep learning

Doctoral thesis

NTNU
Norwegian University of Science and Technology
Thesis for the Degree of
Philosophiae Doctor
Faculty of Engineering
Department of Structural Engineering

NTNU
Norwegian University of
Science and Technology

Muhammad Zohaib Sarwar

Vehicle-assisted bridge damage assessment using deep learning

Thesis for the Degree of Philosophiae Doctor

Trondheim, June 2023

Norwegian University of Science and Technology
Faculty of Engineering
Department of Structural Engineering

NTNU
Norwegian University of
Science and Technology

NTNU
Norwegian University of Science and Technology

Thesis for the Degree of Philosophiae Doctor

Faculty of Engineering
Department of Structural Engineering

ISBN 978-82-326-7119-9 (printed ver.)
ISBN 978-82-326-7120-5 (electronic ver.)
ISSN 1503-8181 (printed ver.)
ISSN 2703-8084 (online ver.)

Doctoral theses at NTNU, 2023:209

Printed by NTNU Grafisk senter

ABSTRACT

This thesis introduces innovative methodologies for vehicle-assisted bridge health monitoring, aiming to improve maintenance procedures of ageing infrastructure, a critical concern for transport network owners. By taking advantage of advancements in sensing technology and the increasing interconnectivity between vehicles and infrastructure, these methodologies focus on developing an automated bridge assessment method that efficiently evaluates the current condition of bridge structures. This approach enables more accurate and timely maintenance decisions.

The primary objective of this thesis is to create an automated bridge assessment framework for existing bridges by harnessing the synergy between sensors installed on structures and signals transmitted by passing vehicles. By gathering comprehensive information from various sources, including vehicles and the bridge itself, and fusing this data using deep learning techniques, the framework efficiently evaluates the current condition of bridge structures, facilitating more precise and prompt maintenance decisions.

The thesis comprises several studies investigating deep learning techniques, such as deep autoencoders (DAE) and probabilistic temporal autoencoders (PTAE), for extracting features and capturing temporal relationships in the data. This enables accurate identification and quantification of potential damage in bridge structures.

The first study (Paper IA IB) examines an indirect bridge monitoring system using vertical acceleration responses from a fleet of vehicles passing over a healthy bridge. This study's findings reveal that the error in signal reconstruction from the trained DAE is sensitive to damage, considering the distribution of results from multiple separate vehicle-crossing events. The proposed method proves effective in detecting damage under operational conditions and demonstrates potential as a new tool for cost-effective bridge health monitoring.

The second study introduces a methodology for assessing bridge conditions using a PTAE and multi-sensor data from a fixed sensing framework, collected during train crossings. The study's results indicate that the proposed method can detect damage with a limited number of sensors, making it a valuable approach to enhance bridge safety. An Exponentially Weighted Moving Average (EWMA) filter and a control chart-based threshold mechanism are applied to further refine the damage assessment process, distinguishing between healthy and progressively deteriorating damage cases.

The third study proposes a Probabilistic Deep Neural Network framework for damage assessment, combining vehicle and bridge responses to extract damage-sensitive features for classifying different damage states. The findings of this study demonstrate that incorporating multiple sensor information reduces uncertainties in damage detection and localisation. The results also suggest that the proposed method is robust in handling measurement noise and varying environmental conditions.

In conclusion, this thesis advances knowledge in the field of structural assessment through structural health monitoring by providing insights and improvements in tech-

niques and methodologies. By taking advantage of the combined strengths of sensors mounted on structures and signals transmitted by moving vehicles, the developed methodologies provide reliable and precise damage evaluation capabilities. These valuable insights enhance bridge safety, improve resource allocation, and contribute to the overall performance of transport networks. Ultimately, this approach leads to more sustainable and resilient infrastructure, better equipped to handle modern society's growing demands.

PREFACE

This thesis has been submitted to partially fulfil the requirements for the degree of Philosophiae Doctor at the Norwegian University of Science and Technology (NTNU). The research took place at the Concrete Group within the Department of Structural Engineering, which is part of the Faculty of Engineering.

The thesis is comprised of a collection of 4 papers, referred as Paper I through III. Papers IA and III have been published in internationally recognised peer-reviewed journals. Paper II is currently submitted for publication, and Paper 1B has been published in an international conference.

Associate Professor Daniel Cantero was the primary supervisor for this thesis, while Professor Terje Kanstad acted as a co-supervisor.

Muhammad Zohaib Sarwar
Trondheim, Norway
April, 2023

PUBLICATIONS

The following papers are included in this thesis:

- M. Z. Sarwar, D. Cantero, **Deep autoencoder architecture for bridge damage assessment using responses from several vehicles**, Engineering Structures 246 (2021) 113064.
- M. Z. Sarwar, D. Cantero, **Data-driven bridge damage detection using multiple passing vehicles responses**, 11th International Conference on Bridge Maintenance, Safety and Management (IABMAS), Taylor Francis, Barcelona, Spain (2022), pp. 1003-1010
- M. Z. Sarwar, D. Cantero, **Probabilistic autoencoder-based bridge damage assessment using train-induced responses**, Submitted for journal publication
- M. Z. Sarwar, D. Cantero, **Vehicle assisted bridge damage assessment using probabilistic deep learning**, Measurement 206 (2023) 112216.

The following paper is published in conference proceedings during this work

- M. Z. Sarwar, D. Cantero, **Unsupervised deep learning-based bridge damage detection using the fleet sourcing concept**, Proceedings of the 10th International Conference on Structural Health Monitoring of Intelligent Infrastructure, SHMII 10, Porto, Portugal, 30 June - 2 July 2021

ACKNOWLEDGEMENTS

First and foremost, I would like to express my heartfelt gratitude to my main supervisor, Associate Professor Daniel Cantero, for providing me with the opportunity to work on this project. His exceptional supervision, unwavering encouragement, invaluable support, and generous sharing of his vast knowledge have been instrumental in helping me achieve success in this endeavour. I am also deeply grateful to Professor Mette Rica Geiker for offering me the chance to work as a researcher, allowing me to extend my stay at NTNU and further develop my skills and expertise.

I would like to express my heartfelt gratitude to all the professors, colleagues, and staff in the concrete group for creating a supportive, lively, and enjoyable work environment. Their combined knowledge and friendship have made my time at NTNU truly unforgettable and valuable.

My heartfelt thanks go out to all my friends who have been by my side throughout this journey, offering their unwavering support and assistance. I would like to give special mention to Asaad, Taimur, Hammad, Hamid, and Waleed, who have made my stay in Trondheim an unforgettable experience filled with cherished memories.

I dedicate this work to my incredible parents, whose love, support, and encouragement have been my pillars of strength throughout this journey. I am forever grateful for their sacrifices and unwavering belief in me. Words cannot adequately express the depth of my appreciation, and I am immensely proud to be their son. I would also like to dedicate this work to my supportive elder brother Junaid, my caring younger sister Iqra, and my spirited younger brother Faheem, all of whom have played an invaluable role in my life.

Lastly, I want to express my deepest appreciation to my cherished wife, Wajeeha, for her love, patience, and steadfast support. Her faith in me and her encouragement have been immeasurable. As we set out on our next adventure together, I eagerly look forward to the experiences and joy that lie ahead.

CONTENTS

CHAPTER

ONE

INTRODUCTION

1.1 Motivation

The maintenance of ageing infrastructure has become a pressing concern for transport network owners, as a significant portion of their budgets is allocated to this task. In particular, the growing stock of ageing bridges poses a serious challenge due to the deterioration of construction material over time, which has been exacerbated by corrosion, degradation, fatigue, and other factors [1, 2]. This is further compounded by the need for increased capacity to accommodate traffic growth, making infrastructure maintenance a critical aspect of overall management.

To address this challenge, responsible authorities have established guidelines and procedures, but these methods are not always optimal. Structural maintenance is a difficult task due to the sheer number of bridges to maintain and the heterogeneity of the constructions. The initial step in the maintenance process is a structural assessment, which requires skilled personnel, and multiple resources, and is time-consuming. Furthermore, there is often limited information about existing damage. Improvements to the assessment procedure would allow infrastructure owners to better utilise their available resources.

In recent years, there have been substantial advancements in fields related to structural assessment. Sensing technology, for example, has introduced energy harvesting and wireless systems that make it more convenient and cost-effective to instrument infrastructure. Simultaneously, vehicles are being equipped with a greater number and variety of complex sensors, enabling increased interconnectivity between vehicles and infrastructure. This interconnectedness has demonstrated potential benefits for improving traffic and resource management through Intelligent Transport Systems (ITS). However, the full potential of this interconnectivity between vehicle sensors and infrastructure sensors has not been completely realised and could be harnessed to benefit infrastructure maintenance.

By leveraging the advancements in sensing technology and the growing interconnectedness of vehicles and infrastructure, maintenance procedures could be enhanced, making it easier to identify and address issues in ageing structures. This would not only improve the efficiency of resource allocation but also contribute to the overall safety and performance of transport networks. Developing more effective maintenance strategies would ultimately lead to a more sustainable and resilient infrastructure, better equipped to handle the growing demands of modern society.

1.2 Structural health monitoring

1.2.1 Overview

The process of implementing an autonomous assessment strategy of engineering infrastructure is referred to as structural health monitoring (SHM). The SHM process involves observing a system over time using periodically sampled response measurements from an array of sensors, the extraction of damage-sensitive features from these measurements, and the statistical analysis of these features to determine the current state of the system's health [3]. For long-term SHM, the output of this process is periodically updated, providing information regarding the ability of the structure to perform its intended function in light of the inevitable ageing and degradation resulting from operational and environmental effects. SHM has emerged as a promising solution to empower bridge owners and inspectors with new capabilities for bridge management systems. Modern SHM systems generally consist of transducers, data acquisition system and communication network. The collected information from a SHM system is analysed through physics- and/or data-driven techniques to extract useful features that can further be used for the decision-making process.

1.2.2 Bridge damage assessment

Early damage detection is one of the core issues in SHM. In civil engineering, traditional SHM has been particularly focused on damage detection, localisation, and quantification. SHM typically involves the direct installation of multiple sensors on a bridge. The measured responses are analysed using signal processing methods to provide information about the structure and possible damage state. Existing methods for damage detection can be classified into global and local techniques.

In a global level damage assessment, system-level characteristics of the structure, such as natural frequency, mode shape, and flexibility matrix, are considered to determine the location and severity of the damage. The main challenges associated with global damage detection techniques are their insensitivity to local damage and high sensitivity to operational conditions [4, 5]. Conversely, local damage detection methods can be used for accurate damage localisation and quantification, but the information is not indicative of the overall structural behaviour. The main challenge with local damage detection techniques is the need for prior information related to the damage state [6]. For instance, a single strain sensor cannot detect an existing crack, but it can be used to further study the development of that crack once it has been identified through visual inspection or non-destructive techniques.

Over recent years, substantial progress has been made in the field of vibration-based damage identification, leading to significant advancements in bridge damage assessment. An et al [4] provided a comprehensive review of the various damage identification algorithms developed and implemented for different bridge types within the last decade. Vibration-based damage identification can be generally classified into two primary approaches: 'model-based' and 'data-based'.

Model-based methods utilise detailed numerical or Finite Element (FE) models of the structure for the purpose of damage identification. During the development phase, these models undergo a process of incremental refinement to ensure accurate representation of the measured structural responses. The models evolve from basic conceptual system representations to advanced, physics-based models that accurately represent the actual asset or reference model. Damage detection algorithms predominantly focus on the discrepancies between the modified model before and after the occurrence of damage [7].

For damage assessment, a reference model is calibrated to reflect the damaged con-

ditions of the structure. Damage assessment is then performed by analysing the changes in the updated parameters of this calibrated reference model. The application of this approach has been reported for damage assessment [8, 9, 10]. However, in the context of damage assessment for bridges, the model-based approach is considered impractical due to several disadvantages. One of the main challenges in using these methods is the time-consuming and computationally demanding nature of developing high-fidelity models. This often requires significant time and computational resources, which may not be feasible. Another drawback is the need for extensive experimental data for calibration and validation of the models [11]. Obtaining such data can be challenging, particularly for large, complex bridges with limited accessibility. This requirement for a substantial amount of experimental data can hinder the practicality of model-based methods for bridge damage assessment. Furthermore, model-based methods may be affected by uncertainties in the material properties, boundary conditions, or other model parameters. These uncertainties can impact the accuracy of damage detection and assessment results, making it difficult to rely on these techniques in certain situations [12]. Consequently, while model-based methods can be valuable under specific conditions where accurate and detailed models are available, alternative approaches such as data-based methods may be more practical and cost-effective for many bridge damage assessment applications.

Data-based methods offer an alternative solution that doesn't require precise geometry or material information. This approach helps to bypass the need for creating an intricate FE model of the structure under observation [13]. The data-based approach primarily focuses on using data mining and advanced signal processing techniques to extract damage-sensitive features. Damage assessment is performed by analysing these damage-sensitive features with statistical pattern recognition methods or machine learning algorithms [14, 15, 16].

In the context of bridge damage assessment, the acquired damage-sensitive features are used to train machine learning models. These trained models are then utilised to identify future variations in features. For training these machine learning models, two training modes are commonly used: supervised and unsupervised. Supervised training requires data from both undamaged situations and abnormal data from various damage scenarios of the monitored bridge structure for damage detection. However, it is often challenging to obtain sufficient data for different damage scenarios from the bridge, and it is practically impossible to induce damage on a perfectly normal bridge. In such situations, it is recommended to use unsupervised training methods, which only require normal data from the intact structure during the training phase. This approach allows for more practical implementation of data-based methods in bridge damage assessment, even when data for damaged scenarios is limited or unavailable.

1.2.3 Vehicles-assisted bridge damage assessment

Vibration-based Structural Health Monitoring (SHM) systems in terms of sensing framework can be divided into two categories: fixed and mobile sensing frameworks [17]. With fixed sensing frameworks, sensors are permanently installed at specific points on the target bridge. This approach faces three primary challenges. First, the high costs and labour associated with deployment make it unsuitable for inspecting short to medium span bridges. Second, fixed sensing systems provide limited spatial information, which negatively impacts the bridge assessment results. Third, vibration data collected during ambient and forced vibrations may not adequately excite the stiff bridge, leading to noisy measurements [18].

Forced vibration responses can be obtained using impact load testing, human-induced loads, or hydraulic actuators, but these methods can negatively affect bridge serviceability and increase maintenance costs. Recently, vehicle-assisted monitoring has emerged

as a promising research area. In this approach, traversing vehicles serve as the excitation source and bridge responses are measured using sensors on the bridge or inside the vehicles. This method is more cost-effective, as bridge vibration data is only collected when vehicles are on the structure [19]. Additionally, when vehicles act as mobile sensors, the measured responses provide comprehensive spatial information, significantly enhancing bridge condition assessments [20, 21].

In recent years, there has been a growing interest in vehicle-assisted monitoring systems for bridge damage assessment. Shokravi et al [22] conducted a thorough review of conventional vehicle-assisted techniques, which can be classified into fixed and mobile sensing frameworks. Using fixed sensing, researchers in studies [19] and [23] applied the Moving Force Identification (MFI) method for bridge damage assessment, while others, such as [24] and [25], focused on measuring rotational responses of bridges under moving loads for the same purpose.

Mobile sensing or drive-by techniques have also been examined for bridge damage assessment, with Wang et al [26] offering a detailed overview of their applications. These methods primarily depend on advanced signal processing techniques and machine learning methods for damage detection. For instance, researchers in [27] and [28] utilised data-driven techniques and statistical analysis for damage detection and quantification, while [29] and [30] estimated the contact point response between the vehicle and the bridge for damage detection and localisation.

Vehicle-assisted monitoring systems hold great potential for damage assessment, but they also face limitations and challenges. These include the influence of vehicle speed, road profiles, and additional random traffic, as well as the need for specialised vehicles [31, 32]. The variability of vehicle speeds can affect the accuracy of measurements and the performance of data-driven methods, while uneven or rough road surfaces can introduce noise and unwanted variations in the measurements, making it difficult for data-driven methods to accurately detect damage [33, 34].

Additional random traffic on the bridge during the assessment can introduce interference and complicate the analysis [20]. Equipping vehicles with the necessary sensors and technology for accurate data collection can be expensive, and data-driven methods typically rely on machine learning algorithms that require sufficient training data to perform accurately. Obtaining adequate training data for various damage scenarios can be challenging.

Environmental factors, such as changes in temperature and humidity, can also influence the structural response of the bridge and complicate the damage assessment process [35]. Ensuring appropriate sensor placement and data quality is crucial for accurate damage assessment, as poor sensor placement or low-quality data can lead to false-positive or false-negative results. Data-driven methods often involve complex signal processing and machine learning techniques, which can be computationally demanding and may require significant computational resources [7].

By combining the advantages of both direct and indirect methods, a more comprehensive and effective approach to bridge damage assessment could be developed, thus overcoming some of these challenges. The recent advancements in wireless sensing systems for infrastructure and the increasing trend of equipping vehicles with multiple sensors pave the way for Vehicle to Infrastructure (V2I) connectivity [36, 37]. This integration not only has shown potential benefits in improving traffic and resource management but could also revolutionise bridge health monitoring and maintenance by providing real-time data and continuous assessment of bridge conditions.

Furthermore, the integration of V2I technology could enable the development of smart infrastructure systems that can autonomously identify and prioritise maintenance needs, thereby optimising resource allocation and reducing costs. Additionally, the fusion of

data from both vehicle and bridge sensors can enhance the accuracy and reliability of damage detection methods, allowing for the early identification of structural issues and more effective maintenance planning.

Although the interconnectivity between vehicle and bridge sensors has not yet been thoroughly explored in the context of damage assessment and bridge maintenance, this thesis aims to address this gap. The research will focus on investigating this interconnectivity, tackling the challenges and limitations of current vehicle-assisted monitoring systems, and devising techniques that take advantage of the strengths of both fixed sensing and mobile sensing methods. The ultimate goal is to improve the efficiency and accuracy of bridge damage assessment, which could significantly enhance the maintenance and management of bridge infrastructure.

1.2.4 Machine learning in bridge damage assessment

The data-based approach to damage assessment leverages machine learning (ML) techniques in either supervised or unsupervised training modes. Supervised training uses data from both normal and various damage scenarios [2]. ML algorithms in this mode perform classification and regression tasks, such as Support Vector Machine (SVM) [38, 39], Decision Tree (DT) [40, 41], and Naive Bayes Classifier (NB) [42]. Some algorithms, like Artificial Neural Networks (ANN) [43], Genetic Algorithm (GA) [44], and Hidden Markov Model (HMM) [45], can be applied in both supervised and unsupervised settings due to their flexibility.

On the other hand, unsupervised training focuses on grouping and interpreting data based solely on input data. An algorithm first defines a reference condition for the bridge by extracting relevant features from the data. Then, using statistical pattern recognition, the features from newly obtained data over time are compared to those from the reference condition. If a significant deviation is observed, the algorithm detects a novelty, suggesting a potential change in the bridge's condition due to damage. Examples of algorithms used in unsupervised training include K-means clustering, Gaussian Mixture Model (GMM), Principal Component Analysis (PCA), and Autoencoders [46, 47, 48, 49, 20]. Furthermore, the versatile algorithms mentioned earlier can be employed in both supervised and unsupervised learning scenarios.

In recent years, Deep Learning (DL) has emerged as a significant area of interest within the field of Structural Health Monitoring (SHM). Traditional machine learning methods necessitate extensive data analysis and rely heavily on expert knowledge to extract damage-sensitive features. In contrast, DL models can automatically learn these features when training data is input into deep neural networks [2]. The features discovered in the hidden layers of these networks can then be utilised for tasks such as classification and novelty detection.

However, the successful application of DL in SHM hinges on the availability of extensive training datasets, as these models are theoretically better equipped to reveal intricate relationships within the data [50]. The practical implementation of DL models in SHM is constrained by the fact that collected training data may not encompass all operational and loading conditions, making it challenging to quantify the uncertainty in the model's decision output. To ensure reliable decision-making, an SHM system must be capable of managing uncertainty in its predictions [51].

Despite these challenges, various algorithms, including Long Short-Term Memory (LSTM) neural networks [52], Autoencoder (AE) neural networks [53, 54], Sparse Autoencoder (SAE) neural networks [55], and Convolutional Neural Networks (CNN) [56, 57], have been used for bridge damage assessments, though on a limited scale. The primary focus of this thesis is to apply DL techniques to bridge damage assessments while addressing and quantifying uncertainties resulting from limited training datasets.

1.3 Challenges in SHM

Within the context of the above discussion, Structural Health Monitoring (SHM) faces numerous challenges that must be addressed to make it an acceptable tool for bridge owners and the industry to use for bridge maintenance. Some of these challenges include:

- **Sensor placement and coverage:** Ensuring appropriate sensor placement and coverage across the entire bridge structure is crucial for accurate damage assessment. Inaccurate or inadequate sensor positioning may result in overlooked or misinterpreted damage indicators, as structural damage is generally localised and may not substantially impact the overall response of the structure.
- **Limited training data:** Developing accurate machine learning models requires a significant amount of high-quality training data that covers various damage scenarios and operational conditions. Obtaining such data is often difficult and time-consuming.
- **Environmental influences:** Factors such as temperature, humidity, and wind can affect the structural response of a bridge and complicate the damage assessment process. Developing algorithms that can account for these environmental influences is a challenge.
- **Uncertainty quantification:** Addressing uncertainties in the ML model's predictions is essential for reliable decision-making in SHM systems. This includes uncertainties due to limited training data, sensor noise, and environmental factors.
- **Computational complexity:** Some SHM methods involve complex signal processing and machine learning techniques, which can be computationally demanding and may require significant computational resources.
- **Scalability and real-time monitoring:** Developing SHM systems that can scale to large, complex bridge networks and provide real-time damage assessment is an ongoing challenge, especially given the increasing volume of data generated by modern sensors.
- **Integration and interoperability:** Combining various sensing technologies, data sources, and algorithms into a cohesive SHM system can be challenging, particularly when dealing with different types of sensing mechanisms.
- **Cost-effectiveness and maintenance:** Implementing SHM systems can be expensive, particularly for sensor installation and maintenance. Developing cost-effective solutions that provide accurate and reliable damage assessment is crucial for widespread adoption.

CHAPTER
TWO

PHD THESIS

2.1 Objectives

The objective of this thesis is to develop an automated bridge assessment system for existing bridges by leveraging the synergy between sensors installed on the structures and signals transmitted by passing vehicles. As illustrated in Figure 2.1.1, the primary goal is to gather comprehensive information about the bridge from various sources, including both vehicles and the bridge itself. By fusing this data and employing deep learning techniques, the system aims to efficiently evaluate the current condition of the bridge structure, enabling more accurate and timely maintenance decisions.

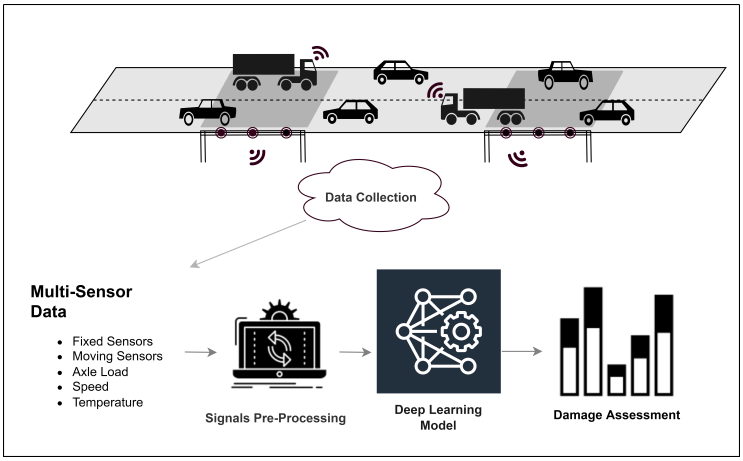

Figure 2.1.1: Main overview of the thesis

The main objectives of this thesis can be organised into the following tasks:

- Carry out a comprehensive review of relevant literature covering key topics, including structural deterioration, long-term behaviour, assessment methodologies, sensor technologies, damage indicators, numerical modelling, as well as machine learning and deep learning techniques.
- Develop a comprehensive bridge damage assessment strategy that focuses on utilising only vehicle response data, while carefully considering the impact of realistic operational and environmental conditions on the assessment process. This approach should account for factors such as varying vehicle speeds, road profiles,

traffic conditions, and weather-related influences to ensure a reliable and accurate evaluation of the bridge's structural health.

- Implement a damage assessment strategy based on a fixed sensing framework, focusing on strategically placed sensors on the bridge structure. Evaluate the effectiveness and reliability of this approach by comparing the results with numerical simulations and real-world experimental data sets, ensuring that the strategy provides accurate and valuable insights into the bridge's structural health.

- Design and evaluate a comprehensive bridge damage assessment mechanism that combines both mobile and fixed sensing frameworks. Investigate and quantify the impact of different sensor information combinations on the accuracy and effectiveness of the assessment process. This integrated approach aims to provide a more holistic and precise understanding of the bridge's structural health, considering a broader range of data sources and sensor inputs.

- Contribute to the progression of knowledge in the field of structural assessment through structural health monitoring by providing insights and advancements in techniques and methodologies. Offer guidance and best practices for devising efficient and robust strategies for conducting monitoring campaigns, ultimately enhancing the reliability and effectiveness of infrastructure maintenance and management.

2.2 Scope of the thesis

The scope of this PhD thesis is defined by certain limitations and focuses. The research aims to develop and assess bridge damage assessment methods using both fixed and mobile sensing frameworks, considering real operational conditions such as measurement noise, vehicle speeds, and environmental factors. However, there are challenges in obtaining measurement data for analysis, as it is not feasible to instrument multiple vehicles and bridges simultaneously during this work. Therefore, the study will primarily rely on numerically simulated responses, utilising a 1D vehicle-bridge interaction model for different damage scenarios.

The investigation will concentrate on damage assessment strategies for bridges, incorporating machine deep learning techniques, as well as the evaluation of uncertainties arising from limited training datasets. The experimental validation of the proposed methods will be limited to the fixed sensing framework due to the availability of bridge acceleration responses. Despite these limitations, the research intends to contribute to the advancement of knowledge in structural assessment using structural health monitoring and provide guidelines for efficient and robust strategies for monitoring campaigns.

Lastly, all methods developed, including machine learning algorithms and numerical simulation data, will be released as open-source resources, fostering transparency and facilitating further research in this area after the final publication of the thesis.

2.3 Workflow of the thesis

The workflow of this thesis is designed to achieve the research objectives in a structured manner. As illustrated in Figure 2.3.1, the study begins with the consideration of a mobile sensing framework for bridge damage assessment. It takes into account signals from multiple passing vehicles with varying properties. The damage detection sensitivity is validated under the influence of random traffic and fluctuating environmental conditions.

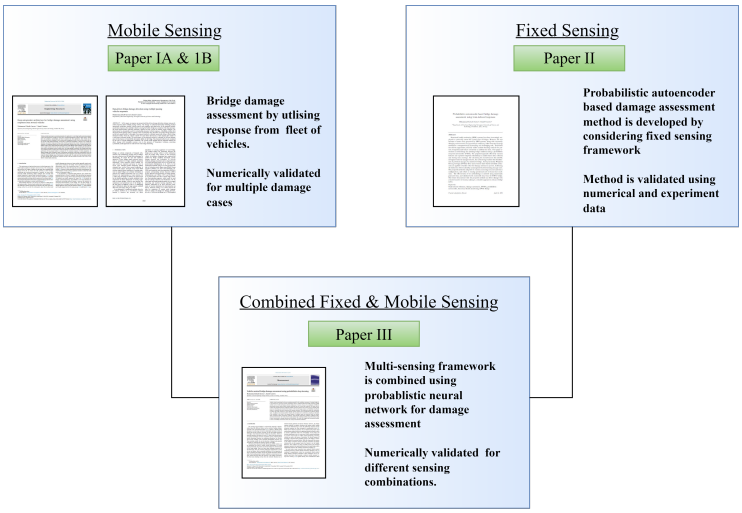

Figure 2.3.1: Workflow of the thesis

In the second phase, a probabilistic autoencoder is proposed for bridge damage assessment using signals from a fixed sensing framework. The method is validated using both numerical and experimental datasets.

In the final stage, both the mobile and fixed sensing frameworks are integrated using a probabilistic neural network to investigate and quantify the influence of different sensor information combinations. This comprehensive approach aims to enhance the accuracy and efficiency of bridge damage assessment, ultimately contributing to more effective monitoring and maintenance strategies for bridge infrastructure.

CHAPTER

THREE

PAPER SUMMARY

3.1 General

This thesis consists of three journal papers, with Paper IA and Paper III published in peer-reviewed international journals, while Paper II has been submitted for review. Additionally, a conference paper, Paper IB, has been published in a peer-reviewed international conference. The summaries of these papers are provided below:

3.2 Paper IA & IB

Deep autoencoder architecture for bridge damage assessment using responses from several vehicles & Data-driven bridge damage detection using multiple passing vehicles responses

These papers present a novel damage assessment technique for bridge health monitoring that leverages deep learning and a statistical distribution-based damage index. The proposed method uses acceleration responses from multiple vehicles traversing the target bridge, addressing the challenge of generalising the relationship between vehicle responses and bridge dynamics by employing a deep autoencoder (DAE) architecture with multiple convolutional and LSTM layers. The DAE is trained on healthy bridge conditions, constructing a feature space sensitive to bridge dynamics and robust against measurement noise and operational conditions. Furthermore, the errors between measured and reconstructed signals are characterised by distributions sensitive to bridge damage, allowing the use of a damage index based on the Kullback-Leibler divergence for damage detection and severity quantification.

The proposed method's effectiveness is evaluated numerically using a 5-axle truck vehicle model traversing both a simply supported bridge and a multi-span continuous bridge. The study takes into account various scenarios, including variability in vehicle properties, operational conditions, random traffic effects, and the influence of temperature changes (as explored in Paper 1B). The results demonstrate the method's ability to detect damage successfully and provide robust outcomes under different operational conditions. However, selecting an appropriate threshold is crucial for reliable damage detection and minimising false alarms. Moreover, crossing events should be considered when a minimum level of daily traffic is present. In summary, the proposed method presents a practical and cost-effective solution for bridge health monitoring that eliminates the need for specialised vehicles and seamlessly integrates with intelligent transport networks. This approach has the potential to significantly enhance the efficiency and affordability of long-term bridge monitoring systems.

3.3 Paper II

Probabilistic autoencoder-based bridge damage assessment using train-induced responses

This paper presents an innovative methodology for assessing bridge conditions using a probabilistic temporal autoencoder (PTAE) in the context of structural health monitoring (SHM) systems with fixed sensing frameworks, which have become increasingly important in maintaining bridge safety. The PTAE methodology addresses the challenges posed by vast amounts of sensor data and constantly changing environmental and operational conditions. By gathering multi-sensor data during train crossings and employing a PTAE with multiple convolutional blocks and an LSTM recurrent neural network, the approach effectively extracts features and captures temporal relationships in the data.

The methodology enables the detection of potential bridge damage by calculating the reconstruction loss and KL divergence-based damage features. Further refining the damage assessment process, an Exponentially Weighted Moving Average (EWMA) filter and a control chart-based threshold mechanism allow for differentiation between healthy and progressively deteriorating damage cases. The proposed method accommodates various monitoring scenarios and sensor configurations, enhancing its robustness against varying operational and environmental conditions.

The results of this study suggest that the proposed method can detect and quantify different types of damage, even without employing any pre-processing method to remove the effects of operational and environmental conditions. The method can be easily integrated with existing monitoring systems and data collection platforms, enabling seamless adoption and implementation in various contexts.

In conclusion, the PTAE methodology holds significant potential for the future of bridge health monitoring and maintenance, offering a data-driven solution that can enhance the safety of infrastructure by effectively detecting damage with a limited number of sensors.

3.4 Paper III

Vehicle assisted bridge damage assessment using probabilistic deep learning

This paper demonstrates the potential of vehicle-assisted bridge monitoring by emphasising the benefits of combining various types of sensory information, including fixed sensors on bridges and moving sensors on vehicles. The proposed PDNN model possesses several strengths, such as scalability, which enables easy integration of different measurements for damage assessment tasks; robustness, attributed to the model's probabilistic nature that ensures accuracy is maintained despite noise and fluctuating loading conditions; simplicity of implementation, as the model works directly with raw signals without the need for heavy pre-processing; and improved damage detection and localisation performance compared to similar methods in the literature.

The innovative aspect of the PDNN model lies in its ability to merge multiple sensors and extract damage-sensitive features without pre-processing input signals, even under realistic operational conditions. This leads to accurate damage assessment across a range of sensor combinations. In contrast to other commonly used data-driven methods, the proposed PDNN model provides added value by quantifying the reliability of its decisions. This is achieved by replacing fixed weights with probabilistic weight distributions, which enhances the model's generalisation ability and offers a measure of decision-making reliability. The study reveals that vehicle-assisted monitoring can effectively identify small and realistic damage cases under various operational and environ-

mental conditions. Combining sensor information from both vehicles and bridges results in more reliable decision-making. However, random traffic on the bridge hinders damage detection when only vehicle sensors are employed.

This study serves as a valuable guideline for future bridge health monitoring systems and planning, benefiting bridge owners when considering monitoring campaigns for specific bridges. Integrating this approach with the fixed and mobile sensing frameworks discussed in papers I and II would lead to a comprehensive and robust solution for bridge health monitoring and maintenance.

3.5 Declaration of Authorship

In papers IA, IB and III, both authors collaborated on the planning of the papers. Muhammad Zohaib Sarwar developed the methodology, wrote all the machine learning and damage assessment codes, performed calculations and analyses of the results, and authored the manuscript. Daniel Cantero contributed by providing the code for the vehicle-bridge interaction model and offering feedback, which led to improvements in the manuscripts.

In Paper II, the planning process was a collaborative effort between both authors. Muhammad Zohaib Sarwar took the lead in developing the methodology, implementing all required codes, including machine learning algorithms, and writing the manuscript. Daniel Cantero supported the project by supplying the train-track model code and providing valuable feedback, resulting in an improved manuscript.

CHAPTER
FOUR

CONCLUSIONS

4.1 Conclusions

This thesis has presented innovative methodologies for damage assessment in bridge health monitoring, emphasising the importance of vehicle-assisted monitoring. Vehicle-assisted monitoring plays a crucial role in these approaches, as it eliminates the need for specialised vehicles for long-term bridge monitoring, making the process more efficient, cost-effective, and accessible for a broader range of infrastructure. Furthermore, the integration of bridge health monitoring with intelligent transport networks is facilitated by leveraging the data generated from regular vehicular traffic. This synergy can enhance the overall efficiency and effectiveness of infrastructure management. For damage assessment, these methodologies employ deep learning techniques and probabilistic approaches that address the challenges posed by the vast amounts of sensor data generated by structural health monitoring (SHM) systems, and the constantly changing environmental and operational conditions. Key aspects of these methodologies include:

- Multi-sensor data: By gathering data from traversing vehicles, such as accelerations, displacements, and rotations, these methods can adapt to various monitoring scenarios and sensor configurations. This eliminates the need for manual feature extraction or single-sensor level model training, streamlining the monitoring process.

- Deep autoencoders (DAE) and probabilistic temporal autoencoders (PTAE): These powerful machine learning techniques effectively extract features and capture temporal relationships in the data. They provide a robust and generalised relationship between vehicle responses and bridge dynamics, making the methodologies applicable across different bridge structures and conditions.

- Damage detection and quantification: The proposed methods employ a statistical distribution-based damage index, the computation of reconstruction loss, and KL divergence-based damage features to accurately identify and quantify various types of damage in bridge structures.

- Enhanced damage assessment process: The Exponentially Weighted Moving Average (EWMA) control chart-based threshold mechanism and wavelet transform-based filter bank further refine the damage assessment process. This allows for early damage detection and differentiation between healthy and progressively deteriorating damage cases, enabling timely maintenance interventions.

- Robustness under varying conditions: The methodologies account for varying operational and environmental conditions, ensuring reliable and accurate damage assessments regardless of factors like measurement noise, temperature variations, and random traffic.
- Better decision-making support: By incorporating model uncertainty and providing accurate damage assessments, these methodologies support improved decision-making in maintenance planning and resource allocation for bridge owners and road authorities.

In conclusion, these data-driven solutions hold significant potential for the future of bridge health monitoring and maintenance. The combination of directly installed sensors and mobile sensing platforms provides a powerful and flexible approach for SHM. By leveraging the strengths of both systems, a comprehensive, robust, and cost-effective framework for assessing and maintaining critical infrastructure assets can be developed, advancing the field of SHM and its practical applications. This approach represents a valuable contribution to the body of knowledge in the field and can serve as a basis for further research and development in the area of structural health monitoring.

CHAPTER
FIVE

FURTHER RESEARCH

5.1 Further research

Further research in the area of structural health monitoring and vehicle-assisted monitoring can explore the following aspects:

- Advanced sensor technology: Examine the integration of cutting-edge sensor technologies, such as LiDAR, cameras, and ultrasonic sensors, alongside traditional sensors to improve data quality and encourage the widespread adoption of vehicle-assisted monitoring.
- Large-scale implementation challenges: Examine the obstacles and requirements for the large-scale deployment of vehicle-assisted monitoring, including regulatory, logistical, and technical aspects, to ensure its success in various contexts.
- Long-term performance evaluation: Conduct in-depth assessments of the long-term performance of vehicle-assisted monitoring systems to gauge their durability, effectiveness, and potential for improvement over time.
- Secure communication and data sharing: Explore secure and efficient communication systems and data sharing protocols to enable seamless integration of vehicle-assisted monitoring with intelligent transport networks and other infrastructure systems.
- Physics-enhanced machine learning and expert knowledge: Develop accurate, reliable, and interpretable models for structural health monitoring by leveraging the combined strengths of physics-based models, data-driven machine learning techniques, and expert knowledge. Incorporating expert insights into the development and interpretation of physics-enhanced machine learning models can lead to more meaningful results.
- Domain adaptation and transfer learning: Investigate innovative algorithms and strategies for transferring knowledge between different bridge structures, allowing for the creation of more effective and efficient damage assessment methodologies applicable across a wide range of bridge structures.

REFERENCES

[1] Bart Peeters, Johan Maeck, and Guido De Roeck. "Vibration-based damage detection in civil engineering: excitation sources and temperature effects". In: *Smart materials and Structures* 10.3 (2001), p. 518.

[2] Onur Avci et al. "A review of vibration-based damage detection in civil structures: From traditional methods to Machine Learning and Deep Learning applications". In: *Mechanical systems and signal processing* 147 (2021), p. 107077.

[3] Charles R Farrar and Keith Worden. *Structural health monitoring: a machine learning perspective*. John Wiley & Sons, 2012.

[4] Yonghui An et al. "Recent progress and future trends on damage identification methods for bridge structures". In: *Structural Control and Health Monitoring* 26.10 (2019), e2416.

[5] Joan R Casas and John James Moughty. "Bridge damage detection based on vibration data: past and new developments". In: *Frontiers in Built Environment* 3 (2017), p. 4.

[6] Edwin Reynders et al. "Damage identification on the Tilff Bridge by vibration monitoring using optical fiber strain sensors". In: *Journal of engineering mechanics* 133.2 (2007), pp. 185–193.

[7] Yang Zhang and Ka-Veng Yuen. "Review of artificial intelligence-based bridge damage detection". In: *Advances in Mechanical Engineering* 14.9 (2022), p. 16878132221122770.

[8] Anne Teughels and Guido De Roeck. "Damage detection and parameter identification by finite element model updating". In: *Revue européenne de génie civil* 9.1-2 (2005), pp. 109–158.

[9] Xin Zhou et al. "Vibration-based Bayesian model updating of an actual steel truss bridge subjected to incremental damage". In: *Engineering Structures* 260 (2022), p. 114226.

[10] Georgios I Dadoulis and George D Manolis. "Model bridge span traversed by a heavy mass: Analysis and experimental verification". In: *Infrastructures* 6.9 (2021), p. 130.

[11] Bjørn T Svendsen et al. "A hybrid structural health monitoring approach for damage detection in steel bridges under simulated environmental conditions using numerical and experimental data". In: *Structural Health Monitoring* (2022), p. 14759217221098998.

[12] Hassan Sarmadi, Alireza Entezami, and Mansour Ghalehnovi. "On model-based damage detection by an enhanced sensitivity function of modal flexibility and LSMR-Tikhonov method under incomplete noisy modal data". In: *Engineering with Computers* 38.1 (2022), pp. 111–127.

[13] Bjørn T. (Bjørn Thomas) Svendsen. "Numerical and experimental studies for damage detection and structural health monitoring of steel bridges". PhD thesis. 2021. ISBN: 9788232663279.

[14] Ana C Neves et al. "Structural health monitoring of bridges: a model-free ANN-based approach to damage detection". In: *Journal of Civil Structural Health Monitoring* 7 (2017), pp. 689–702.

[15] Yuequan Bao and Hui Li. "Machine learning paradigm for structural health monitoring". In: *Structural Health Monitoring* 20.4 (2021), pp. 1353–1372.

[16] Kun Feng, Arturo González, and Miguel Casero. "A kNN algorithm for locating and quantifying stiffness loss in a bridge from the forced vibration due to a truck crossing at low speed". In: *Mechanical Systems and Signal Processing* 154 (2021), p. 107599.

[17] Muhammad Zohaib Sarwar and Daniel Cantero. "Vehicle assisted bridge damage assessment using probabilistic deep learning". In: *Measurement* 206 (2023), p. 112216.

[18] Premjeet Singh and Ayan Sadhu. "Limited sensor-based bridge condition assessment using vehicle-induced nonstationary measurements". In: *Structures* 32 (2021), pp. 1207–1220.

[19] Shuo Wang, Eugene J OBrien, and Daniel P McCrum. "A Novel Acceleration-Based Moving Force Identification Algorithm to Detect Global Bridge Damage". In: *Applied Sciences* 11.16 (2021), p. 7271.

[20] Muhammad Zohaib Sarwar and Daniel Cantero. "Deep autoencoder architecture for bridge damage assessment using responses from several vehicles". In: *Engineering Structures* 246 (2021), p. 113064.

[21] Abdollah Malekjafarian et al. "A machine learning approach to bridge-damage detection using responses measured on a passing vehicle". In: *Sensors* 19.18 (2019), p. 4035.

[22] Hoofar Shokravi et al. "Vehicle-assisted techniques for health monitoring of bridges". In: *Sensors* 20.12 (2020), p. 3460.

[23] Eugene OBrien, Ciaran Carey, and Jennifer Keenahan. "Bridge damage detection using ambient traffic and moving force identification". In: *Structural Control and Health Monitoring* 22.12 (2015), pp. 1396–1407.

[24] C McGeown et al. "Using measured rotation on a beam to detect changes in its structural condition". In: *Journal of Structural Integrity and Maintenance* 6.3 (2021), pp. 159–166.

[25] Eugene J Obrien et al. "Identifying damage on a bridge using rotation-based Bridge Weigh-In-Motion". In: *Journal of Civil Structural Health Monitoring* 11 (2021), pp. 175–188.

[26] ZL Wang et al. "Recent Advances in Researches on Vehicle Scanning Method for Bridges". In: *International Journal of Structural Stability and Dynamics* 22.15 (2022), p. 2230005.

[27] Robert Corbally and Abdollah Malekjafarian. "A data-driven approach for drive-by damage detection in bridges considering the influence of temperature change". In: *Engineering Structures* 253 (2022), p. 113783.

[28] Zhenkun Li, Weiwei Lin, and Youqi Zhang. "Drive-by bridge damage detection using Mel-frequency cepstral coefficients and support vector machine". In: *Structural Health Monitoring* (2023), p. 14759217221150932.

[29] Robert Corbally and Abdollah Malekjafarian. “Examining changes in bridge frequency due to damage using the contact-point response of a passing vehicle”. In: *Journal of Structural Integrity and Maintenance* 6.3 (2021), pp. 148–158.

[30] YB Yang, YC Li, and Kai Chun Chang. “Constructing the mode shapes of a bridge from a passing vehicle: a theoretical study”. In: *Smart Structures and Systems* 13.5 (2014), pp. 797–819.

[31] Abdollah Malekjafarian, Patrick J McGetrick, and Eugene J OBrien. “A review of indirect bridge monitoring using passing vehicles”. In: *Shock and vibration* 2015 (2015).

[32] Abdollah Malekjafarian, Robert Corbally, and Wenjie Gong. “A review of mobile sensing of bridges using moving vehicles: Progress to date, challenges and future trends”. In: *Structures*. Vol. 44. Elsevier. 2022, pp. 1466–1489.

[33] George Lederman et al. “Damage quantification and localization algorithms for indirect SHM of bridges”. In: *Proc. Int. Conf. Bridge Maint., Safety Manag., Shanghai, China*. 2014, pp. 640–647.

[34] Jingxiao Liu et al. “Diagnosis algorithms for indirect structural health monitoring of a bridge model via dimensionality reduction”. In: *Mechanical Systems and Signal Processing* 136 (2020), p. 106454.

[35] William Locke et al. “Using drive-by health monitoring to detect bridge damage considering environmental and operational effects”. In: *Journal of Sound and Vibration* 468 (2020), p. 115088.

[36] Reza Malekian et al. “Design and implementation of a wireless OBD II fleet management system”. In: *IEEE Sensors Journal* 17.4 (2016), pp. 1154–1164.

[37] Holger Billhardt et al. “Dynamic coordination in fleet management systems: Toward smart cyber fleets”. In: *IEEE Intelligent Systems* 29.3 (2014), pp. 70–76.

[38] Yanqi Wu and Shengli Li. “Damage degree evaluation of masonry using optimized SVM-based acoustic emission monitoring and rate process theory”. In: *Measurement* 190 (2022), p. 110729.

[39] Han-Bing Liu and Yu-Bo Jiao. “Application of genetic algorithm-support vector machine (GA-SVM) for damage identification of bridge”. In: *International Journal of Computational Intelligence and Applications* 10.04 (2011), pp. 383–397.

[40] Sujith Mangalathu et al. “Rapid seismic damage evaluation of bridge portfolios using machine learning techniques”. In: *Engineering Structures* 201 (2019), p. 109785.

[41] Ji-Gang Xu et al. “Data-driven rapid damage evaluation for life-cycle seismic assessment of regional reinforced concrete bridges”. In: *Earthquake Engineering & Structural Dynamics* 51.11 (2022), pp. 2730–2751.

[42] Shuang Sun et al. “Multidamage detection of bridges using rough set theory and naive-Bayes classifier”. In: *Mathematical Problems in Engineering* 2018 (2018).

[43] Jordan C Weinstein, Masoud Sanayei, and Brian R Brenner. “Bridge damage identification using artificial neural networks”. In: *Journal of Bridge Engineering* 23.11 (2018), p. 04018084.

[44] Frank L Wang et al. “Correlation-based damage detection for complicated truss bridges using multi-layer genetic algorithm”. In: *Advances in Structural engineering* 15.5 (2012), pp. 693–706.

[45] Shenfang Yuan et al. “A uniform initialization Gaussian mixture model–based guided wave–hidden Markov model with stable damage evaluation performance”. In: *Structural Health Monitoring* 18.3 (2019), pp. 853–868.

[46] YB Yang, Yi He, and Hao Xu. "Automatically extracting bridge frequencies using SSA and K-Means clustering from vehicle-scanned accelerations". In: *International Journal of Structural Stability and Dynamics* 22.08 (2022), p. 2250079.

[47] Shinji Baba and Jun Kondoh. "Damage evaluation of fixed beams at both ends for bridge health monitoring using a combination of a vibration sensor and a surface acoustic wave device". In: *Engineering Structures* 262 (2022), p. 114323.

[48] Adam Santos, Eloi Figueiredo, and Joao Costa. "Clustering studies for damage detection in bridges: A comparison study". In: *Structural Health Monitoring 2015* (2015).

[49] Gabriele Comanducci et al. "On vibration-based damage detection by multivariate statistical techniques: Application to a long-span arch bridge". In: *Structural health monitoring* 15.5 (2016), pp. 505–524.

[50] XW Ye, T Jin, and CB Yun. "A review on deep learning-based structural health monitoring of civil infrastructures". In: *Smart Struct Syst* 24.5 (2019), pp. 567–585.

[51] Davið Steinar Ásgrımsson et al. "Bayesian deep learning for vibration-based bridge damage detection". In: *Structural health monitoring based on data science techniques* (2022), pp. 27–43.

[52] Smriti Sharma and Subhamoy Sen. "Real-time structural damage assessment using LSTM networks: regression and classification approaches". In: *Neural Computing and Applications* 35.1 (2023), pp. 557–572.

[53] Zhiqiang Shang et al. "Vibration-based damage detection for bridges by deep convolutional denoising autoencoder". In: *Structural Health Monitoring* 20.4 (2021), pp. 1880–1903.

[54] Zilong Wang and Young-Jin Cha. "Unsupervised deep learning approach using a deep auto-encoder with a one-class support vector machine to detect damage". In: *Structural Health Monitoring* 20.1 (2021), pp. 406–425.

[55] Rafaelle Piazzaroli Finotti et al. "Numerical and Experimental Evaluation of Structural Changes Using Sparse Auto-Encoders and SVM Applied to Dynamic Responses". In: *Applied Sciences* 11.24 (2021), p. 11965.

[56] Bo Zhao et al. "A robust construction of normalized CNN for online intelligent condition monitoring of rolling bearings considering variable working conditions and sources". In: *Measurement* 174 (2021), p. 108973.

[57] Jongbin Won et al. "Automated structural damage identification using data normalization and 1-dimensional convolutional neural network". In: *Applied Sciences* 11.6 (2021), p. 2610.

APPENDICES

PAPER IA

Muhammad Zohaib Sarwar, Daniel Cantero

Deep autoencoder architecture for bridge damage assessment using responses from several vehicles, Engineering Structures 246 (2021) 113064.

IA

Engineering Structures 246 (2021) 113064

Contents lists available at ScienceDirect

Engineering Structures

journal homepage: www.elsevier.com/locate/engstruct

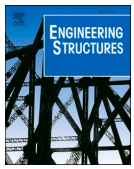

Deep autoencoder architecture for bridge damage assessment using responses from several vehicles

Muhammad Zohaib Sarwar *, Daniel Cantero

Department of Structural Engineering, NTNU Norwegian University of Science and Technology, Trondheim 7491, Norway

ARTICLE INFO

Keyword:
Structural Health Monitoring
Damage detection
Indirect monitoring
Deep learning
Autoencoders
Convolutional neural network
Vehicle-bridge interaction

ABSTRACT

Vehicle-assisted monitoring is a promising alternative for rapid and low-cost bridge health monitoring compared to direct instrumentation of bridges. In recent years, centralized management systems for fleets of heavy vehicles have been adopted in transportation networks for logistics and other applications. These vehicles can be instrumented and easily integrated with the existing fleet management systems to provide information that can be used for bridge health monitoring. In this study, a numerical investigation is carried out to evaluate the feasibility of an indirect bridge monitoring system considering responses from several vehicles under operational conditions. The proposed method uses the vertical acceleration responses from a fleet of vehicles passing over a healthy bridge to train a deep autoencoder model (DAE) for bridge damage sensitive features. It is shown that the error in signal reconstruction from the trained DAE is sensitive to damage, when considering the distribution or results from several separate vehicle-crossing events. The bridge damage is quantified with a damage index based on the Kullback-Leibler divergence that evaluates the change in the distributions of the reconstruction errors. The performance of the proposed method is evaluated for two numerical scenarios of vehicle populations, for different damage cases including the effect of operational uncertainties (road profile, measurement noise, and variability in vehicle properties). The proposed method is also evaluated for more realistic multi-span continuous bridge for different damage cases in the presence of random traffic. The result show that the proposed method can detect damage under operational conditions and that it has the potential to become a new tool for cost-effective bridge health monitoring.

1. Introduction

The maintenance of ageing infrastructure is taking large parts of the total budget available to transport network owners. The continuously growing stock of bridges is getting old and many have exceeded their design service life. To ensure the safe operation of these bridges, monitoring and continuous assessment is essential. In recent years, structural health monitoring (SHM) strategies have evolved from manual inspection to sensors-based monitoring systems [1,2]. Sensor-based monitoring solutions require the direct installation of multiple sensing instruments on bridges and the analysis of the collected data [3]. The collected information from sensors is analysed through physics and/or data-driven techniques to extract useful features[4].

Early damage detection is one of the core objective in SHM and to that purpose many vibration-based methods have been proposed [4,5]. The measured vibration responses are analysed with some signal processing method to provide the information about the structure and possible damage state. However, these methods generally require multiple sensors installed on the bridge, which increases installation and maintenance costs of the monitoring system. In addition, it is challenging to effectively utilize the large data sets generated daily for each bridge [6]. Because of these practical and economic considerations, the implementation of such systems is generally limited to a relatively small amount of long-span bridges [7].

As an alternative to traditional SHM methods, many studies have proposed indirect or 'Drive-by' methods. This idea utilizes the measured responses from a moving vehicle while traversing the bridge of interest. The method was initially proposed by Yang et al. [8] to identify the bridge's natural frequencies. This method is a low-cost alternative to traditional monitoring methods because it removes the necessity for individual instrumentation of each bridge. Over the past decade, researchers have investigated and provided many solutions for different damage detection levels using the indirect method [9]. These methods are broadly categorized into two main groups: (1) modal-based; (2) non-

* Corresponding author.
E-mail addresses: muhammad.z.sarwar@ntnu.no (M.Z. Sarwar), daniel.cantero@ntnu.no (D. Cantero).

https://doi.org/10.1016/j.engstruct.2021.113064
Received 24 February 2021; Received in revised form 10 July 2021; Accepted 18 August 2021
Available online 2 September 2021

modal-based.

The modal-based indirect method identifies the bridge modal properties, which in turn can be used for damage detection [7,10]. Experimental validation of bridge frequency identification is done in [11] using instrumented trailer. Similarly, Yang et al. [12] and Zhu et al. [13] used empirical mode decomposition (EMD) and ensemble empirical mode decomposition (EEMD) for pre-processing the vehicle's acceleration response to extract higher mode frequencies of a bridge. O'Brien et al. [14] and Kildashti et al. [15] used the EMD and corresponding intrinsic mode functions (IMFs) to define a damage indicator. Modal-based indirect methods have been also used for mode shape identification, which allowed the detection and localisation of damage by analysing the mode shape curvature [16,17]. Yang et al. [18] proposed using the Hilbert amplitude of the acceleration response of passing vehicles to find bridge mode shapes. Likewise, Malekjafarian et al. [19] used the short-time frequency domain decomposition for bridge mode identification. Eshkevari et al. [20] proposed the novel pipeline methods together with EMD and structural identification using expectation maximization (STRIDEX) to identify mode shapes. Despite the advancements in the modal-based method, there are still critical challenges associated with it. Arguably, the main challenge is the need of low vehicle speeds in order to achieve sufficient resolution to accurately extract the modal parameters. Also, the performance of these methods is affected by the presence of the road profile and measurement noise.

In contrast, several other indirect methods did not directly extract modal parameters. These non-modal-based methods, which mainly rely on signal processing and machine learning, have been proven effective in detecting and localising damage [21–28]. For instance, Zhang et al. [27] proposed the estimation of contact-point response to detect damage. The vehicle-bridge contact point was estimated using acceleration measured on a vehicle. Then an indicator based on the Hilbert instantaneous amplitude was proposed for damage detection and localization. O'Brien et al. [21] effectively applied the moving force identification method for damage detection in a numerical study and verified it in an experimental investigation [29]. Both studies assume prior knowledge of the vehicle's dynamic properties (masses and suspension stiffness and viscous damping). Additionally, several authors have used wavelet transform in indirect methods. McGetrick and Kim [30] proposed a damage indicator based on the coefficients from the continuous wavelet transform (CWT), which was capable of identifying different crack levels on a bridge. Similarly, Hester and González [31] use CWT with the Mexican Hat basis for the detection of cracks on the bridge. Liderman et al. [32] applied signal processing and principle component analysis (PCA) to diagnose numerically simulated damage. Liu et al. [33] proposed a nonlinear dimensionality reduction method for damage diagnosis, studied it numerically for a single degree of freedom vehicle and verified it with laboratory experiments. Therefore, it is well acknowledged that these methods can perform well for damage detection and can be used to quantify the severity of the damage. However, their practical viability still requires significant physical insights for model and method selection.

Despite the reported progress in indirect health monitoring, several challenges and limitations still exist for its practical implementation. Bridge damage detection is a task that requires several vehicle passages and most of the 'Drive-by' methods generally use a single specialized vehicle. Thus, arguably the main challenge in this scenario is that it is practically impossible to have the same vehicle with the same properties over an extended period of time. In addition, operational and environmental conditions also directly affect the damage diagnosis process. To address these issues multiple frequent runs are an alternative approach for bridge monitoring. Miyamoto et al. [34] proposed the idea of using a fleet of public transport buses to monitor short and medium span bridges. A damage indicator was developed based on the average characteristic deflection curve. The authors suggested that heavy vehicle responses can be a better option for damage detection because of high flexural stiffness of short and medium-span bridges. Mei et al. [25] used cepstrum analysis and PCA for damage detection from several vehicle-crossing events. Similarly, Malekjafarian et al. [26] and Locke et al. [35] proposed the idea of using artificial neural network (ANN) and deep learning respectively for damage detection using multiple vehicles measurement responses based on numerically generated vehicle-bridge interaction (VBI) data. In [26] the authors employed a two-stage approach using an ANN model and gaussian process (GP) to detect damage features from acceleration responses measured at the vehicles' axles. The combination of ANN and statistical analysis proved to be successful in the detection of damage even in the presence of surface roughness and measurement noise. Locke et al. [35] further explored this idea to only use a single deep learning model for feature extraction and damage diagnosis while considering operational and environmental affect. The main drawback was that it required labelled data of damaged cases, which is not possible in a real case scenario. The above-mentioned methods demonstrated that multiple vehicle responses analysed with different tools (signal processing, ANN and/or statistical analysis) can be successfully employed in indirect SHM. However, generally these studies are based on numerical simulations of simple vehicle models (mainly quarter-car). Furthermore, these studies consider only a small variation in vehicle properties and limited effect of road profile roughness.

On the other hand, recent developments in intelligent transportation systems has created the possibility to manage the information from multiple vehicles using a centralized system [36]. With progress in telemetric technology, the perspective of an on-board monitoring system for multiple vehicles managed via a centralized system opens new prospects for SHM. The multi-sensor (GPS, acceleration, speed, etc.) data from a fleet of vehicles can be remotely accessed regularly by system managers [37,38]. The big data that is collected from multiple vehicles can be further analysed and used for SHM. For big data analysis machine learning algorithms have proven to be a valuable tool to extract reliable information. Hinton and Salakhutdinov [39] introduced the idea of the deep learning (DL) model in machine learning to address the issue of gradient vanishing and convergence to local minima associated with shallow ANN architecture models. Since then deep neural networks have attracted attention in a wide range of applications, mainly in object recognition, speech recognition and natural language processing [40,41]. For SHM, DL models have been widely explored recently [42], where convolution neural networks (CNN) or recursive neural networks (RNN) are some of the DL algorithm types used. Abdeljaber et al. [43] proposed applying 1D CNN to extract structural damage features from the time histories of vibration responses. Similarly, Ni et al. [44] and Zhang et al. [45] used 1D CNN for data compression for anomaly detection in acceleration data for bridge health monitoring. Wang and Cha [46] and Shang et al. [47] used deep convolutional autoencoder to detect damage using directly measurements from the structure. For more details on recent advancements in vibration-based condition assessment, refer to [42,48], which provide a comprehensive review of DL and CNN applications in SHM.

To address the challenges discussed earlier, we propose a bridge damage detection method considering the dynamic responses from a fleet of vehicles traversing the target bridge. The idea is explored numerically with a 5-axle truck model considering a range of vehicle properties and speeds, as well as, the presence of road profiles and measurement noise. An autoencoder based DL framework is trained to extract damage-sensitive features, where the inputs are the vehicles' vertical accelerations while traversing the bridge. Once the model is trained it is used to predict subsequent vehicle responses. The difference between model-based and actual vehicle responses is the prediction error. A damage index is proposed based on the distance between the distributions of prediction errors. The numerical study evaluates the performance of the proposed method for a range of different damage scenarios.

The remainder of the paper is organized as follows. Section 2 provides an overview of the proposed methodology, including the

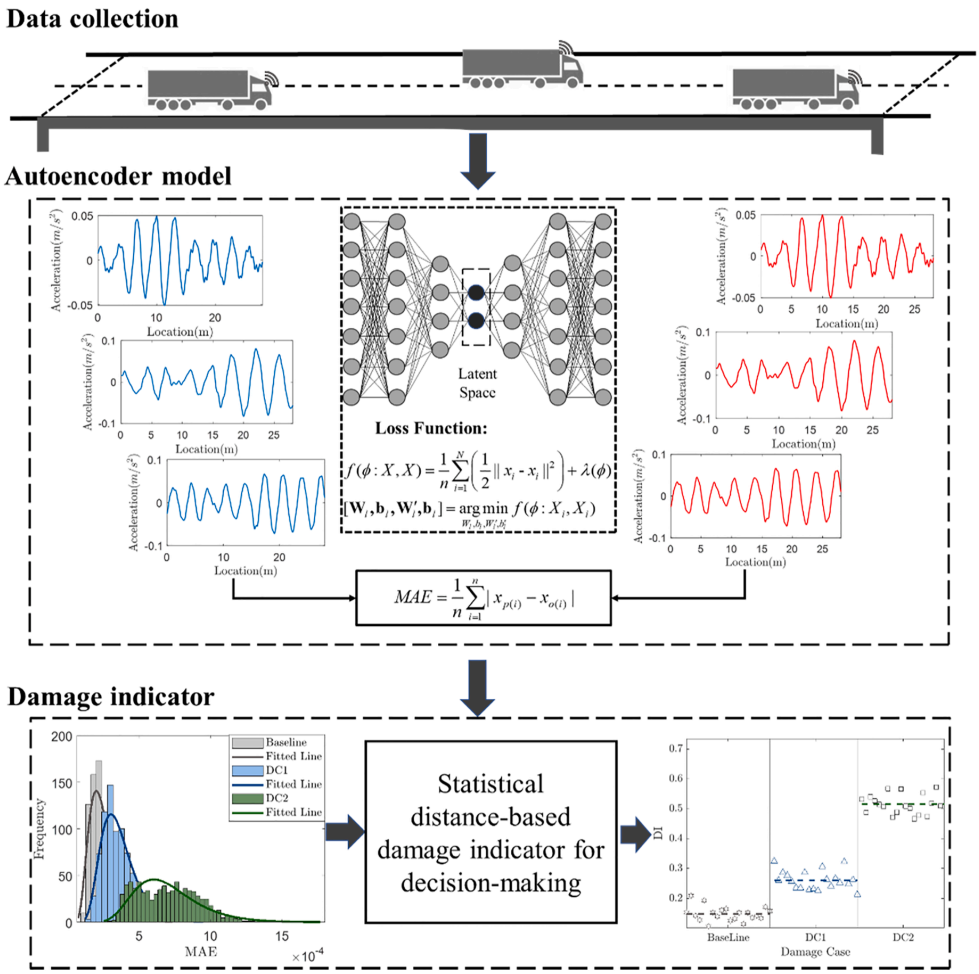

Fig. 1. Overview of the proposed framework.

architecture of the deep neural network model and damage index. Section 3 presents the vehicle-bridge interaction model and details about the training of the deep learning model. Section 4 evaluates the performance of deep learning model. Section 5 provides the numerical validation of the proposed damaged detection approach. Section 6 provides the validation of damage detection for multi-span continuous bride model. Section 7 discusses the practical considerations for real life application of the proposed method

2. Proposed method

The framework proposed in this paper for damage detection is mainly divided into three phases. The first phase involves the collection of vehicle information and responses (speed and vertical acceleration) from a number of vehicle-crossing events. The collected data is then used to train a deep autoencoder for damage sensitive features in the second phase. The autoencoder architecture is developed using 1D CNN and Long short-term memory (LSTM) recurrent neural network. In the third phase, the trained model is used to compute the reconstruction error for testing data. The KL (Kullback-Leibler) divergence-based damage index is proposed to assess the severity of the damage. Fig. 1 shows a schematic overview of the proposed framework. More details about the data collection, autoencoder, and damage index are discussed in subsequent sections.

2.1. Data collection

The proposed framework assumes that vehicle responses are measured using on-board systems, information that could be accessed remotely by a central fleet management system. Different sensor types could be used at different vehicle locations to measure a range of responses. However, due to their low cost and ease of installation, this study assumes that accelerometers are installed on each passing vehicle's tractor and trailer. Also, this study considers single- vehicle crossing events where the entry and exit times on the bridge are known.

2.2. Deep autoencoder (DAE)

Autoencoder is an unsupervised neural network model that is used for dimensionality reduction and feature extraction. The traditional architecture of autoencoder model is consists of an encoder and a decoder module, each with a single hidden layer. The encoder module

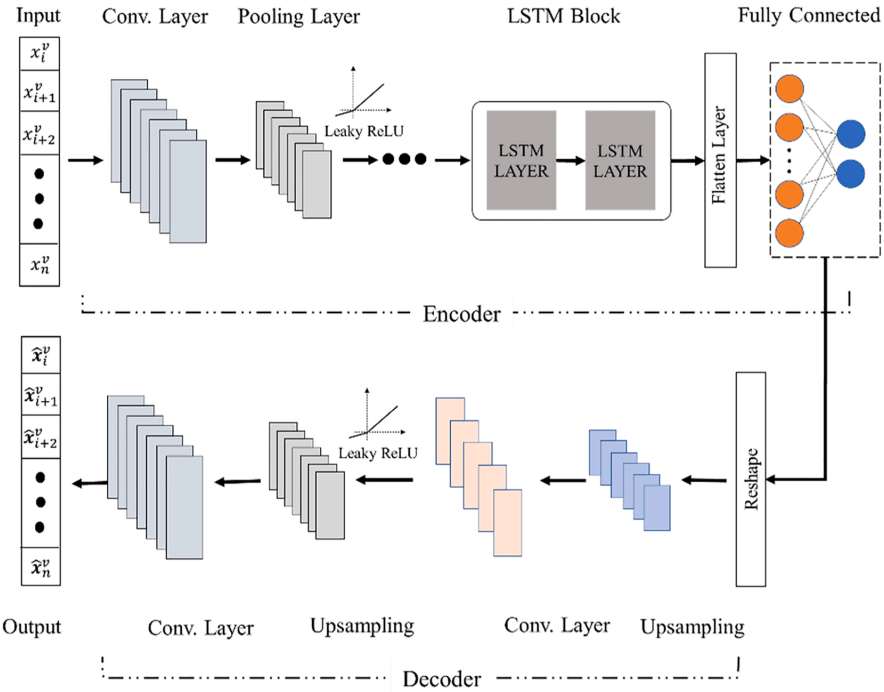

Fig. 2. Architecture of the proposed deep autoencoder model (DAE).

maps the input data x into arbitrary lower dimensional space $\boldsymbol{h}$ while the decoder modules reconstruct the original input using $\boldsymbol{h}$ as an output $\hat{x}$. The transfer function of each module is expresses as follows:

$$\boldsymbol{h} = f(x) = \Phi(\boldsymbol{W}x + \boldsymbol{b}) \tag{1}$$

$$\hat{x} = g(\boldsymbol{h}) = \Phi^{'}(\boldsymbol{W}^{'}x + \boldsymbol{b}^{'}) \tag{2}$$

where $\boldsymbol{W}, \boldsymbol{W}^{'}$ and $\boldsymbol{b}, \boldsymbol{b}^{'}$ are the weight matrices and bias vectors for encoder and decoder modules, while $\Phi, \Phi^{'}$ are the activation functions of encoder and decoder, which are usually the nonlinear functions *sigmoid* or *hyperbolic tangent*. The autoencoder optimizes the learning parameters $\boldsymbol{W}, \boldsymbol{W}^{'}, \boldsymbol{b}, \boldsymbol{b}^{'}$ using mean squared error as the loss function $\mathscr{L}$ between input and its reconstruction at the decoder's output.

In comparison to traditional autoencoders, deep autoencoders (DAE) contain more than one hidden layer (depending on the input data's complexity) in the encoder and the decoder. The DAE model allows for the effective feature extraction through hierarchical nonlinear mapping via multiple hidden layers, resulting in a significant reduction of training dataset [46]. For a DAE model, the loss function can be expressed for an unlabelled dataset $X = [x_1, x_2, x_3, \cdots x_n]$ as follows:

$$\mathscr{L} = f(\phi : X, X) = \frac{1}{n}\sum_{i=1}^{N}\left(\frac{1}{2}||\hat{x}_i - x_i||^2\right) + \lambda(\phi) \tag{3}$$

$$\left[\boldsymbol{W}_l, \boldsymbol{b}_l, \boldsymbol{W}_l^{'}, \boldsymbol{b}_l^{'}\right] = \underset{W_l, b_l, W_l^{'}, b_l^{'}}{argmin} f(\phi : X, X); \quad l = 1, 2, 3, \cdots \tag{4}$$

Where subscript l is the number of hidden layers and λ is a regularization factor imposed at the weights of the specific layer to prevent overfitting.

2.2.1. Network architecture for DAE

Autoencoders have been used in literature, among other applications, for feature extraction and dimensionality reduction [49,50]. In the proposed framework, these functionalities are utilised to learn the compressed feature representation of multiple vehicles' acceleration responses, which can further be used for robust damage detection.

For feature extraction from time-series, recurrent neural network (RNN) and 1D convolutional neural network (1D CNN) are widely used. RNN is specifically designed for sequential data to extract and augment the time-dependent features. However, according to the existing investigations, it is difficult to train RNN for long term sequences because of gradient vanishing during backpropagation [51]. To address this Long short-term memory (LSTM) is introduced [52]. LSTM is explicitly designed to avoid the long-term dependency problem because of its internal gates-like architecture that can be used to control the flow of information. LSTM has a threshold-based mechanism to fuse similar information and filter out redundant information. More details regarding LSTMs can be found in [52].

A CNN usually consists of a convolutional layer, pooling layer, and activation function. In the convolutional layer, the convolutional operations are performed on the input by different convolutional filters, which essentially perform cross-correlation on multiple local regions of the input to extract low-level features from the raw response. The pooling layer aggregates the information from all local regions and downsamples the overall feature space. The pooling layer makes the learned feature robust and reduces the model's number of parameters, resulting in a computationally efficient model. The activation function is applied for nonlinear transformation in each layer.

DAE architecture is developed as shown in Fig. 2 to extract the compact hidden representation of the training dataset. The model can reconstruct the input data with high accuracy and is mostly sensitive to damage information. The hidden layers of the encoder have two levels. The first level includes multiple convolutional blocks, where each extract multiple local features from the input data and reduces the

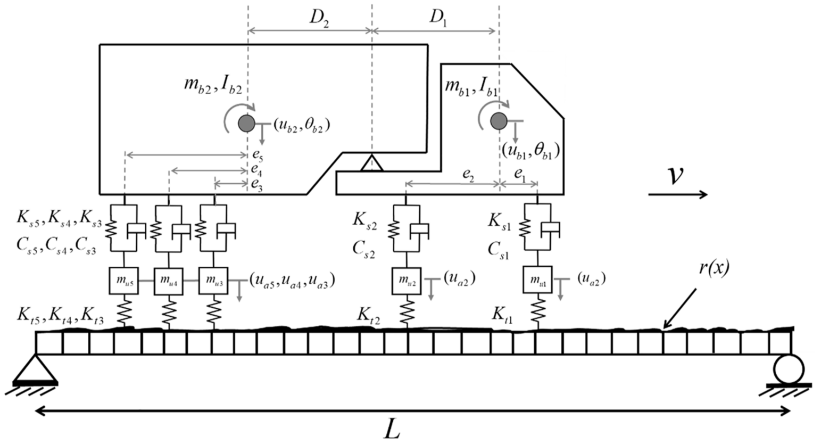

Fig. 3. Vehicle-bridge interaction model.

number of parameters by pooling layers. Here, the Leaky-ReLU activation function is used. In this first level, the time-series response is reduced to a more compact representation of the most relevant features. The extracted features using convolutional blocks are strongly dependent upon each other. However, 1-D CNN did not able produce smooth and compact latent representation that can be applied for reconstruction of the original response. For a robust latent representation, learning feature's temporal dependencies are crucial. A fully connected layer is normally used to simply combine the feature with its adjusted weight. However, in this case for smooth latent representation, the first level feature map is fed into a second-level LSTM layers for retaining the temporal dependencies of similar features which would further be used for extracting smooth latent space. Then the last LSTM layer is flattened and mapped to the bottleneck layer to obtain a fixed latent space representation. For the decoder, each convolutional block is comprised of deconvolutional layers followed by up-sampling and nonlinear activation function Leaky-ReLU. The proposed architecture optimization of weight and bias parameters is done by an end-to-end method, in contrast to stepwise training of hidden layers, and staking of pre-trained layers for final fine-tuning.

2.3. Damage index (DI)

For damage detection and severity evaluation, the reconstruction loss is evaluated by the mean absolute error (MAE) using Eq. (5). The MAE calculates for each vehicle, the difference between the measured response and the reconstructed response estimated by the trained DAE model.

$$\mathrm{MAE} = \frac{1}{n}\sum_{i=1}^{n} |\hat{x}(t_i) - x(t_i)| \tag{5}$$

where $\hat{x}(t_i)$ and $x(t_i)$ are the reconstructed and measured responses respectively at sample i for a total of n samples.

When considering a fleet of vehicles, the MAE error significantly varies between crossing events because of the different vehicle properties and speed. However, batches of these events result in distributions of MAE values that can be used to differentiate a healthy bridge (baseline) from a damaged one. It is possible to assess the bridge condition by evaluating the difference between MAE distributions from different batches. In this study, KL divergence is computed to quantify how different two distributions are [53]. The KL divergence is the method that comes from information theory and measures the information loss when a probability distribution p is used to approximate a distribution q. The general form of KL divergence is expressed as follows:

$$D_{KL}(p\|q) = \int_x p \log \frac{dp}{dq} \tag{6}$$

In this paper the MAE distributions are assumed to follow the log-normal distribution for each batch of vehicles crossing the bridge. These distributions are defined in terms of their corresponding mean μ and standard deviation $\sigma$for the baseline condition ($p_0 = logN(x|\mu_0, \sigma_0)$) and for an unknown condition ($q_1 = logN(x|\mu_1, \sigma_1)$). By using the probability density functions definitions in Eq. (6) the KL divergence between two distributions can be written as:

$$D_{KL}(p_0\|q_1) = ln\left[\frac{\sigma_1}{\sigma_0}\right] + \frac{1}{2\sigma_1^2}\left[(\sigma_1^2 - \sigma_0^2) + (\mu_1 - \mu_0)^2\right] \tag{7}$$

One can see in Eq. (7) that the relationship between the distributions and KL divergence is exponential with a range of $[0, \infty]$. To obtain a robust damage index (DI) the expression is transformed into a linearized relationship as Eq. (8) as proposed in [54]. From Eq. (8) it is clear that DI value depends upon the batch size of vehicles. If sufficient amount of vehicle-crossing data is available, this DI could be used for damage detection. This would be later illustrated with numerical results in Section 5.

$$\mathrm{DI} = ln[D_{KL}(p_0\|q_1) + e] \tag{8}$$

where is e is Euler number.

3. Numerical modelling

This section presents the numerical model that simulates the responses of a vehicle-bridge interaction system with road profile. The numerical model would be used to generate dataset for training and evaluation of DAE. This section also discusses the configuration and hyperparameters for DAE training used in this study.

3.1. Vehicle-bridge interaction model

Fig. 3 shows the vehicle-bridge system used for numerical simulations. The coupled system is modelled as a simply supported beam crossed by a 5-axle truck.

3.1.1. Vehicle model

The vehicle model consists of an articulated tractor-trailer configuration with two and three axles respectively. Fig. 3 shows that the tractor

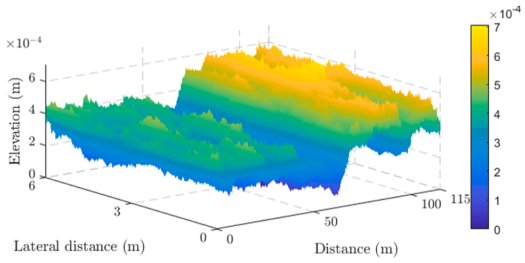

Fig. 4. Road profile of class A (according to ISO 8608).

and trailer are represented as rigid bodies, whereas the axles are modelled as lumped masses. These bodies are interconnected with spring and dashpot systems representing the suspensions. The axle tyre is modelled as a single spring connecting the axle mass and road profile. The vehicle model has a total of 8 independent degrees of freedom (DOF's): vertical displacements of five axles ($u_{a,i}$), tractor's vertical displacement (u_{b1}) and pitch rotation (θ_{b1}), and pitch rotation (θ_{b2}) of the trailer. The trailer's vertical displacement (u_{b2}) can be expressed in terms of the other DOFs by the geometric relation given in Eq. (9) arising from the articulation between tractor and trailer.

$$u_{b2} = u_{b1} + D_1\theta_{b1} + D_2\theta_{b2} \tag{9}$$

The equation of motion of the vehicle can be represented by:

$$\boldsymbol{M_v}\ddot{u}_v + \boldsymbol{C_v}\dot{u}_v + \boldsymbol{K_v}u_v = f_v \tag{10}$$

where $\boldsymbol{M_v}$, $\boldsymbol{C_v}$, and $\boldsymbol{K_v}$ are the mass, damping and stiffness matrices of the vehicle respectively. The u_v vector contains the displacements of all DOFs and f_v is the external force applied to the vehicle system. The extended formulation can be found in [55]. The vehicle model assumes constant speed for each run. Table A1 in appendix provides the vehicle parameters adopted for the numerical studies. The values of the vehicles' parameters are based on European 5-axle trucks, which are adopted from [56–58]. Reference [58] also provides the parameters for distributions (mean, standard deviation, minimum and maximum) that are the basis for generation of batch of vehicles used for Monte Carlo simulations.

3.1.2. Bridge and road profile

The bridge is modelled as a simply supported beam of 15m span length. Its section and material properties are: second moment of area $I = 0.5273\ m^4$, modulus of elasticity $E = 3.5 \times 10^{10}\ N/m^2$, and mass per unit length $\rho = 28125\ kg/m$, deemed to represent a generic reinforced concrete highway bridge. A 2% damping is considered for all modes. The finite element model is discretised into 30 elements (each element 0.5 m length). The equation of motion of the bridge is described as follows:

$$\boldsymbol{M_b}\ddot{u}_b + \boldsymbol{C_b}\dot{u}_b + \boldsymbol{K_b}u_b = f_b \tag{11}$$

where $\boldsymbol{M_b}$, $\boldsymbol{C_b}$, and $\boldsymbol{K_b}$ are the global mass, damping and stiffness matrices of the bridge respectively and u_b is the vector of nodal displacements.

A road profile is also added to the bridge model. A 6 m wide carpet road profile of ISO class 'A' is generated as shown in Fig. 4. A 100 m approach distance is considered before entering the bridge to allow that traversing vehicles reach dynamic equilibrium. The transverse vehicle position on the road profile is randomly varied for each run following a normal distribution. A moving average filter of 0.24 m width is applied to the profile to represent the actual contact of a truck tyre [59]

3.1.3. Vehicle-bridge interaction:

The response of a vehicle traversing a bridge is characterised by the dynamic interaction between both systems. This vehicle-bridge interaction is achieved by coupling the equations of motion of vehicle Eq. (10) and bridge Eq. (11). The final system of coupled equations of motions can be expressed as:

$$\boldsymbol{M_g}\ddot{u}_g + \boldsymbol{C_g}\dot{u}_g + \boldsymbol{K_g}u_g = f_g \tag{12}$$

where $\boldsymbol{M_g}$, $\boldsymbol{C_g}$, and $\boldsymbol{K_g}$ are the time-varying system mass, damping and stiffness matrices respectively and u is the vector of combined bridge and vehicle displacements. $u_g = \{u_b, u_v\}$. The vector f_g contains the external forces applied to the coupled system [55]. To solve the coupled system, the equation of motions are integrated using Newmark-β scheme and solved iteratively to obtain the system responses, which has been implemented in MATLAB. More details of the coupling procedure and numerical solution can be found in [55,60].

3.2. Data generation and pre-processing

Numerical evaluation of the proposed damage detection method is performed using simulated data generated by solving the vehicle-bridge interaction system presented in Section 3.1. In this study, two different scenarios are considered based on the degree of variation in vehicle properties.

1. Scenario-1: The dataset is generated assuming that a fleet of similar vehicles is traversing the bridge. In this case, the variation in vehicle properties is considered in such a way that their standard deviation is small, while the geometry of the vehicles is identical. Variation in vehicle masses and suspension properties is applied to account for normal fluctuations in payload and to account for the inherent uncertainty of the reported vehicle properties.
2. Scenario-2: This data represents a more generic scenario where the responses of different 5-axle trucks is considered. Compared to Scenario-1, the dataset is generated by randomly varying the vehicle properties with a larger standard deviation, while at the same time introducing also random variations in vehicle geometry, rendering different vehicles for each event.

The particular vehicle properties and the statistical variability of the parameters (i.e. maximum, minimum, and standard deviation) for both scenarios are presented in Table A1 in the appendix. For both datasets, the vehicle properties are randomly sampled based on the given statistical variation within a Monte Carlo simulation. For each scenario, a batch of 1000 vehicle events are created. Each dataset contains the vehicle's speed (v) and the vertical acceleration response from tractor ($\ddot{u}_{b1}$) and trailer ($\ddot{u}_{b2}$) with a sampling frequency of 500 Hz. The length of these signals is not uniform across the events in the datasets because of the varying vehicle's speed. For DAE input, the acceleration signals of each event are resampled into the spatial domain by multiplying signal in time by the vehicle's speed. Therefore, for each vehicle crossing the bridge of 15 m, 1500 samples are recorded. Therefore, the size of a dataset X, for either tractor ($\ddot{u}_{b1}$) or trailer ($\ddot{u}_{b2}$), is 1000 × 1500. Each dataset is normalized using Eq. (13) for better reconstruction performance of DAE[47].

$$X_n = \frac{X - \mu_X}{\sigma_X} \tag{13}$$

where X_n is the normalized dataset, while μ_X and σ_X is the mean and standard deviation of the original data set X.

3.3. Configuration of DAE

The architecture of DAE is designed by using TensorFlow modules, and the implementation code is developed using python 3.7. The configuration of the autoencoder model was selected based on lowest reconstruction loss after an extensive trial and error process. The detail of different model configurations and parameters used in trial and error

Table 1
Different network architectures and hyper-parameters used for model selection.

Architecture	Latent size	Activation function	L_2 regularization
conv.-latent-conv. [{4,6,8}-1- {4,6,8}]	{8,16,32,64}	{tanh, ReLU, leaky-ReLU}	$\{10^{-2},10^{-4},10^{-6}\}$
conv.-LSTM-latent-conv. [{4,6,8}-{1,2,3}-1-{4,6,8}]	{8,16,32,64}	{tanh, ReLU, leaky-ReLU}	$\{10^{-2},10^{-4},10^{-6}\}$

*conv: convolutional block, LSTM: Long short-term memory layers.

Table 2
Architecture of proposed deep autoencoder.

Layers	Output shape	Kernel size	Activation
Encoder			
Input	(1500 × 1)	–	–
Conv_1D	(1500 × 256)	1 × 7	Leaky-ReLU
Max-pooling	(500 × 256)	1 × 7	–
Conv_1D	(500 × 128)	1 × 5	Leaky-ReLU
Max-pooling	(250 × 128)	1 × 5	–
Conv_1D	(125 × 64)	1 × 3	Leaky-ReLU
Max-pooling	(125 × 64)	1 × 3	–
Conv_1D	(125 × 32)	1 × 3	Leaky-ReLU
LSTM	(125 × 32)	–	Leaky-ReLU
LSTM	(125 × 32)	–	Leaky-ReLU
Flattened	(2000)	–	–
Fully connected	(16)	–	Leaky-ReLU
Decoder			
Fully connected	(4000)	–	Leaky-ReLU
Reshape	(125 × 32)	–	–
Conv_1D	(125 × 64)	1 × 3	Leaky-ReLU
Up-sampling	(250 × 64)	1 × 3	–
Conv_1D	(250 × 128)	1 × 3	Leaky-ReLU
Up-sampling	(500 × 128)	1 × 3	–
Conv_1D	(500 × 256)	1 × 3	Leaky-ReLU
Up-sampling	(1500 × 256)	1 × 3	–
Output	(1500 × 1)	–	Linear

*Conv_1D: 1-Dimenasional convolutional layer, Leaky ReLU: Leaky-Retified linear unit, LSTM: Long short-term memory

process is summarized in Table 1. The final architecture's encoder module includes an input layer, four convolutional blocks, two LSTM layers, and fully connected layers. Each convolutional block has a 1D convolutional layer and a max-pooling layer followed by Leaky-ReLU as an activation function. For the decoder module, the same number of convolutional blocks is used as in encoder but in the reverse direction. In the decoder module, a max-pooling layer is replaced with up-sampling layer and at the output layer linear activation function is used. For robust model performance and to avoid overfitting, a regularization term is used as an additional hyperparameter. The regularization term applies penalties on weight parameters of the layers. In the proposed model, L_2 regularization is applied at the bottleneck layer with the value of 1×10^{-4}. The detailed architecture of the proposed DAE with different hyperparameters (activation function, filters and kernel size) is

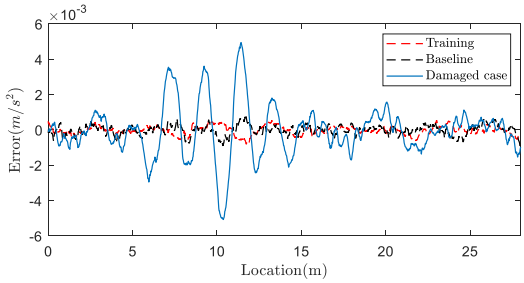

Fig. 6. Comparison of the difference between measured and reconstructed signals for three different vehicle-crossing events.

shown in Table 2. For evaluation of proposed method in subsequent sections same hyperparameters would be used for all scenarios.

The learning and decay rates are set to 0.001 and 0.0001 respectively for model optimization and training, adaptive moment estimation (Adam) with a batch size of 64 samples is considered. For efficient training, early stopping criteria is added to the network, which stops the training when the model achieves the loss criteria of 1×10^{-6} or 1500 epochs. All models training and numerical computations are performed on a standard PC with Intel Core i9-10900 K CPUs with 64 GB RAM and NVIDIA GTX 2080Ti graphic card.

4. Damage detection using DAE

This section evaluates the DAE for damage detection using Scenario-1, in which the crossing event correspond to a fleet of similar vehicles as discussed in Section 3.2. For this demonstration, the DAE model is trained with the acceleration responses from the tractor of the vehicles ($\ddot{u}_{b1}$). For training, the dataset is divided into 700 and 300 vehicle-crossing events for training and validation respectively. After training, the model achieves mean squared errors of 1.2908×10^{-6} and 1.2119×10^{-6} for training and validation data. The total training time was 1 h and 16 min. To demonstrate how the trained model can be used for damage detection, seven new datasets with different damage severities are generated for Scenario-1, in which the damage is modelled as a stiffness reduction of a single beam element. The details for the different damage cases (DC) are:

- Baseline: Dataset with no damage
- DC1: Dataset with 5% damage at midspan
- DC2: Dataset with 10% damage at midspan
- DC3: Dataset with 15% damage at midspan
- DC4: Dataset with 20% damage at midspan
- DC5: Dataset with 25% damage at midspan
- DC6: Dataset with 30% damage at midspan

To visualize the model's reconstruction performance, two random cases are illustrated for the baseline data (undamaged bridge) and

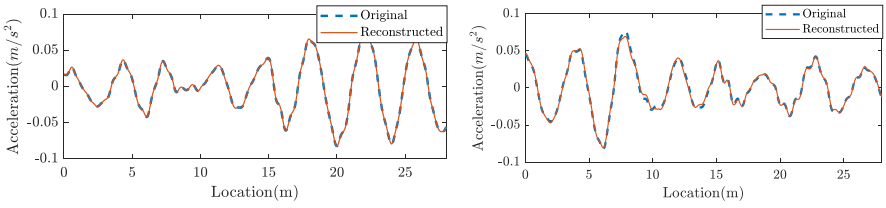

Fig. 5. Comparison of original and reconstructed vertical accelerations of two separate events for: (a) healthy and (b) damaged case.

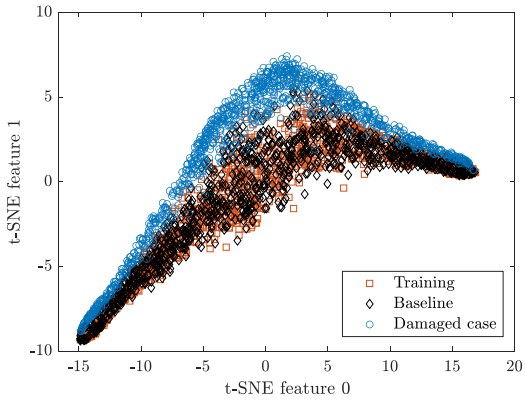

Fig. 7. Feature space visualization using t-SNE on the encoder output.

damage case (DC4). Fig. 5 shows the measured and predicted signals for two particular vehicle responses from different datasets. The trained DAE model is able to reconstruct the response for the healthy bridge case (Fig. 5(a)) with great accuracy, whereas for the damaged case (Fig. 5(b)) the match between measured and reconstructed signals is somewhat different. The proposed method exploits precisely this difference to detect damage. This reconstruction error shows large fluctuations between individual events but remains approximately constant when larger populations of events are analysed statistically.

To further quantify the loss in signal reconstruction, three particular vehicle-crossing events are investigated. The measured acceleration responses are compared to DAE's reconstructed response in Fig. 6 that shows the difference between both. The errors for vehicles from the training dataset and baseline are very small and almost the same, while for a damaged case event, the model could not reconstruct the response with the same accuracy. The reason for the higher reconstruction loss is due to the damage in the bridge. Then, the dynamic behaviour of the bridge changes, which leads to inaccuracies in vehicle response reconstruction. Because the DAE is trained only for the healthy condition, the model cannot reconstruct the response accurately when data from a damaged case is used.

The DAE model generalises the feature space into a continuous domain. This capability makes it possible to correctly predict the responses of events with different vehicle properties and travelling at different speeds, while at the same time distinguish changing bridge conditions. This is achieved because the encoder module in the DAE compresses the input data and transforms it into a latent space that generalises the feature space. To visualise this capability of the DAE model, the t-Distributed Stochastic Neighbour Embedding (t-SNE) is applied, which is used to compare high-dimensional datasets [61]. Fig. 7 shows a two-dimensional visualization of the feature space for the input data from three datasets (training, baseline, DC4). This confirms that the DAE model produces distinctive clusters for events with different damage conditions.

The studied example shows that it is possible to distinguish the structural condition by evaluating the reconstruction error for batches of events. To further illustrate this idea, Fig. 8 shows the histogram of the reconstruction errors in terms of MAE (Eq. (5)). The figure directly compares the distribution of errors of the baseline dataset with the different damage cases considered in this study (DC1 to DC6). The results show that as the damage increases, the mean absolute error distribution changes compared to the baseline. In the proposed method, this variation in the statistical distribution of different bridge conditions is exploited for damage detection and severity quantification.

In order to quantify the differences between batches of events, log-normal distributions are fitted to the histograms of mean absolute error. As shown in Fig. 8 the distribution of MAE is always positive, is skewed to the right and has a long tail because of outliers. The log-normal distribution has similar characteristics, namely a lower bound of zero and a positive skewness. Thus the log-normal distribution is deemed suitable for representation of the distribution of MAE. The statistical parameters of those fits are then used to define the damage index discussed in Section 2.3. Fig. 9 shows the fitted distributions to the results in Fig. 8. Each distribution has distinct statistical parameters (μ, σ) that are then used to compute the corresponding DI following Eq. (8).

5. Performance of damage detection method

This section evaluates the performance of the proposed damage detection method using vehicle responses for the two different scenarios

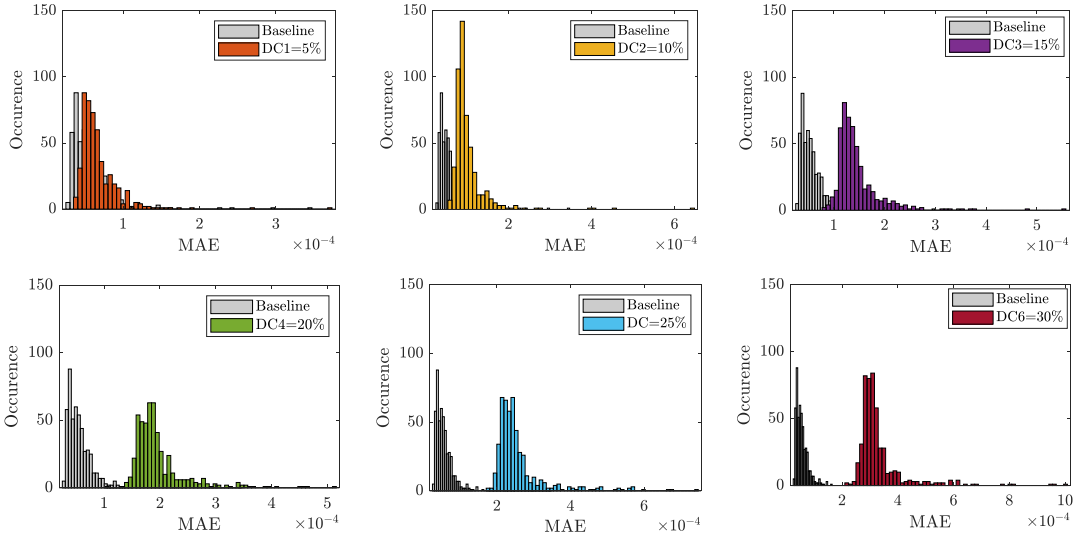

Fig. 8. Histogram of mean absolute error for batches of events for different bridge damage cases.

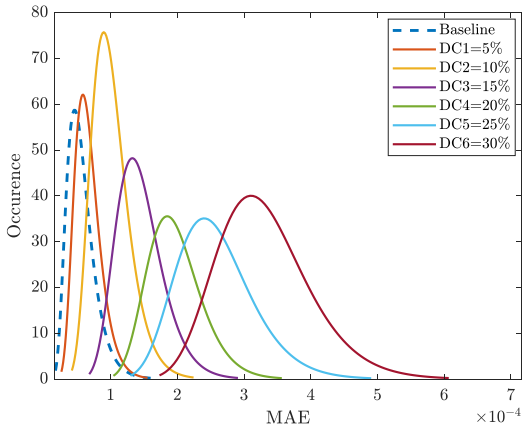

Fig. 9. Comparison of log-normal distributions of reconstruction loss for different damage cases.

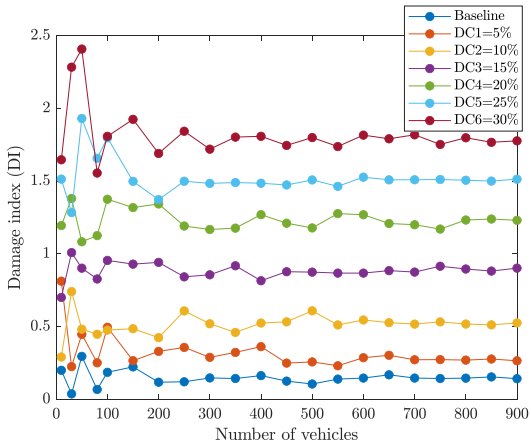

Fig. 11. Influence of batch size (number of vehicle-crossing events) in the calculation of the damage index.

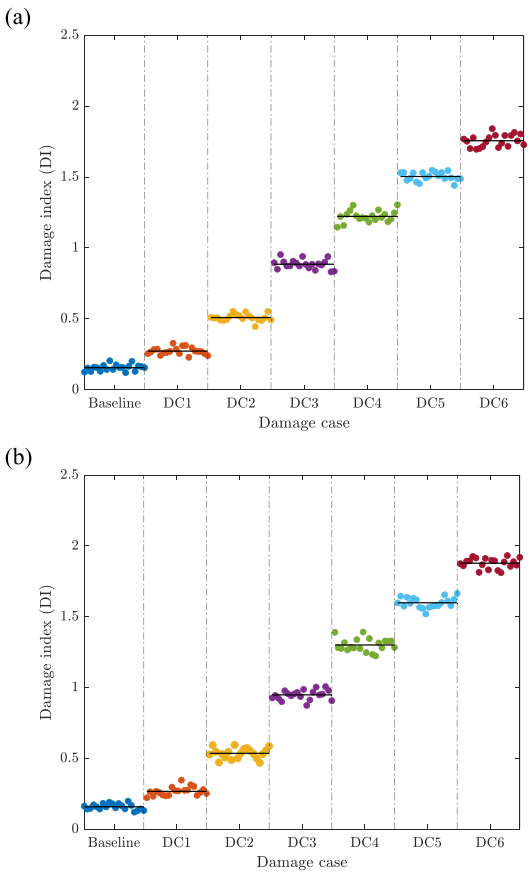

Fig. 10. Evolution of daily damage index (300 events/day) during progressive bridge condition change (every 20 days), for Scenario-1. Solid line indicates 20-day average value, using signals from: (a) tractor response (b) trailer response.

presented in Section 3.2. The analysis studies the sensitivity of the proposed damage index to damage severity and location. In addition, this section explores the influence of number of vehicles, their speeds and effect of measurement noise.

5.1. Damage detection for Scenario-1

This section illustrates how damage detection can be performed by using vehicle responses from a fleet of similar vehicles (Scenario-1) when there is a progressive bridge deterioration. This analysis assumes that for every given day, 300 vehicle-crossing events are available. The condition of the bridge is changed with increases of 5% damage severity every 20 days, starting from a perfectly healthy beam (baseline) until a 30% stiffness reduction at midspan (DC6). For comparison, this scenario is studied for acceleration responses from the tractor ($\ddot{u}_{b1}$) and the trailer ($\ddot{u}_{b2}$). Two separate DAE models are trained with acceleration responses from both locations on the vehicles.

Fig. 10 shows the damage index (DI) calculated using Eq. (8) for the discussed scenario. The DI values are distinctively different for different bridge conditions. In the case of the baseline, the magnitude of DI is small and close to zero. As the severity of the damage increases DI grows proportionally. The operational conditions and varying vehicle properties affect the magnitude of DI, which result in daily variations. However, for any given bridge condition the average value of the DI remains constant. The sensitivity of the index to the damage severity is clear, which allows the identification of damage even considering the daily dispersion in results. Therefore, it is evident that the proposed method can successfully be used to monitor the evolution in time of the condition of a bridge.

Fig. 10 also allows for a direct comparison of the damage detection method using signals from different locations in the vehicles. While the results in Fig. 10(a) come from the analysis of the vertical accelerations in the tractors, Fig. 10(b) shows the same analysis but based on the signals recorded on the trailers. Both sources of vehicle responses yield similar results in terms of sensitivity and variability of the DI. Therefore, in subsequent studies in this section only the tractor response ($\ddot{u}_{b1}$) will be considered.

5.1.1. Influence of the number of vehicles

The robustness and accuracy of the proposed method depends on the number of vehicles considered for a given batch of events. The damage index (Eq. (8)) directly relates to the probability distribution of the reconstruction error (MAE). Errors for individual events usually

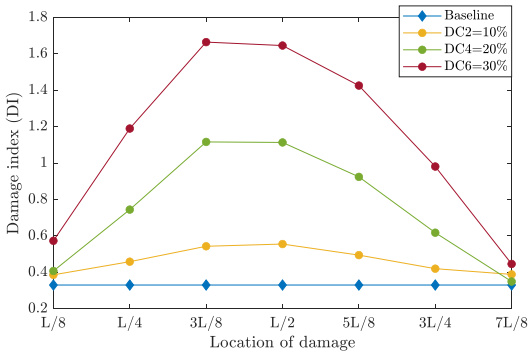

Fig. 12. Effect on damage index of different bridge damage locations (Scenario-1).

fluctuate because of operational effects and varying vehicle properties, but the distribution of errors tends to a remain fixed. The characterization of that distribution is more precise when larger the number of events considered in its calculation. As shown in Fig. 11, the damage index fluctuates quite significantly for small fleet sizes. However, with increasing number of vehicles, variations in DI decrease. This shows that for a sufficiently large fleet size, the effect of operational conditions can be reduced. In this study a batch size of 250 vehicle-crossing events are deemed appropriate because it results in sufficiently small variations in DI.

5.1.2. *Influence of location*

In practical cases, the location of damage can be anywhere along the bridge's length and it has been often reported that it is difficult to detect damage close to the bridge's supports under realistic vehicle and operational conditions [7]. In vibration-based damage detection methods, the sensitivity to damage depends on the location. For instance, in the case of a damage close to the bridge support the variation in frequencies (mainly the lower frequencies) would be much less compared to the case with midspan damage. To detect the damage at different locations of the beam it is important to consider the full spectra of the signals. The proposed method considers time series responses, which include the complete frequency content, that enables the damage detection at different locations, to some extent.

To illustrate the robustness and accuracy of the proposed method, damage identification is conducted for different beam damage locations. The trained model for Scenario-1 is considered with batch sizes of 250 vehicle-crossing events. Fig. 12 shows the sensitivity of DI for damage cases at seven different locations along the beam. The variation in magnitude of the damage index for locations between $L/4$ and$3L/4$ is significant and comparable in order of magnitude to results at $L/2$. In case of locations closer to the supports ($L/8$ and $7L/8$) the magnitude of damage index for low damage severity cases is not distinguishable. However, if larger batch sizes were considered the robustness of the method increases. Then it would be possible to consistently distinguish smaller variations of DI due to damages near the supports.

5.1.3. *Effect of vehicle speed*

In vehicle assisted damage assessment, speed and mass of traversing vehicle is critical in the presence of road surface. Previously published studies [7,27] have shown that vehicles with relatively small masses travelling at high speeds cannot detect damage with sufficient accuracy. This is mainly due to the short duration of the vehicle signals, hence a poor resolution in the frequency domain, but also due to low levels of bridge excitation and the presence of road profile. In lightweight vehicles at high speeds, the bridge response component is masked by the dynamic effects induced by the road profile. Compared to that,

Table 3
Vehicle speed variability (in km/h).

Dataset name	Min.	Max.	Mean	SD
Dataset V1	25	40	36	7
Dataset V2	40	70	55	7
Dataset V3	70	120	90	7

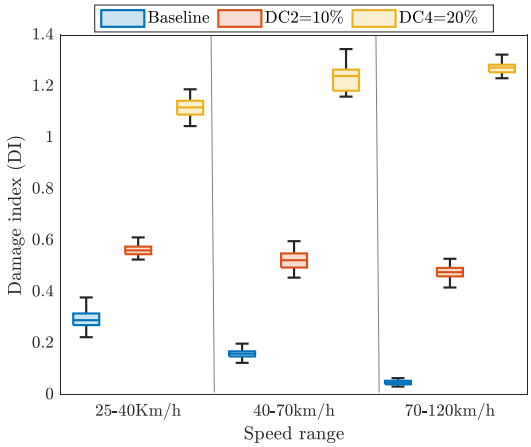

Fig. 13. Damage index performance comparison for different speed ranges.

heavyweight vehicles can sufficiently excite the bridge and are therefore considered more suitable for indirect bridge monitoring [34]. However, the amount of dynamic interaction between vehicle and bridge depends on the traversing speed. To study the effect of vehicle speed, three different speed ranges are studied for Scenario-1. New datasets are generated with the same properties as shown in Table A1 of the appendix except for the vehicle speeds. For each new dataset, the vehicle speeds are randomly sampled following normal distributions defined by the values provided in Table 3. Three DAE models are trained using tractor accelerations ($\ddot{u}_{b1}$), one for each new dataset. The trained models have tested against the baseline and two damage cases (DC2 and DC4). To consider the uncertainty in operational conditions (number of vehicle's, road profile etc) 20 randomly selected fleet size is considered from range of 200 to 400.

Fig. 13 compares the damage index distributions for three damage cases (baseline, DC2 and DC4) for three speed ranges (using datasets V1, V2 and V3). The comparison is done using a box plot representation, which shows the 25th and 75th percentile values in a box together with the median value and indicates the maximum and minimum results of the DI distribution. The results in all speed ranges allow for the clear distinction between healthy and damaged cases. It also shows that at lower speed the performance of the trained model is less accurate than at higher speeds. The magnitude of the damage index for the baseline condition shows that at lower speeds the feature space is not well generalised for the damage-sensitive features, compared to higher speeds. The physical interpretation on why damage detection is more robust at higher speed might be in the relative magnitudes between static and dynamic components of the bridge response. At lower speeds the bridge behaviour captured by the vehicle response is dominated by the quasi-static component. Only a small proportion of energy is present at the bridge frequencies, which are therefore hardly captured by the passing vehicle. It is found the proposed damage detection method performs well using responses of vehicles travelling at normal operational speeds.

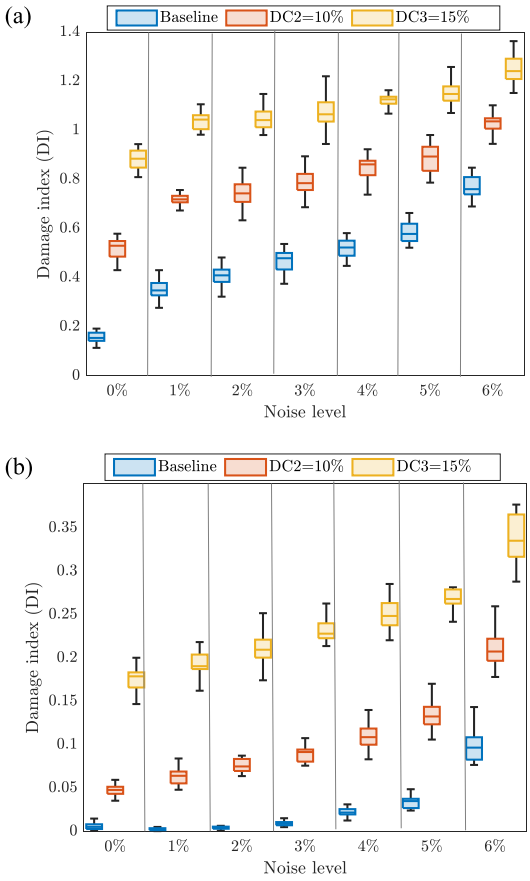

Fig. 14. Effect of measurement noise on the sensitivity of the damage index: (a) noise-free; (b) with noise.

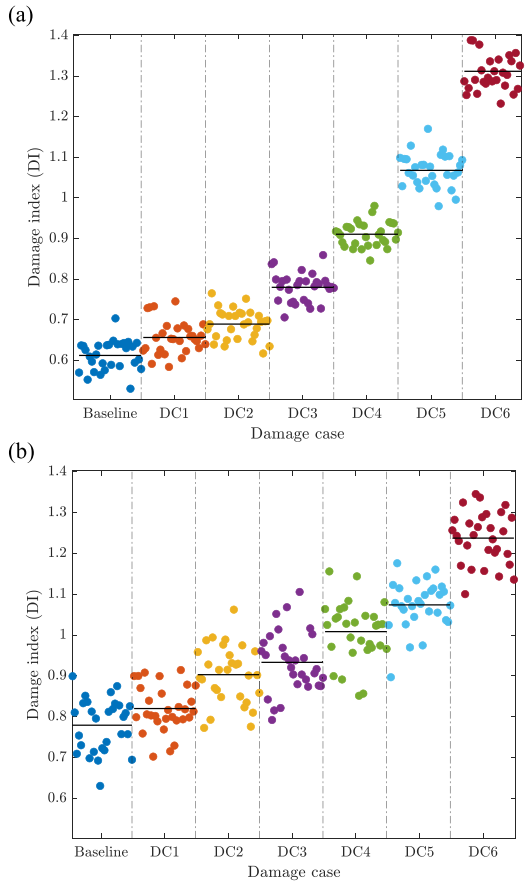

Fig. 15. Evolution of daily damage index (450 events/day) during progressive bridge condition change (every 30 days), for Scenario-2. Solid line indicates 30-day average value, using signals from: (a) tractor response (b) trailer response.

5.1.4. *Influence of measurement noise*

This section presents the sensitivity and performance of the proposed damage detection method to measurement noise. In order to analyse the effect of noise, two separate datasets of 1000 vehicle-crossing events are considered. Dataset N1 was formed by noise-free samples and dataset N2 by adding normally distributed noise. Noise in acceleration response ($\ddot{u}_{b1,noise}$) is defined according to Eq. (14), for an equivalent nose level E_{level}.

$$\ddot{u}_{b1,noise} = \ddot{u}_{b1} + E_{level} \cdot N_{noise} \cdot \sigma(\ddot{u}_{b1}) \tag{14}$$

where, N_{noise} is a vector of standard normal distribution $N(0,1)$ and $\sigma(\ddot{u}_{b1})$ is the standard deviation of the measured response. In dataset N2, the noise level for each event is randomly sampled for E_{level} $N(2.5, 0.5)$ with value in the range $[0, 5]$. Both datasets (N1 and N2) are trained using the architecture and hyperparameters discussed in Section 3.3. The trained models are then tested for three damage conditions (baseline, DC2 and DC3) by including a variations in noise levels E_{level} (noise-free or 0%, 1%, 2%, 3%, 4%, 5% and 6%). For each noise level to consider the statistical uncertainties because of operational variabilities 20 repeated simulation are computed with randomly selected fleet size from range of 200 to 400.

The noise sensitivity analysis of the proposed damage index (DI) for the two datasets is presented in Fig. 14. The results from both datasets clearly show that different levels of damages are separable even when including large noise magnitudes in the signals. For dataset N1, when the model is trained with noise-free samples and tested with different noise levels, DI increases linearly with the increase in noise level (Fig. 14 (a)). It shows that the trained model starts overfitting with increases in noise and that variations in the noise level at baseline condition could be interpreted as damage. However, Fig. 14(b) shows the results of the same model but trained with dataset N2. The magnitude of DI for baseline condition remains approximately constant for a range of different noise levels compared to the noise-free model. The introduction of noise levels during the training process helped the DAE model to generalise the latent feature for healthy conditions under uncertainty. From these results, it can be said that the introduction of uncertainty in the form of measurement noise during model training results in a more stable performance for the baseline condition.

5.2. *Damage detection for Scenario-2*

This section discusses the damage assessment performance of the proposed method for Scenario-2, i.e. a more challenging scenario that uses a broader range of vehicle properties (as described in Section 3.2). For Scenario-2, separate DAE models are trained for both tractor and trailer responses of the vehicles. The trained models are tested for the damage cases discussed in Section 4, with the only difference that each

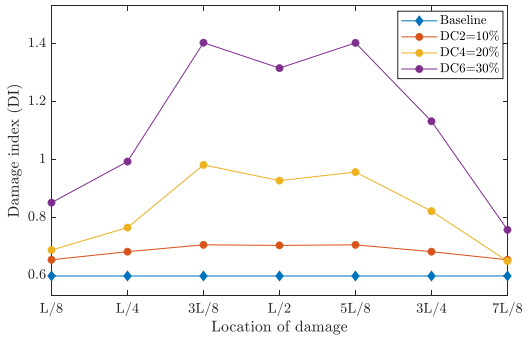

Fig. 16. Effect on damage index for different location of the bridge (Scenario-2).

case is simulated for the dataset of Scenario-2. Because of the inherent broader variability of the vehicle properties, the damage detection method benefits of larger sets of data. This is why 450 vehicles/day and intervals of 30 days are considered to illustrate the performance of the method, where the damage intensity is increased in 5% increments after 30 days. The results in terms of DI are shown in Fig. 15.

It is evident from Fig. 15, when compared to Scenario-1, that the daily variation in DI and the magnitude of DI for baseline condition are much higher. The trained models cannot fully generalise the latent space for damage sensitive features to accommodate the large variation in vehicles properties. However, the average value after 30 days is more robust and can easily distinguish different damage cases. Furthermore, as can be observed in Fig. 15(a), the daily fluctuation in DI when using the tractor signals is much less than for the model using the trailer signals Fig. 15(b). This significant difference between model results can be attributed to the inherent larger variability in properties of trailers. More in particular, trailers can vary considerably in dimensions, mass, and inertia properties, factors that have been accounted for during the random vehicle generation for Scenario-2. Therefore, the DAE model has more difficulties discerning damage sensitive features when using trailer responses, which in theory could be improved by increasing the number of events.

5.2.1. *Influence of location*

Finally, this section evaluates the sensitivity of the proposed method to damage location under the conditions of Scenario-2. Seven damage locations along the beam have been studied for different levels of damage severity. The trained model for tractor response is used with a batch size of 450 vehicles. Fig. 16 shows the damage index values for baseline condition and three damage cases (DC2, DC4, and DC 6). The magnitude of DI changes quite significantly for different locations. However, for a given damage location it is possible discern a healthy bridge (baseline) from a damaged one. The proposed method has clear damage detection capabilities, and since it is sensitive to damage location it could potentially be further developed to a damage localisation tool.

In summary, it is shown that the proposed method can be used effectively for damage assessment using multiple vehicles responses. A DAE can be implemented that finds an adequate generalisation of the feature space together with damage sensitive features provided that enough data for training is available.

Table 4
Bridge model properties and first three fundamental frequencies.

Symbol	Description	Value
L	Total span length (m)	89
E	Young's modulus (N/m^2)	$3.5 \cdot 10^{10}$
I	Second moment of area (m^4)	1.3427
A	Cross section area (m^2)	5.6180
ρ	Mass per unit length (kg/m)	2500
$k_{r,\,(1,2,3)}$	Rotational stiffness for supports (Nm/rad)	$4.5 \cdot 10^9$
$k_{v,\,(1,2,3)}$	Vertical stiffness for supports (N/m)	$3.5 \cdot 10^{10}$
ζ	Damping (%)	2
$f_{1,2,3}$ *(model)*	First three calculated frequencies (Hz)	[4.91, 6.54, 13.45]
$f_{1,2,3}$ [62]	First three measured frequencies (Hz)	[4.91, 6.53, 12.84]

6. Performance validation on multi-span bridge

This section evaluates the performance of the proposed method simulating the behaviour of an existing multi-span continuous highway bridge. Furthermore, this study is extended to evaluate the effect of additional random traffic and its influence on the sensitivity of proposed damage index.

6.1. *Voigt Drive I-5 bridge*

The Voigt Drive I-5 bridge is located on the Eastern edge of the University of California, San Diego (UCSD). The four span reinforced concrete box girder structure is 89 m long and constitutes a typical large highway overpass. More details on the structure's properties, dimensions and configuration can be found in [62]. The bridge is modelled here as a multi-span continuous beam. The section properties of the beam are computed from the cross-section dimensions of the real bridge. The intermediate supports are modelled using vertical and rotational springs, as shown in Fig. 17. The values of the support springs are manually tunned to match the first three natural frequencies reported in [62].

Table 4 lists the final section and material properties and the first three natural frequencies of the model compared to the measured bridge frequencies.

In line with the studies performed in previous sections, the finite element model of the bridge is made of 0.5 m long elements (178 elements in total). A similar carpet road profile of class 'A' is included on bridge and vehicle's path, with a 100 m approach distance (as discussed in section 3.1.2). The coupled vehicle-bridge interaction model is solved using Eq. (12) to extract vehicle body acceleration responses.

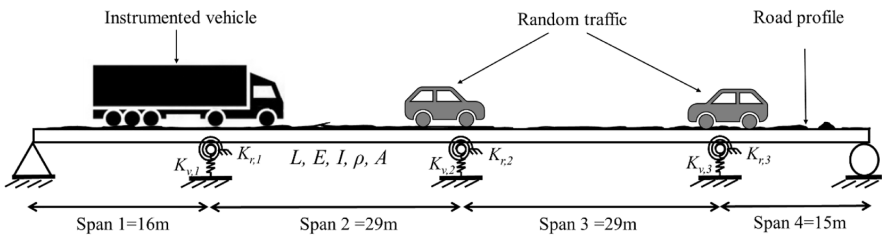

Fig. 17. Model of Voigt Drive I-5 bridge with instrumented vehicle and random traffic.

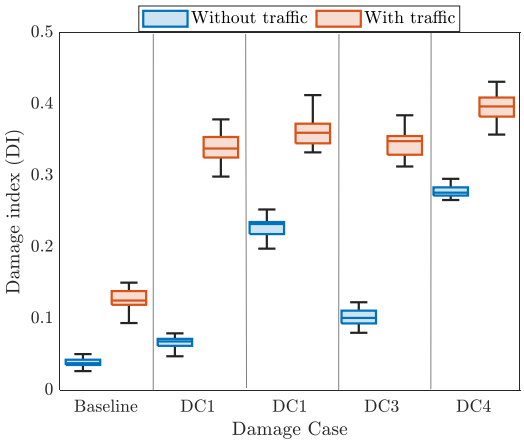

Fig. 18. Damage index performance comparison for multi-span bridge considering without traffic and with traffic.

6.2. Data generation and DAE training

To examine the sensitivity of the proposed damage index on the multi-span continuous bridge, two new scenarios are studied. One scenario consists of single 5-axle truck crossing events, which is subsequently referred to as 'Without traffic'. On the other hand, the second new scenario includes additional random traffic on the bridge, which is termed 'With traffic'. The dataset for both scenarios was generated by solving the vehicle-bridge interaction system presented in Section 3.1. For dataset generation the statistical variabilities of the 5-axle truck parameters remained the same as for Scenario-1 discussed in Section 3.2. However, for modelling the additional random traffic on the bridge for the 'With traffic' scenario, two 2-axle vehicles are included in the crossing event as shown in Fig. 19. These additional vehicles are assigned randomly sampled properties within a Monte Carlo simulation, allowing the vehicles to enter randomly from either left or right side of the bridge. Additional details on the 2-axle vehicle model and their statistical variabilities are provided in Table A2 in the Appendix.

For each new scenario batches, of 1000 vehicle events are created. Each dataset contains the vertical acceleration response from tractor ($\ddot{u}_{b1}$) and vehicle speed (v) of the traversing 5-axle truck. Each dataset is resampled from time-domain to space-domain to compute fixed length vectors with 1500 samples. A random sampled noise level of $E_{level}\ N(2.5, 0.5)$ with value in the range $[0, 5]$ is added to the datasets using Eq. (14). The DAE model with the same configuration and hyperparameters as discussed in Section 3.3 is used to train the model for a healthy bridge condition. The datasets are divided into 700 and 300 vehicle crossing events respectively for training and validation of the model.

To investigate the performance of the DAE and the sensitivity of the damage index, five new damage cases are defined. The type of damage and their location of each damage case are:

- Baseline: Healthy bridge
- DC1: 30% mid-span stiffness reduction on span 1 (at 8.5 m of the bridge)
- DC2: 30% mid-span stiffness reduction on span 2 (at 31 m of the bridge)
- DC3: 30% rotational stiffness ($k_{r,1}$) reduction at support 1
- DC4: 30% rotational stiffness ($k_{r,2}$) reduction at support 2

6.3. Damage detection for multi-span bridge

The five new damage cases are investigated for both new scenarios ('Without traffic" and 'With traffic') to assess the performance of the proposed method. For each damage case, 20 repeated simulation are computed with randomly selected fleet sizes ranging from 400 to 500 events. Then, as in Section 5, the distribution of the reconstruction loss is computed using Eq. (5) and the statistical parameters of fitted distributions are further used to compute the Damage index (DI) with Eq. (7).

Fig. 18 shows the damage sensitivity analysis for both new scenarios and the five new damage cases for the multi-span continuous bridge. The results suggest that in both scenarios, there is a clear distinction between baseline and damage cases. However, it is also evident from the figure that for the scenario with additional random traffic the severity comparison of different damage cases is relatively poor, compared to the scenario when no traffic is present on the bridge. This is because the trained model cannot fully generalise the latent space for damage sensitive features to accommodate the contribution of excitations from additional random traffic vehicles. However, broadly speaking this problem could be resolved by fine tuning the DAE model's hyperparameters and increasing the training dataset. Nevertheless, aside from the performance degradation of the method when considering additional random traffic, the proposed method can clearly detect and quantify the severity of damages for the multi-span bridge model for all other cases. Therefore, the results suggest that the proposed method can be used for a wide range of structural configurations, making it a potentially useful approach for network-wide road bridge monitoring.

7. Practical consideration for real-life application

The method proposed in this paper may be useful to monitor bridges and assess their condition. The method relies on the fact that local damage, resulting in local bending stiffness reductions, directly affect the modal properties of the bridge. These variations can be identified from the vertical acceleration signals recorded by the on-board sensors of the traversing vehicles. However, it is impossible to identify these variations solely using signals from single events, due to the inherent fluctuations under operational conditions (e.g. vehicle velocity, road profile and signal noise). Instead, this study proposes the use of signals from a fleet of vehicles to capture the variations in bridge behaviour. The collected signals from multiple vehicles could then be used to extract the bridge dynamic features using DAE.

However, there exist multiple challenges for the practical implementation of the proposed method, including signal collection and synchronization, variable vehicle speed, threshold definition and other loads (wind, earthquake, temperature). Each of these challenges could potentially be adequately addressed by fully utilizing existing technologies.

Arguably, the main challenge to apply the proposed method is the collection of the necessary signals and related crossing event information from passing vehicles. However, this is gradually becoming a real possibility considering the current trends in the transport industry. Modern trucks are getting an increasing number of built-in sensors, which could include (if not already) also sensors measuring the vertical acceleration of the tractor. While entry and exit times of the vehicle on the bridge can be determined via global positioning systems. Furthermore, many truck vendors offer also comprehensive fleet management system solutions that could seamlessly accommodate the gathered information. In turn, this information can be used to devise correction measures on operational conditions such as variable vehicle speed or individual truck mechanical properties. In such a near future scenario, a fleet of transport trucks that regularly roam the road network would provide a reliable and abundant source of information to put the proposed idea into practice.

On the other hand, bridges are subjected not only to traffic loading but also to other types of actions. It is generally known that ambient

Table A1
5-axle truck model parameters.

5-Axle-truck	Scenario-1				Scenario-2			
Parameters	Min.	Max.	Mean	SD	Min.	Max.	Mean	SD
Mass (kg)								
Tractor body m_{b1}	2800	3400	3100	80	2500	4000	3200	250
Trailor body m_{b2}	15,000	25,000	20,000	1000	10,000	40,000	25,000	4500
Tractor axles m_{u1}, m_{u2}	500	1000	750	30	300	1000	600	100
Trailer axles m_{u3}, m_{u4}, m_{u5}	800	1400	1100	50	600	1600	1100	100
Moment of inertia (kg·m^2)								
Tractor body I_{b1}	4250	5500	4875	50	4000	5800	4900	150
Trailer body I_{b2}	112,000	135,000	123,000	2500	106,000	140,000	123,000	6000
Viscous damping (N·s/m)								
Front suspensions C_{s1}, C_{s2}	$1.0 \cdot 10^4$	$8.0 \cdot 10^4$	$4.0 \cdot 10^4$	$0.5 \cdot 10^4$	$1 \cdot 10^4$	$12 \cdot 10^4$	$6 \cdot 10^4$	$2 \cdot 10^4$
Rear suspensions C_{s3}, C_{s4}, C_{s5}	$2 \cdot 10^5$	$16 \cdot 10^5$	$8 \cdot 10^4$	$1 \cdot 10^4$	$2 \cdot 10^4$	$24 \cdot 10^4$	$12 \cdot 10^4$	$4 \cdot 10^4$
Spring stiffness (N/m)								
Front suspensions K_{s1}, K_{s2}	$4.0 \cdot 10^6$	$8.0 \cdot 10^6$	$6.0 \cdot 10^6$	$0.5 \cdot 10^6$	$1 \cdot 10^6$	$12 \cdot 10^6$	$6 \cdot 10^6$	$1 \cdot 10^6$
Rear suspensions K_{s3}, K_{s4}, K_{s5}	$5.0 \cdot 10^6$	$15 \cdot 10^6$	$10 \cdot 10^6$	$0.5 \cdot 10^6$	$2.5 \cdot 10^6$	$15.0 \cdot 10^6$	$10.0 \cdot 10^6$	$2.0 \cdot 10^6$
Front tyre K_{t1}, K_{t2}	$1.25 \cdot 10^6$	$2.25 \cdot 10^6$	$1.75 \cdot 10^6$	$0.20 \cdot 10^6$	$1.0 \cdot 10^6$	$4.0 \cdot 10^6$	$2.0 \cdot 10^6$	$0.7 \cdot 10^6$
Rear tyre K_{t3}, K_{t4}, K_{t5}	$2.75 \cdot 10^6$	$4.75 \cdot 10^6$	$3.50 \cdot 10^6$	$0.20 \cdot 10^6$	$2.0 \cdot 10^6$	$8.0 \cdot 10^6$	$4.0 \cdot 10^6$	$1.0 \cdot 10^6$
Geometry (m)								
D_1	–	–	5	–	3.5	6.5	5.0	0.1
D_2	–	–	4	–	3.0	5.0	4.0	0.02
e_1	–	–	−1.09	–	−0.50	−1.20	−0.80	−0.01
e_2	–	–	3.5	–	3.00	4.00	3.50	0.05
e_3	–	–	1.2	–	–	–	1.2	–
e_4	–	–	2.2	–	–	–	2.2	–
e_5	–	–	3.2	–	–	–	3.2	–
Velocity (km/h)								
Velocity v	36	60	40	5	36	60	40	8

temperature fluctuations produce variations in the modal properties of bridges. Also, wind loading can be an important source of dynamic excitation, particularly on longer bridges. These effects could be compensated using dedicated sensors on the bridge to monitor these loads or utilizing the information available from nearby weather stations. In case of seismic activity, the duration of this exceptional load is very short. Any vehicle crossing event during earthquake excitation could be discarded without affecting the overall performance of the proposed method. However, if some damage occurs as result of an earthquake, the proposed method could be used to detect that damage.

Moreover, to implement a successful structural health monitoring system based on the proposed method, it is required to identify adequate thresholds for the damage index. The system has to identify potential damage occurrences while minimizing the number of false alarms. This challenge can be tackled using statistical techniques on the continuous stream of calculated damage indicators from each individual event. Over time, the study of statistical moments (mean and standard deviations) would provide indications of normal damage index values under operational conditions. Then large deviations on the damage index would indicate significant variations in the structural behaviour that could be attributed to a possible damage.

8. Conclusion

This study proposed a damage assessment technique based on deep learning and a statistical distribution-based damage index. The suggested SHM method uses the acceleration responses from multiple traversing vehicles over the target bridge. The major challenge in damage detection using the response from several different vehicles is to generalise the relationship between vehicle responses and bridge dynamics. To address this issue, this paper used deep autoencoders (DAE) architecture, considering multiple convolutional layers and LSTM layers for dimensionality reduction. The DAE is trained for healthy (or existing) bridge conditions, which constructs a feature space that is sensitive to bridge dynamics and robust enough against measurement noise and operational conditions. Moreover, the errors between measured and reconstructed signals are characterized by distributions that are sensitive to bridge damage. The damage index based on the KL divergence of these distributions can be used for damage detection and severity quantification.

The proposed method's effectiveness is evaluated numerically with a 5-axle truck vehicle model traversing a simply supported bridge and multi-span continuous bridge. Two scenarios are considered based on the level of variability in vehicle properties and operational conditions for simply supported beam model. Similarly, for multi-span bridge model, effect of random traffic is also considered. The results show that the outlined method is able to detect damage successfully, providing robust results under operational conditions (road profile, vehicle properties variability and measurement noise). In conclusion, the proposed method has potential to become a practical tool as it removes the need of specialised vehicles for long-term bridge monitoring. Additionally, the proposed method can easily be integrated with an intelligent transport network and can be used as a cost-effective solution for bridge health monitoring.

CRediT authorship contribution statement

Muhammad Zohaib Sarwar: Conceptualization, Methodology, Software, Formal analysis, Writing – original draft. **Daniel Cantero:** Conceptualization, Supervision, Software, Writing – review & editing.

Declaration of Competing Interest

The authors declare that they have no known competing financial

Table A2
2-axle vehicle model parameters.

2-Axle-vehicle	'With traffic' scenario			
Parameters	Min.	Max.	Mean	SD
Mass (kg)				
Body mass m_b	5000	16,000	10,500	500
Tractor axles m_{s1}, m_{s2}	600	1200	900	100
Moment of inertia (kg·m^2)				
Body I_b	45,000	65,000	53,651	2000
Viscous damping (N·s/m)				
Front suspensions C_{s1}, C_{s2}	$0.5 \cdot 10^4$	$1.5 \cdot 10^4$	$1.0 \cdot 10^4$	$0.2 \cdot 10^4$
Spring stiffness (N/m)				
Front suspensions K_{s1}, K_{s2}	$4.0 \cdot 10^6$	$8.0 \cdot 10^6$	$6.0 \cdot 10^6$	$0.5 \cdot 10^6$
Front tyre K_{t1}, K_{t2}	$1.25 \cdot 10^6$	$2.25 \cdot 10^6$	$1.75 \cdot 10^6$	$0.20 \cdot 10^6$
Axle spacing (m)				
e_1	4	9	–	–
Velocity (km/h)				
Velocity v	40	70	55	5

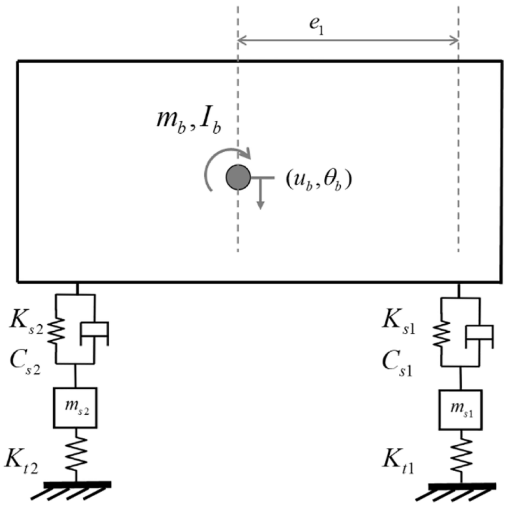

Fig. 19. 2-axle vehicle model.

interests or personal relationships that could have appeared to influence the work reported in this paper.

Appendix

Table A1 provides the model parameters with their statistical variability for simulation of 5-axle truck as shown in Fig. 3. Monte Carlo simulation used the statistical variability of the parameter to generate the dataset for two scenarios. Table A2 provides the model parameters with their statistical variability of 2-axle vehicles as shown in Fig. 19, which are used in the 'With traffic' scenario in Section 6

References

[1] Jang S, Jo H, Cho S, Mechitov K, Rice JA, Sim S-H, et al. Structural health monitoring of a cable-stayed bridge using smart sensor technology: deployment and evaluation. Smart Struct Syst 2010;6:439–59. https://doi.org/10.12989/sss.2010.6.5_6.439.

[2] Spencer BF, Ruiz-Sandoval ME, Kurata N. Smart sensing technology: opportunities and challenges. Struct Control Health Monit 2004;11(4):349–68. https://doi.org/10.1002/stc.48.

[3] Spencer BF, Park J-W, Mechitov KA, Jo H, Agha G. Next Generation Wireless Smart Sensors Toward Sustainable Civil Infrastructure. Proc Eng 2017;171:5–13. https://doi.org/10.1016/j.proeng.2017.01.304.

[4] An Y, Chatzi E, Sim S-H, Laflamme S, Blachowski B, Ou J. Recent progress and future trends on damage identification methods for bridge structures. Struct Control Health Monitoring 2019;26(10). https://doi.org/10.1002/stc.2416.

[5] Casas JR, Moughty JJ. Bridge Damage Detection Based on Vibration Data: Past and New Developments. Front Built Environ 2017;3. https://doi.org/10.3389/fbuil.2017.00004.

[6] Çelebi M. Real-Time Seismic Monitoring of the New Cape Girardeau Bridge and Preliminary Analyses of Recorded Data: An Overview. Earthquake Spectra 2006;22(3):609–30. https://doi.org/10.1193/1.2219107.

[7] Yang YB, Wang Z-L, Shi K, Xu H, Wu YT. State-of-the-Art of Vehicle-Based Methods for Detecting Various Properties of Highway Bridges and Railway Tracks. Int J Str Stab Dyn 2020;20(13):2041004. https://doi.org/10.1142/S0219455420410047.

[8] Yang Y-B, Lin CW, Yau JD. Extracting bridge frequencies from the dynamic response of a passing vehicle. J Sound Vib 2004;272(3-5):471–93. https://doi.org/10.1016/S0022-460X(03)00378-X.

[9] Malekjafarian A, McGetrick PJ, OBrien EJ. A Review of Indirect Bridge Monitoring Using Passing Vehicles. Shock Vib 2015;2015:1–16. https://doi.org/10.1155/2015/286139.

[10] Matarazzo TJ, Kondor D, Santi P, Milardo S, Eshkevari SS, Pakzad SN, et al. Crowdsourcing Bridge Vital Signs with Smartphone Vehicle Trips. ArXiv: 201007026 [Physics]; 2020.

[11] Lin CW, Yang YB. Use of a passing vehicle to scan the fundamental bridge frequencies: An experimental verification. Eng Struct 2005;27(13):1865–78. https://doi.org/10.1016/j.engstruct.2005.06.016.

[12] Yang YB, Chang KC. Extracting the bridge frequencies indirectly from a passing vehicle: Parametric study. Eng Struct 2009;31(10):2448–59. https://doi.org/10.1016/j.engstruct.2009.06.001.

[13] Zhu L, Malekjafarian A. On the Use of Ensemble Empirical Mode Decomposition for the Identification of Bridge Frequency from the Responses Measured in a Passing Vehicle. Infrastructures 2019;4:32. https://doi.org/10.3390/infrastructures4020032.

[14] OBrien EJ, Malekjafarian A, González A. Application of empirical mode decomposition to drive-by bridge damage detection. Eur J Mech A Solids 2017;61:151–63. https://doi.org/10.1016/j.euromechsol.2016.09.009.

[15] Kildashti K, Makki Alamdari M, Kim CW, Gao W, Samali B. Drive-by-bridge inspection for damage identification in a cable-stayed bridge: Numerical investigations. Eng Struct 2020;223:110891. https://doi.org/10.1016/j.engstruct.2020.110891.

[16] Zhu XQ, Law SS. Wavelet-based crack identification of bridge beam from operational deflection time history. Int J Solids Struct 2006;43(7-8):2299–317. https://doi.org/10.1016/j.ijsolstr.2005.07.024.

[17] OBrien EJ, Malekjafarian A. A mode shape-based damage detection approach using laser measurement from a vehicle crossing a simply supported bridge. Struct Control Health Monitoring 2016;23(10):1273–86. https://doi.org/10.1002/stc.1841.

[18] Yang YB, Li YC, Chang KC. Constructing the mode shapes of a bridge from a passing vehicle: a theoretical study. Smart Struct Syst 2014;13:797–819. https://doi.org/10.12989/sss.2014.13.5.797.

[19] Malekjafarian A, OBrien EJ. On the use of a passing vehicle for the estimation of bridge mode shapes. J Sound Vibrat 2017;397:77–91. https://doi.org/10.1016/j.jsv.2017.02.051.

[20] Sadeghi Eshkevari S, Matarazzo TJ, Pakzad SN. Bridge modal identification using acceleration measurements within moving vehicles. Mech Syst Sig Process 2020;141:106733. https://doi.org/10.1016/j.ymssp.2020.106733.

[21] OBrien EJ, McGetrick PJ, Gonzalez A. A drive-by inspection system via vehicle moving force identification. Smart Struct Syst 2014;13:821–48. https://doi.org/10.12989/sss.2014.13.5.821.

[22] Quirke P, Bowe C, OBrien EJ, Cantero D, Antolin P, Goicolea JM. Railway bridge damage detection using vehicle-based inertial measurements and apparent profile. Eng Struct 2017;153:421–42. https://doi.org/10.1016/j.engstruct.2017.10.023.

[23] Zhu XQ, Law SS, Huang L, Zhu SY. Damage identification of supporting structures with a moving sensory system. J Sound Vib 2018;415:111–27. https://doi.org/10.1016/j.jsv.2017.11.032.

[24] Liu J, Bergés M, Bielak J, Garrett JH, Kovačević J, Noh HY. A damage localization and quantification algorithm for indirect structural health monitoring of bridges using multi-task learning. AIP Conf Proc 2019;2102:090003. https://doi.org/10.1063/1.5099821.

[25] Mei Q, Gül M, Boay M. Indirect health monitoring of bridges using Mel-frequency cepstral coefficients and principal component analysis. Mech Syst Sig Process 2019;119:523–46. https://doi.org/10.1016/j.ymssp.2018.10.006.

[26] Malekjafarian A, Golpayegani F, Moloney C, Clarke S. A Machine Learning Approach to Bridge-Damage Detection Using Responses Measured on a Passing Vehicle. Sensors (Basel) 2019;19. https://doi.org/10.3390/s19184035.

[27] Zhang B, Qian Y, Wu Y, Yang YB. An effective means for damage detection of bridges using the contact-point response of a moving test vehicle. J Sound Vib 2018;419:158–72. https://doi.org/10.1016/j.jsv.2018.01.015.

[28] Fitzgerald PC, Malekjafarian A, Cantero D, OBrien EJ, Prendergast LJ. Drive-by scour monitoring of railway bridges using a wavelet-based approach. Eng Struct 2019;191:1–11. https://doi.org/10.1016/j.engstruct.2019.04.046.

[29] McGetrick PJ, Kim C-W, González A, Brien EJO. Experimental validation of a drive-by stiffness identification method for bridge monitoring. Struct Health Monitoring 2015;14(4):317–31. https://doi.org/10.1177/1475921715578314.
[30] McGetrick PJ, Kim CW. A Parametric Study of a Drive by Bridge Inspection System Based on the Morlet Wavelet. Key Eng Mater 2013;569–570:262–9. https://doi.org/10.4028/www.scientific.net/KEM.569-570.262.
[31] Hester D, González A. A discussion on the merits and limitations of using drive-by monitoring to detect localised damage in a bridge. Mech Syst Sig Process 2017;90:234–53. https://doi.org/10.1016/j.ymssp.2016.12.012.
[32] Lederman G, Wang Z, Bielak J, Noh HY, Garrett J, Chen S, et al. Damage quantification and localization algorithms for indirect SHM of bridges. 2014. https://doi.org/10.1201/B17063-93.
[33] Liu J, Chen S, Bergés M, Bielak J, Garrett JH, Kovačević J, et al. Diagnosis algorithms for indirect structural health monitoring of a bridge model via dimensionality reduction. Mech Syst Sig Process 2020;136:106454. https://doi.org/10.1016/j.ymssp.2019.106454.
[34] Miyamoto A, Yabe A, Brühwiler E. A Vehicle-based Health Monitoring System for Short and Medium Span Bridges and Damage Detection Sensitivity. Proc Eng 2017;199:1955–63. https://doi.org/10.1016/j.proeng.2017.09.299.
[35] Locke W, Sybrandt J, Redmond L, Safro I, Atamturktur S. Using drive-by health monitoring to detect bridge damage considering environmental and operational effects. J Sound Vib 2020;468:115088. https://doi.org/10.1016/j.jsv.2019.115088.
[36] Relationship with the ITS Action Plan and ITS Directive | FRAME ARCHITECTURE n.d. https://frame-online.eu/frame-architecture/detailed-information/relationship-with-the-its-action-plan-and-its-directive (accessed January 3, 2021).
[37] Malekian R, Moloisane NR, Nair L, Maharaj BT, Chude-Okonkwo UAK. Design and Implementation of a Wireless OBD II Fleet Management System. IEEE Sens J 2017;17(4):1154–64. https://doi.org/10.1109/JSEN.2016.2631542.
[38] Billhardt H, Fernandez A, Lemus L, Lujak M, Osman N, Ossowski S, et al. Dynamic Coordination in Fleet Management Systems: Toward Smart Cyber Fleets. IEEE Intell Syst 2014;29(3):70–6. https://doi.org/10.1109/MIS.2014.41.
[39] Hinton GE, Salakhutdinov RR. Reducing the Dimensionality of Data with Neural Networks. Science 2006;313:504–7. https://doi.org/10.1126/science.1127647.
[40] Arel I, Rose DC, Karnowski TP. Deep Machine Learning - A New Frontier in Artificial Intelligence Research [Research Frontier]. IEEE Comput Intell Mag 2010;5(4):13–8. https://doi.org/10.1109/MCI.2010.938364.
[41] Schmidhuber J. Deep learning in neural networks: An overview. Neural Networks 2015;61:85–117. https://doi.org/10.1016/j.neunet.2014.09.003.
[42] Avci O, Abdeljaber O, Kiranyaz S, Hussein M, Gabbouj M, Inman DJ. A review of vibration-based damage detection in civil structures: From traditional methods to Machine Learning and Deep Learning applications. Mech Syst Sig Process 2021;147:107077. https://doi.org/10.1016/j.ymssp.2020.107077.
[43] Abdeljaber O, Avci O, Kiranyaz S, Gabbouj M, Inman DJ. Real-time vibration-based structural damage detection using one-dimensional convolutional neural networks. J Sound Vib 2017;388:154–70. https://doi.org/10.1016/j.jsv.2016.10.043.
[44] Ni F, Zhang J, Noori MN. Deep learning for data anomaly detection and data compression of a long-span suspension bridge. Comput-Aided Civ Infrastruct Eng 2020;35(7):685–700. https://doi.org/10.1111/mice:v35.710.1111/mice:12528.
[45] Zhang Y, Miyamori Y, Mikami S, Saito T. Vibration-based structural state identification by a 1-dimensional convolutional neural network. Comput-Aided Civ Infrastruct Eng 2019;34(9):822–39. https://doi.org/10.1111/mice:v34.910.1111/mice:12447.
[46] Wang Z, Cha Y-J. Unsupervised deep learning approach using a deep auto-encoder with an one-class support vector machine to detect structural damage. 1475921720934051 Struct Health Monitoring 2020. https://doi.org/10.1177/1475921720934051.
[47] Shang Z, Sun L, Xia Y, Zhang W. Vibration-based damage detection for bridges by deep convolutional denoising autoencoder. Struct Health Monitoring 2021;20(4):1880–903. https://doi.org/10.1177/1475921720942836.
[48] Sony S, Dunphy K, Sadhu A, Capretz M. A systematic review of convolutional neural network-based structural condition assessment techniques. Eng Struct 2021;226:111347. https://doi.org/10.1016/j.engstruct.2020.111347.
[49] Zhang Q, Barri K, Babanajad SK, Alavi AH. Real-Time Detection of Cracks on Concrete Bridge Decks Using Deep Learning in the Frequency Domain. Engineering 2020. https://doi.org/10.1016/j.eng.2020.07.026
[50] Liu T, Li Z, Yu C, Qin Y. NIRS feature extraction based on deep auto-encoder neural network. Infrared Phys Technol 2017;87:124–8. https://doi.org/10.1016/j.infrared.2017.07.015.
[51] Pascanu R, Mikolov T, Bengio Y. On the difficulty of training recurrent neural networks. International Conference on Machine Learning, PMLR 2013:1310–8.
[52] Hochreiter S, Schmidhuber J. Long Short-Term Memory. Neural Comput 1997;9(8):1735–80. https://doi.org/10.1162/neco.1997.9.8.1735.
[53] Joyce JM. Kullback-Leibler Divergence. In: Lovric M, editor. International Encyclopedia of Statistical Science. Berlin, Heidelberg: Springer; 2011. p. 720–2. https://doi.org/10.1007/978-3-642-04898-2_327.
[54] Mei Q, Gül M. A crowdsourcing-based methodology using smartphones for bridge health monitoring. Struct Health Monitoring 2019;18(5-6):1602–19. https://doi.org/10.1177/1475921718815457.
[55] Cantero D, O`Brien EJ, González A. Modelling the vehicle in vehicle—infrastructure dynamic interaction studies. Proc Inst Mech Eng, Part K: J Multi-Body Dyn 2010;224:243–8. https://doi.org/10.1243/14644193JMBD228.
[56] Harris NK, OBrien EJ, González A. Reduction of bridge dynamic amplification through adjustment of vehicle suspension damping. J Sound Vib 2007;302(3):471–85. https://doi.org/10.1016/j.jsv.2006.11.020.
[57] González A, Mohammed O. Dynamic Amplification Factor of Continuous versus Simply Supported Bridges Due to the Action of a Moving Vehicle. Infrastructures 2018;3:12. https://doi.org/10.3390/infrastructures3020012.
[58] González A, Cantero D, OBrien EJ. Dynamic increment for shear force due to heavy vehicles crossing a highway bridge. Comput Struct 2011;89:2261–72. https://doi.org/10.1016/j.compstruc.2011.08.009.
[59] Zhou X-Y, Treacy M, Schmidt F, Brühwiler E, Toutlemonde F, Jacob B. Effect on Bridge Load Effects of Vehicle Transverse In-Lane Position: A Case Study. J Bridge Eng 2015;20(12):04015020. https://doi.org/10.1061/(ASCE)BE.1943-5592.0000763.
[60] Cantero D, González A, OBrien EJ. Comparison of Bridge Dynamic Amplifications Due to Articulated 5-Axle Trucks and Large Cranes. Baltic J Road Bridge Eng 2011;6:39–47. https://doi.org/10.3846/bjrbe.2011.06.
[61] van der Maaten L, Hinton G. Visualizing Data using t-SNE. J Machine Learning Res 2008;9:2579–605.
[62] Fraser M, Elgamal A, He X, Conte JP. Sensor Network for Structural Health Monitoring of a Highway Bridge. J Comput Civil Eng 2010;24(1):11–24. https://doi.org/10.1061/(ASCE)CP.1943-5487.0000005.

PAPER IB

Muhammad Zohaib Sarwar, Daniel Cantero

Data-driven bridge damage detection using multiple passing vehicles responses, 11th International Conference on Bridge Maintenance, Safety and Management (IABMAS), Taylor Francis, Barcelona, Spain (2022), pp. 1003-1010

IB

PAPER II

Muhammad Zohaib Sarwar, Daniel Cantero

Probabilistic autoencoder-based bridge damage assessment using train-induced responses, Submitted for journal publication

II

Probabilistic autoencoder-based bridge damage assessment using train-induced responses

Muhammad Zohaib Sarwar[a], Daniel Cantero[a]

[a]*Department of Structural Engineering Norwegian University of Science and Technology, Trondheim, 7491, Norway*

Abstract

Structural health monitoring (SHM) systems have been increasingly employed to continually assess the current state of bridges. However, the vast amounts of sensor data generated by SHM systems, along with constantly changing environmental and operational conditions, make structural damage assessment a computationally demanding and challenging task. Traditional data-driven approaches primarily utilise machine learning methods for pattern recognition and feature extraction to address this issue. This paper introduces a methodology for assessing bridge conditions using a probabilistic temporal autoencoder (PTAE). The proposed approach effectively extracts features and captures temporal relationships in multi-sensor data collected only during train crossings. By calculating the reconstruction loss and KL divergence-based of damage features, the methodology enables the identification of potential damage of a monitored bridge. An Exponentially Weighted Moving Average (EWMA) filter and a control chart-based threshold mechanism are applied to further refine the damage assessment process, facilitating the distinction between healthy and progressively deteriorating damage cases. The proposed method is adaptable to various monitoring scenarios and sensor configurations, and robust to varying operational and environmental conditions. The effectiveness of the methodology is assessed using numerically generated data and validated with real-world data from the KW51 bridge. The results demonstrate that the proposed method can detect damage with a limited number of sensors, making it a valuable approach to enhance bridge safety.

Keywords:
Train-induced vibration, damage assessment, EWMA, probabilistic autoencoder, Structural health monitoring, KW51 Bridge

1. Introduction

The rapidly ageing bridge infrastructure has become a growing concern worldwide, as a significant number of bridges in developed countries reach the end of their design life. Increased mobility, traffic volume, and climate change have resulted in deviations from original design assumptions, accelerating the deterioration process [1, 2]. Presently, bridge maintenance decisions rely primarily on manual and visual inspections, which are time-consuming, expensive, and partly subjective. As a result, there is an urgent need for more efficient and objective methods to monitor and maintain ageing bridges. Structural Health Monitoring (SHM) techniques present a promising alternative to traditional manual inspections, providing real-time, objective data on bridge conditions [3]. Among various SHM techniques, vibration-based methods have attracted considerable attention due to their ability to capture a structure's global behaviour and detect damage without prior knowledge of the damage location [4].

Vibration-based SHM approaches for detecting damage can generally be divided into model-based and data-driven methods. The model-based approach involves using a numerical model combined with experimental data to obtain information about the structural integrity. Although widely popular and known for their accuracy, these methods possess inherent computational complexity, rendering them less appropriate for extensive SHM applications [5]. Conversely, data-driven or non-model-based methods primarily focus on utilising data mining and advanced signal processing techniques to derive valuable insights directly from the sensor data collected from the target bridge. Due to their computational simplicity, data-driven methods are more attractive and cost-efficient for real-time damage assessment in large-scale structures [6].

There has been extensive discussion in the literature regarding strategies for identifying bridge damage using data-driven methods. One such approach, proposed by Alamdari et al. [7], involves identifying rotation influence lines using only two instrumented locations at the bridge bearings. This technique was implemented to evaluate cable losses in a cable-stayed bridge. Similarly, Huseynov et al. [8] and O'Brien et al. [9] used accelerometers to determine structural rotation and the corresponding influence lines for identifying damage related to the loss of bending stiffness in the bridge

deck. In addition, authors Quqa et al. [10, 11] showed that filter banks consisting of low and bandpass filters can be used to identify damage-sensitive structural features from acceleration measurements. Although these methods have been effective in assessing damage, practical implementation remains a challenging task due to the uncertainty associated with varying operational and environmental conditions in long-term monitoring data.

Continuous structural health monitoring (SHM) systems face challenges in dealing with the influence of operational and environmental conditions due to the complex, nonlinear relationship between the mechanical and material properties of the structure and external factors [12]. This has led to increasing interest in the application of machine learning (ML) techniques, which are effective in handling these challenges [13, 5]. ML models are essentially black box models that automatically extract information from datasets, identify patterns, and make predictions about future outcomes. There are two types of ML methods: supervised and unsupervised. Supervised ML requires input and output labels, while unsupervised ML only requires input data. In situations where only data obtained from the original state of the structure is available, unsupervised ML is particularly relevant [14, 15]. This is often the case in civil structures, where monitoring data frequently lacks information for damage cases. Overall, ML methods have significant potential for improving the accuracy and reliability of SHM systems in the face of operational and environmental uncertainties [16].

In the context of unsupervised machine learning methods, Principal Component Analysis (PCA) is often considered the simplest and most common approach [17]. PCA computes the linear relationship between measured features and the deviation of features from the identified relationship, referred to as the damage state. Due to its efficiency and practicality, many researchers prefer using PCA for dimensionality reduction and damage detection [18]. For instance, Ni et al. [19] proposed a damage detection and localisation method based on fixed moving principal component analysis, where principal components and eigenvalues are used as damage-sensitive features. Similarly, Ma et al. [20] introduced a probabilistic variant of PCA for anomaly detection. Although PCA constitutes the majority of commonly used dimensionality reduction techniques in SHM, other methods such as tensor decomposition and autoencoders are also prevalent [21]. In recent years, autoencoders have gained significant attention in the SHM field. Researchers in various studies have used modal parameters to train autoencoders for damage detection [22, 23]. Ma et al. [24] and Silva et al. [25] introduced a

damage-sensitive feature extraction method using an autoencoder by utilising raw acceleration data. Wang and Cha [26] combined autoencoders with one-class support vector machines for damage assessment. Giglioni et al. [27] expanded upon Wang and Cha's idea by introducing ensemble learning and a threshold mechanism. In their work, the authors developed a methodology that uses an autoencoder to reconstruct the acceleration response. The damage-sensitive feature is computed by calculating the reconstruction loss, and a number of short sequences are grouped to form a macro sequence for damage detection. Moreover, Zhang et al. [28] and Sarwar and Cantero [29] presented the idea of using a 1D convolutional autoencoder. The convolutional autoencoder is trained on acceleration data of the undamaged state of bridges and then the trained model is further used for damage assessment. Shang et al. [30] used a deep convolutional denoising autoencoder to combine multiple sensors and extract damage-sensitive features. Compared to ordinary autoencoders, convolution-based autoencoders enable the possibility of combining multiple sensors to extract damage-sensitive features. This makes convolutional autoencoders more attractive for applications in SHM, where multiple sensor fusion has proven to be beneficial. For more detail on the application of convolutional autoencoders and their application refer to [15].

The majority of research conducted on data-driven methods for bridge damage assessment primarily relies on ambient vibration data or static effects. However, recent studies have acknowledged that structural responses generated by vehicle crossings can also be effective for bridge damage assessments [16]. In this context, most research related to monitoring techniques and data interpretation focuses on highway bridges, but these techniques are generally applicable to railway bridges as well [31]. Gonzalez and Karoumi [32] proposed an artificial neural network (ANN)-based damage detection method. Their approach utilises deck acceleration and bridge weigh-in-motion data to train a machine learning model, which is then used in conjunction with statistical processes for classifying the bridge's health and damage states. In [33], the authors validated this idea using real bridge measurements. One of the main drawbacks of this strategy is the need to train an ANN model for each individual sensor. Azim and Gul [34] proposed a time series analysis-based method for the global monitoring of railway bridges using operational data. Their method employs the autoregressive moving average (ARMA) model to analyse the free vibration response of the bridge, in order to extract damage features. Similarly, Meixedo et al. [35] presented the idea of using autoregressive (AR) models to extract damage-

sensitive features from traffic-induced vibration responses. Their method effectively removes the influence of temperature, train type, and speed from the damage-sensitive features using Multiple Linear Regression (MLR) and Principal Component Analysis (PCA). However, the main challenge with their proposed method is the manual extraction of damage-sensitive features for each sensor, which requires careful analysis of the AR parameters.

Despite the strong potential, the real-world application of vehicle-induced dynamic response for Structural Health Monitoring (SHM) implementation remains limited. Most of the existing works and methodologies have certain limitations, such as disregarding the influence of environmental and operational conditions, specific loading effects, and validating methods using simple numerical models. Consequently, this study aims to develop a methodology for damage assessment that can automatically extract damage-sensitive features from responses generated by trains crossing at varying speeds and loading conditions. To this end, a multivariate temporal convolutional autoencoder is proposed. The proposed autoencoder is first trained using the current, healthy state of the bridge. Then, the trained model is utilised for damage assessment. In practice, it is impossible for training data to encompass all varying conditions, such as temperature and loading conditions. Therefore, it is crucial that the proposed autoencoder can generalise the feature space for the healthy state of the bridge and quantify the uncertainty arising from limited data. This challenge is addressed by developing a temporal convolutional autoencoder as a Bayesian deep learning approach. Moreover, for damage assessment, the features extracted from the autoencoder are combined with an Exponentially Weighted Moving Average (EWMA) filter, a pattern recognition algorithm capable of distinguishing minor damage cases under varying operational conditions. The EWMA control chart is employed for threshold selection in damage detection. Likewise, a one-class Support Vector Machine (OC-SVM) is implemented using the input from the EWMA output for damage detection. The proposed methodology is evaluated across a range of different damage scenarios using both numerical and real-life field data.

The remainder of the paper is structured as follows. Section 2 offers an overview of the suggested methodology, encompassing details of the probabilistic deep autoencoder and the damage index. Section 3 presents the specifics of the numerical case study, which includes the train-track bridge model used to generate data, as well as an evaluation of the proposed method's performance for the numerical case study. Section 4 describes the monitoring

details of railway bridge KW51 and validates the proposed method by detecting various bridge conditions. Lastly, Section 5 summarises the findings of this research.

2. Proposed methodology

2.1. Overview

The main overview of the proposed methodology is shown in Fig. 1, which involves collecting sensor data as trains cross the bridge. The sensor data for a single event is further divided into n windows. The collected data is then utilised to train a probabilistic temporal autoencoder (PTAE). The architecture of the PTAE consists of multiple convolutional blocks and a Long Short-Term Memory (LSTM) recurrent neural network. For damage assessment, the reconstruction loss of each window is computed first, followed by the calculation of a KL (Kullback-Leibler) divergence-based damage feature between the baseline condition and a subsequent single train crossing. In the final step, an Exponentially Weighted Moving Average (EWMA) filter is applied to the damage feature. The EWMA control chart-based threshold mechanism is developed to distinguish between healthy and subsequent damage states. Further details about each step are discussed in subsequent sections.

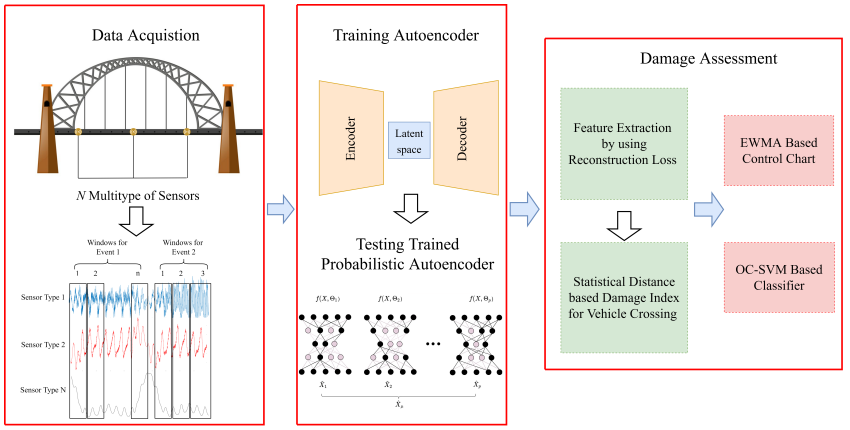

Figure 1: Overview of proposed damage detection framework

2.2. Probabilistic deep autoencoder

An autoencoder is a neural network architecture designed to replicate its input X to itself, namely $Y = X$ via a bottleneck structure. A deep autoencoder consists of two main components: an encoder and a decoder. The encoder maps the input data X to a lower-dimensional latent representation z, also known as the bottleneck layer, while the decoder reconstructs the input data from this latent representation. This means that in an autoencoder, we select a model $F^{W,b}(X)$ to concentrate the information required to accurately recreate X. Suppose that we have N input vectors $X = \{x_1, \ldots, x_N\} \in \mathbb{R}^{M \times N}$. The transfer function of the encoder and decoder can be expressed by Eq. 1 and Eq. 2 respectively.

$$\begin{aligned} z^{(0)} &= X \\ z^{(l)} &= \phi(W^{(l)} z^{(l-1)} + b^{(l)}), \text{ for } l = 1 \text{ to } L \end{aligned} \tag{1}$$

$$\begin{aligned} y^{(0)} &= z^{(L)} \\ y^{(l-L)} &= \phi'(W'^{(l)} y^{(l-L-1)} + b'^{(l)}), \text{ for } l = L+1 \text{ to } 2L \end{aligned} \tag{2}$$

where ϕ, ϕ' are the activation functions of the encoder and decoder modules, while W, W' and b, b' are the weights and biases of each module, and L is the number of hidden layers in the encoder. In an autoencoder, we fit the model $F^{W,b}(X)$ and optimise the weights W, W' and biases b, b' parameters using the backpropagation algorithm by employing the mean squared error as the loss function, which is expressed as:

$$\mathcal{L} = f(X : \Theta) = \frac{1}{n} \sum_{i=1}^{N} \left(\frac{1}{2} \left\| \widehat{x}_i - x_i \right\|^2 \right) + \lambda(\Theta) \tag{3}$$

where λ is a regularisation factor applied to the weights of a specific layer in order to prevent overfitting. In a standard autoencoder, the learning parameters are optimised as single deterministic estimates based on a given dataset. However, in various applications, the ability to represent uncertainty is of paramount importance. Unfortunately, standard autoencoders do not possess the capability to account for or represent model uncertainty.

Bayesian neural networks (BNN) or probabilistic neural networks (PNN) can incorporate uncertainty in a systematic manner, as opposed to standard neural networks. BNNs handle uncertainty by treating weights as stochastic variables with a prior distribution. One major drawback of BNNs is

their computational cost. In the case of deep networks, BNNs need to obtain posterior distributions across the network's parameters, which become high-dimensional probability distributions as the model complexity increases. To address this issue, Gal and Ghahramani [36] proposed a more computationally efficient algorithm called Monte Carlo Dropout (MC Dropout). In their work, the authors showed that applying dropout before weight layers in any neural network, regardless of its depth and non-linearities, can be interpreted as a Bayesian approximation of the probabilistic deep Gaussian process. Dropout, which randomly deactivates neurons in a neural network during training, is typically employed as a regularisation technique to reduce overfitting, without being used during prediction. However, when each unit is dropped during prediction with some probability p the output ceases to be probabilistic. Training a neural network with dropout can be considered as training a set of pruned networks with extensive weight sharing. Each dropout configuration corresponds to a sub-network, producing multiple output predictions for a given input, as illustrated in Fig. 2. Uncertainty can be quantified by calculating the variance of numerous predictions across different dropout configurations, while the predictive mean of the output is represented by the mean of these multiple predictions.

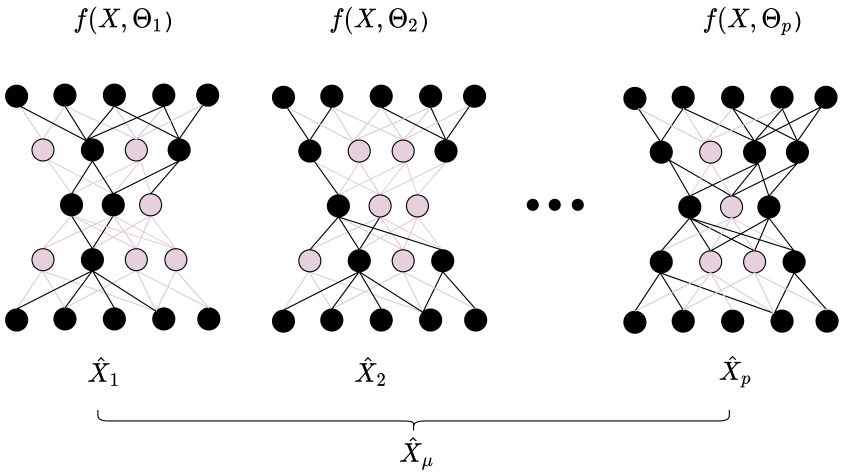

Figure 2: Different MC-Dropout configurations for autoencoder

2.3. Network architecture of probabilistic temporal autoencoder

Deep learning models have shown great promise in combining information from multiple sensors to perform a range of tasks, including classification and regression [16]. Automatic feature extraction from time series data often relies on the use of 1D convolutional neural networks (1D CNN) and recurrent neural networks (RNN). However, training RNNs for long-term sequences can be challenging due to the vanishing gradient problem encountered during backpropagation [37]. To address this issue, Long Short-Term Memory (LSTM) networks were introduced [38]. In this study, the network architecture of the proposed probabilistic temporal autoencoder (PTAE) is primarily built using 1D CNN and LSTM. The architecture of the proposed PTAE is primarily inspired by the temporal autoencoder proposed by Madiraju [39].

In this study, the input dataset for damage assessment comprises multi-sensor information, including accelerations, displacements, and rotations. Time series data from different sensors exhibit considerable variations in important properties and features on the temporal scale and dimensionality. Considering the nature of multi-sensor information in the time series data, the network architecture is designed to ensure that each time scale contains informative features.

For an autoencoder, it is crucial to have an effective latent representation that can be used to reconstruct the input. In this study, this is achieved by employing PTAE, as shown in Fig. 3. The model's architecture is divided into two stages. The first stage consists of 1D convolutional layers that extract key short-term features, followed by a pooling layer of size P, activation functions, and an MC-dropout layer. The first stage reduces the time series data to a more compact representation of the most relevant features. To obtain a latent representation and learn temporal changes, the output of the first stage is fed into an LSTM. The LSTM module learns temporal changes across each time step, collapsing the input signals into all dimensions except the temporal one and casting the inputs into a much smaller latent space. For reconstruction, the decoder is developed by using an upsampling layer of size P followed by a deconvolutional layer to obtain the autoencoder output.

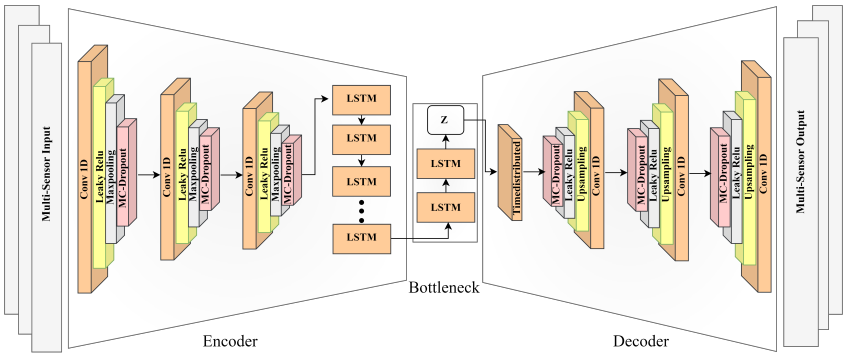

Figure 3: Architecture of proposed Probabilistic Temporal Autoencoder (PTAE)

The proposed PTAE is implemented using TensorFlow and Keras. The optimisation of weight and bias parameters in the proposed architecture is performed using an end-to-end approach, taking into account the loss function as illustrated in Eq. 3.

2.4. Data collection and preprocessing

In the proposed framework, a permanent Structural Health Monitoring (SHM) system is assumed to be installed on the bridge, capable of capturing multiple sensor data such as accelerations, displacements, and rotations at various locations. Sensor measurements are collected exclusively when a train crosses the bridge, with known entry and exit times. It is important to note that due to varying train speeds, each crossing event produces signals of different lengths.

Signal preprocessing is a critical step for both damage assessment and training of the PTAE. This process involves standardising the time series data collected by each sensor, ensuring zero mean and unit variance. Additionally, for every individual train crossing event, the time series signals are divided into appropriate window lengths. Each sliced window's data matrix consists of sensors as rows and sequences of measured responses as columns, as shown in Fig. 4.

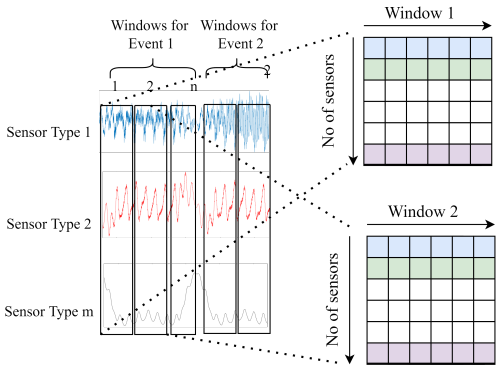

Figure 4: Illustration of the windowing of single event

To train the autoencoder, numerous train crossing events are gathered when the bridge is in a healthy condition. These events are standardised and divided into fixed-length windows, as previously described. During training, the PTAE focuses on reconstructing the time series sequences present in each data matrix.

2.5. Damage feature

To evaluate damage, the discrepancy between original and reconstructed time series signals within fixed-length windows is quantified by computing the normalised root mean square error (NRMSE) for each sensor. This calculation is performed using Eq. 4.

$$\text{NRMSE} = \frac{\sqrt{\frac{1}{n}\sum_{i=1}^{n}(x_i - \hat{x}_{\mu i})^2}}{\sigma_x} \tag{4}$$

where x_i is the actual value of the i^{th} sample, and $\hat{x}_{\mu i}$ is the mean predicted value of PTAE, while σ_x is the standard deviation of the measured time series sequence of each sensor.

During the training phase, considering multiple train crossing events, the NRMSE of each window for various sensors varies between events due to fluctuating train speeds and loading conditions. Nonetheless, the NRMSE distributions for individual events can be employed to distinguish between healthy and damaged states. This can be accomplished by calculating the

statistical variation between the NRMSE distributions of baseline conditions and subsequent train crossing events. To quantify the dissimilarity between two distributions, this study utilises the Kullback–Leibler (KL) divergence. The KL divergence is a technique that measures the information loss when a probability distribution p is employed to approximate a distribution q.

In this study, it is assumed that the NRMSE distributions follow a Gaussian distribution for both the baseline condition and each subsequent train crossing event. For multiple sensors, these distributions are characterised by their respective mean vectors $(\boldsymbol{\mu}_1, \boldsymbol{\mu}_2)$ and covariance matrices (Σ_1, Σ_2). The KL divergence between two multivariate Gaussian distributions can be expressed using Eq. 5.

$$D_{kl}(p\|q) = \frac{1}{2}\left(\mathrm{tr}(\Sigma_2^{-1}\Sigma_1) + (\boldsymbol{\mu}_2 - \boldsymbol{\mu}_1)^T\Sigma_2^{-1}(\boldsymbol{\mu}_2 - \boldsymbol{\mu}_1) - m + \log\frac{|\Sigma_2|}{|\Sigma_1|}\right) \quad (5)$$

where $\boldsymbol{\mu}_1$ and Σ_1 denote the mean vector and covariance matrix of the multivariate Gaussian distribution for the baseline condition, respectively. Similarly, for subsequent events, $\boldsymbol{\mu}_2$ and Σ_2 represent the mean vector and covariance matrix of the multivariate Gaussian distribution, respectively. In addition, m corresponds to the number of sensors in use, and $\mathrm{tr}(\cdot)$ signifies the trace of a matrix. From Eq. 5 it is evident that the KL divergence is exponentially related to the distance between distributions. For damage detection, the equation is mapped to a linear relationship, as shown in Eq. 6, where e is Euler number.

$$\mathrm{DF} = \ln\left[D_{kl}\left(p\|q\right) + e\right] - 1 \quad (6)$$

2.6. Exponentially weighted moving average

For damage assessment, it is crucial to employ a robust method capable of identifying small changes caused by structural damage. To this end, statistical process-based control charts have been used as a novelty detection method [40, 30]. One such technique is the Exponentially Weighted Moving Average (EWMA), a widely used statistical method for detecting underlying patterns in time series data [41]. EWMA calculates the average of a series of data points while assigning exponentially decreasing weights to older data points. This allows EWMA to respond more quickly to recent changes in the data, making it effective for detecting small shifts in the underlying process. The EWMA process can be defined as follows:

$$Z_t = \alpha X_t + (1 - \alpha) Z_{t-1} \tag{7}$$

where Z_t is the EWMA value at time t, which is typically the control variable to be monitored, X_t is the observed data point at time t, and α is the smoothing parameter, with $0 < \alpha \leq 1$. The parameter α determines the degree of weight given to the most recent data points. When α is close to 1, more weight is assigned to recent data points, whereas when α is close to 0, the weight is distributed more evenly across the entire series.

In the context of this study, the control variable is the Damage Index (DI), and the observed variable is the Damage Feature (DF) defined by Eq. 6. Therefore, we modify Eq. 7 for this study as follows:

$$DI_j = \alpha DF_j + (1 - \alpha) DF_{j-1} \tag{8}$$

where j is the number of inspections or train crossing events.

For effectively assessing the structural condition, it is essential to establish a fixed threshold to monitor the Damage Index (DI_j). In the context of the EWMA control chart, two thresholds, known as the Upper Control Limit (UCL) and Lower Control Limit (LCL), are utilised to determine whether the process is in control or not. The UCL and LCL are defined as follows:

$$\text{UCL} = \mu_0 + L\sigma \sqrt{\frac{\alpha}{(2 - \alpha)} \left[1 - (1 - \alpha)^{2j}\right]} \tag{9}$$

$$\text{LCL} = \mu_0 - L\sigma \sqrt{\frac{\alpha}{(2 - \alpha)} \left[1 - (1 - \alpha)^{2j}\right]} \tag{10}$$

In these equations, μ_0 represents the average value of the EWMA statistics when the process is in control, while σ denotes the standard deviation of the Damage Feature (DF) values. The parameter L is a constant that determines the width of the control chart.

These limits allow for the identification of anomalies or shifts in the process. If the Damage Index (DI_j) lies within the UCL and LCL, the process is considered to be in control, indicating that the structural condition remains unchanged. However, if the DI_j exceeds the UCL or falls below the LCL, it signals a potential anomaly or change in the structural condition that warrants further investigation.

3. Numerical case study

3.1. Model description

This section presents the numerical model used to validate the strategies and techniques proposed in this study. The numerical model integrates the behaviour of the train, ballasted track, and bridge, as depicted in Fig. 5. A 2D representation is utilised for the entire problem, an approach that has been widely adopted by researchers for analogous studies. Each modelling component is briefly discussed next.

Firstly, the train is modelled as a sequence of individual vehicles, each characterised by a multibody system with a six-degree-of-freedom configuration. A primary suspension connects the two axles of each bogie, while a secondary suspension system supports the main body on two bogies. This vehicle model has been extensively employed in the literature and effectively captures the primary components. Rail irregularities, which serve as a significant source of excitation, contribute to the combined dynamic response of the vehicle and infrastructure [42]. In this study, Class 6 track irregularities from the Federal Railroad Administration are employed [43].

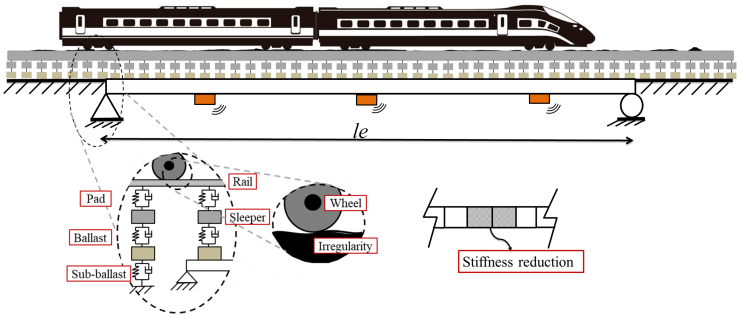

Figure 5: Overview of the Train-Track-Bridge model

The track model comprises a combination of elements, as illustrated in Fig. 5, including rail, pad, sleeper, ballast, and sub-ballast. The rail is modelled as a beam, with the remaining components represented as lumped masses. Dashpot and spring systems interconnect these elements, exhibiting the viscoelastic behaviour of each component. The bridge is represented as

an Euler-Bernoulli beam using a Finite Element Model (FEM) with beam elements, each consisting of two nodes and two degrees of freedom per node. he bridge's specifications are based on a simply supported concrete bridge, as reported in [44]. The bridge has a length of $le = 50m$, a second moment of area $I = 51.3m^4$, a mass per unit length $\rho = 69000kg/m$, and a modulus of elasticity $E = 3.5 \times 10^{10} N/m$.

The subsystems are integrated into a unified system, with the equations of motion for the train, track, and bridge coupled together through the mass, stiffness, damping, and force matrices, These matrices are time-varying and change according to the vehicle's position. The time-varying equations of motion are solved using numerical integration with the Newmark-β scheme, yielding the dynamic response of the train as it traverses the bridge. The reader can refer to [45] for a complete description and more detail of the coupling procedure and its validation.

In this study, the vehicle configuration of the ICE3 Velaro train is considered, comprising a convoy of eight wagons. The mechanical properties and dimensions are provided in Gia et al. [46]. To establish the dynamic equilibrium of the vehicle before it enters the bridge, a track 100m longer than the bridge is modelled. The rail is designed as a standard UIC60 rail with a sleeper spacing of 0.6m. The Matlab implementation of the train-track model for numerical simulation is available at [42]

3.2. Modelling of damage and temperature effect

For damage assessment using the train-track model, damage is simulated by implementing a localised stiffness reduction in the beam elements. The bridge is discretised into 160 elements, resulting in elements with a length of 0.3m. Damage is modelled at the mid-span of the bridge by reducing the stiffness of two elements, which is approximately equal to 1.2% of the total bridge length.

Another critical aspect of long-term bridge monitoring is accounting for the influence of temperature, as it directly affects the bridge's material properties and, consequently, its modal properties. In the present study, the temperature's effect is modelled using an empirical model derived from real bridge measurements, which establishes the relationship between temperature and bridge properties. One such model proposes a bi-linear equation for the bridge's elastic modulus [47], as shown in Eq. 11.

$$E_T = E_0 \left[Q + S, T + R \left(1 - erf \left(\frac{T - \kappa}{\tau} \right) \right) \right] \tag{11}$$

In Eq. 11, the temperature-dependent elastic modulus is denoted by E_T, while E_0 represents its value at a specific reference temperature. The parameters Q and S establish the linear relationship, and the expression $R\left(1 - erf\left(\frac{T-\kappa}{\tau}\right)\right)$ modifies the relationship to account for sub-zero temperatures. In Eq. 11, the temperature is expressed in degrees Celsius as T, with κ and τ serving as parameters that dictate the transition around the freezing point.

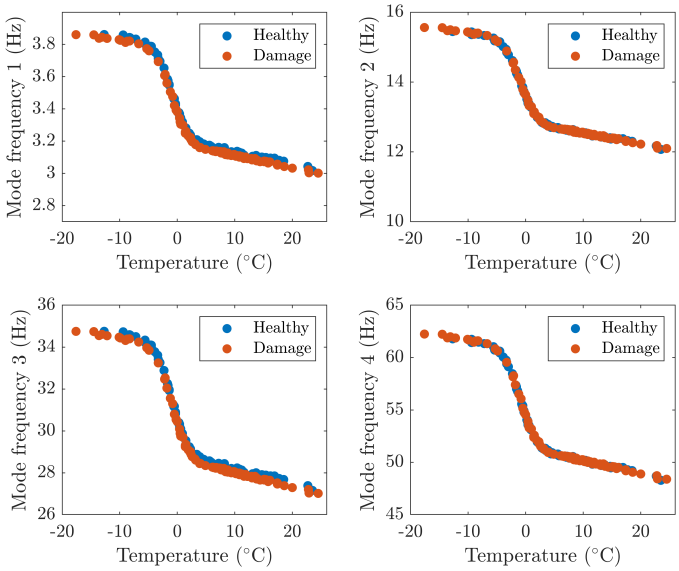

Figure 6: Effect of temperature on modes of the bridge

In this study, the effect of temperature is assessed using a 1-year dataset of temperature records from a weather station in Trondheim, Norway. In the numerical model, temperatures for each train crossing event are randomly chosen from these records. The elastic modulus of the concrete is then adjusted accordingly with Equation 11. To accommodate possible uncertainties, parameters within this equation are also randomly sampled, following

the suggestion in [47], based on the mean and standard deviation values listed in Table 1. Fig. 6 illustrates the influence of fluctuating temperature on the first four modes of the bridge, both in its healthy condition and with damage introduced. All modes exhibit a bi-linear relationship with varying temperature.

Table 1: Mean and standard deviation values for the modelling of the effect of temperature on concrete's elastic modulus

	Q	S	κ	τ	R
μ	1.0129	-0.0048	0.1977	3.1466	0.1977
σ	0.003	0.0001	0.0027	0.0861	0.0027

3.3. Data generation

The evaluation of the proposed damage assessment method is carried out using numerically simulated data generated by solving the Train-Track-Bridge interaction model presented in Section 3.1. The dataset is created by assuming that the train speed varies for each crossing, while the vehicle's suspension properties remain constant. Small variations in the body mass of each train wagon are also considered to account for the inherent uncertainty in the payload. The varying train parameters and the statistical variability of these parameters (i.e., maximum, minimum, and standard deviation) are presented in Table 2. To generate the dataset, these parameters are randomly sampled based on the given statistical variation within a Monte Carlo simulation. For the healthy case, a batch of 200 events is created. For each event, displacement, rotation, and acceleration responses are measured at three locations on the beam, as shown in Fig. 5, with a sampling frequency of 1000Hz. To account for a realistic scenario for each event, noise levels are randomly sampled from a Gaussian distribution $\mathcal{N}$(30dB, 1dB) with values in the range [30dB, 40dB] signal-to-noise ratio, and added to all measured responses.

To demonstrate the performance of the proposed method, this study considers four different scenarios. Each scenario is defined based on the available sensor information:

- Scenario-1: The data contains only displacement responses from 3 locations on the bridge.

- Scenario-2: The data contains only rotation responses from 3 locations on the bridge.
- Scenario-3: The data contains only acceleration responses from 3 locations on the bridge.
- Scenario-4: The data contains all responses, including acceleration, rotation, and displacement from 3 locations on the bridge.

For PTAE input in each scenario, all measured signals are standardised to have zero mean and unit variance. Each event is then sliced into windows of length 128, as discussed in Section 2.4, resulting in a dataset shape of $(N \times l \times m)$, where N is the number of windows in a single event, l is the length of the window, and m is the number of variables or sensors. For the 200 events, considering only acceleration responses at three different bridge locations, the size of the dataset becomes $(8847 \times 128 \times 3)$.

Table 2: Train model parameters variability

	Min.	Max.	Mean	SD
Velocity (km/h)	150	170	160	3
Body Mass (kg)	42100	53500	47800	500

3.4. Training and evaluation method

The PTAE architecture is built using TensorFlow modules, and the code is developed in Python 3.9. The selected network architecture is based on achieving the lowest reconstruction loss after carrying out a random search for hyperparameter optimisation. The encoder module of the PTAE comprises three convolutional blocks, followed by two LSTM layers. Each convolutional block consists of a 1D convolutional layer, Leaky-ReLU activation function, max-pooling layer and an MC-Dropout layer. The decoder utilises the same number of convolutional blocks arranged in reverse order, with the max-pooling layer replaced by an up-sampling layer. An MC-Dropout rate of 0.5 is chosen, meaning that during each forward pass, 50% of the connections are dropped, enhancing the model's robustness and preventing overfitting. Table 3 displays the detailed architecture of the proposed PTAE, including various hyperparameters such as activation function, filters and kernel size, and dropout rate.

The training process employs adaptive moment estimation (Adam) with a batch size of 128 samples, while setting learning and decay rates at 0.001 and 0.0001 respectively. The model undergoes training for 1500 epochs. All training and numerical computations for the models are conducted on a standard PC fitted with an Intel Core i9-10900 K CPU, 64 GB RAM and an NVIDIA GTX 2080Ti graphics card.

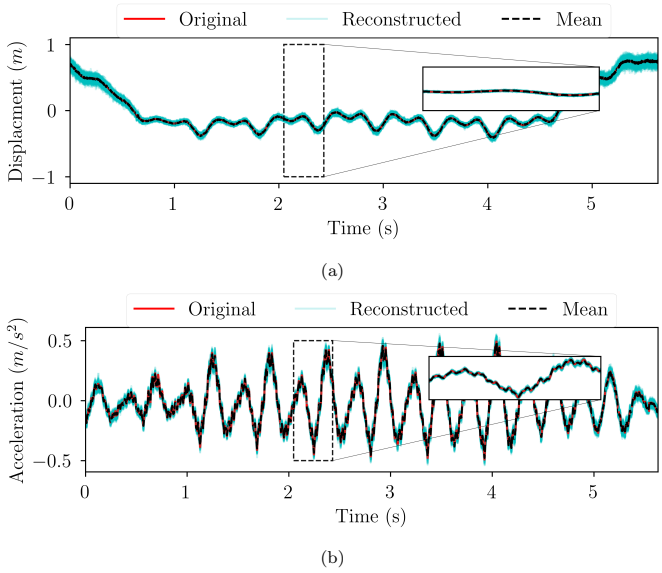

Figure 7: Comparison of original and reconstructed signals of two different type of sensors; (a) Displacement signal at mid-span of the bridge, (b)Acceleration signal at mid-span of the bridge

The proposed PTAE architecture is trained separately for all four scenarios, maintaining the same network architecture as presented in Table 3, with $m = 3$ and the size of the latent space dimension $z = 1$. However, for Scenario-4, the value of m increases to 9 and the dimension of the latent space to $z = 3$. Each model is trained using only the healthy bridge data. For training, 70 train crossing events are selected from the available dataset of 200 events. To visualise the model's reconstruction performance, two random cases from the validation dataset are illustrated in Fig. 7. These cases

are reconstructed using the PTAE model trained for Scenario-4. The trained model undergoes 50 simulations, with each layer's 50% connection randomly pruned, as discussed in Section 2.2. Fig. 7 displays the reconstructed output for each forward pass and compares the mean value of all forward passes to the original input signal. The zoomed-in section of the figure reveals an almost perfect match between the input signals and the mean of the reconstructed signals. The results demonstrate the PTAE-trained model's ability to replicate the bridge's healthy state.

Table 3: Architecture of proposed PTAE

Layers	**Output shape**	**Kernel size**	**Activation**
Encoder			
Input	$(128 \times m)$	–	–
Conv_1D	(128×512)	1×5	Leaky-ReLU
Max-pooling	(64×512)	1×5	–
MC-Dropout	(64×512)	–	–
Conv_1D	(64×256)	1×5	Leaky-ReLU
Max-pooling	(64×256)	1×5	–
MC-Dropout	(64×256)	–	–
Conv_1D	(64×128)	1×3	Leaky-ReLU
Max-pooling	(64×128)	1×3	–
MC-Dropout	(64×128)	–	–
LSTM	(64×128)	–	Leaky-ReLU
LSTM	$(64 \times z)$	–	Leaky-ReLU
Decoder			
TimeDistributed	(64×128)	–	Leaky-ReLU
Up-sampling	(64×128)	1×5	Leaky-ReLU
Conv_1D	(64×128)	1×5	–
MC-Dropout	(64×128)	–	–
Up-sampling	(128×128)	1×5	Leaky-ReLU
Conv_1D	(128×256)	1×5	–
MC-Dropout	(128×256)	–	–
Up-sampling	(128×256)	1×5	Leaky-ReLU
Conv_1D	(128×512)	1×5	–
MC-Dropout	(128×512)	–	–
Conv_1D	$(128 \times m)$	–	Linear

[m] Number of sensors. [z] Size of latent space dimension.

3.5. Damage detection using PTAE

In order to demonstrate the performance of PTAE, and how it can be utilised for damage detection, four new datasets with different damage severities are simulated, where damage is modelled as a stiffness reduction as discussed in Section 3.2. Each dataset consists of 100 train crossing events. The details for different damage cases are:

- DC0: Healthy case
- DC1: Damage at mid-span with 10% stiffness reduction
- DC2: Damage at mid-span with 20% stiffness reduction
- DC3: Damage at mid-span with 30% stiffness reduction

To demonstrate the capability of the proposed method for damage detection, for each damage case, NRMSE is computed for each window sequence to quantify the discrepancies between the original and the reconstructed sequence as discussed in Section 2.5. Similarly, NRMSE is also computed for the window sequence of the training dataset. The mean vector ($\boldsymbol{\mu}_1$) and covariance matrices (Σ_1) of multiple events of the training dataset establish a baseline condition. For subsequent inspections, the distribution of NRMSE of each single crossing event with mean vector ($\boldsymbol{\mu}_2$) and covariance matrices (Σ_2) is used to compute the variation in distribution using Eq. 6. The damage feature (DF) is computed for all four scenarios. Here it is important to mention that the damage index based on EWMA proposed in this paper is sensitive to outliers, so it is important to carefully analyse the computed damage feature and if there are outliers that need to be taken care of with the appropriate method.

3.5.1. Outlier removal using Tukey's method

Tukey's method is a robust technique employed to detect outliers in a dataset [48]. This approach is based on the interquartile range (IQR), which is the difference between the first quartile (Q_1) and the third quartile (Q_3) of a dataset. The (IQR) represents the central 50% of the data, and Tukey's method identifies data points outside this range as potential outliers. When using a fixed window size, this method can be applied to detect outliers within each window of the dataset. In this method, the lower and upper bounds

for outliers are determined using $Q_1 - I \times \text{IQR}$ and $Q_3 - I \times \text{IQR}$, respectively, where I is a constant typically ranging from 1.5 to 3. This method is advantageous for outlier detection because it is less sensitive to extreme values compared to methods based on the mean and standard deviation. By employing a fixed window size, this approach facilitates the detection and removal of local outliers within each window, which is particularly useful when dealing with non-stationary or heterogeneous datasets.

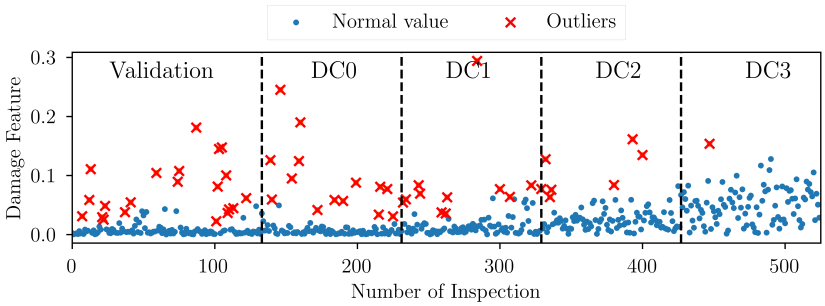

Figure 8: Removal of outliers using Tukey's method

To compute the damage index using Eq. 8 for all scenarios, the outlier removal method is utilised. To illustrate how the outlier removal method is employed, the damage feature (DF) for Scenario-1 is computed where displacement sensors are used. Outlier analysis is performed considering a non-overlapping window size of 20. For each window, Tukey's method is applied with the value of $I = 3$ as discussed previously, and outliers are marked in red as shown in Fig. 8. The figure demonstrates that the outlier removal method effectively removes outliers with progressively varying damage features due to increasing damage severity.

3.6. Results

In the numerical case study, all four scenarios mentioned in the previous section are examined. Each scenario involves separately training PTAE and computing damage features for each trained model. The outlier removal method discussed earlier is applied before utilising EWMA to calculate the damage index. To compute the damage index using EWMA, the value of α is set to 0.02, while $L = 4$. The LCL and UCL are determined using

the validation dataset according to Eq. 10 and Eq. 9 respectively. These values will be employed to establish the threshold for differentiating between the healthy and damaged conditions of the bridge. For comparison, the threshold-based system is also examined alongside the commonly used one-class support vector machine (OC-SVM) anomaly detector. The OC-SVM is implemented with an RBF kernel function and regularisation parameters $\nu = 0.1$ and $\gamma = 10$, which define the decision boundary's shape. The OC-SVM is trained using damage features from the validation dataset, similar to the threshold selection in the EWMA-based damage index.

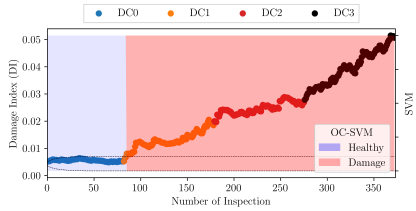

(a) Scenario-1

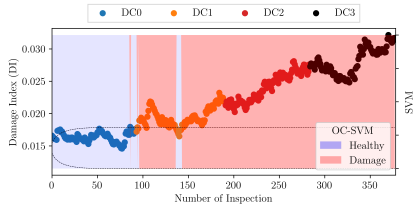

(b) Scenario-2

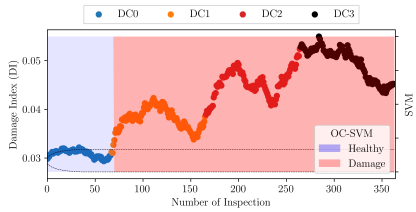

(c) Scenario-3

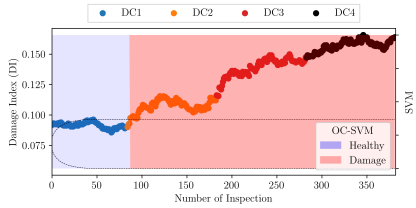

(d) Scenario-4

Figure 9: Evolution of damage index during progressive bridge condition change for different scenarios. Dashed line indicate the UCL and LCL threshold values.

To demonstrate the performance of the proposed method, the results of all four scenarios for different damage cases are illustrated in Fig. 9. In the figure, the black dashed lines represent the UCL and LCL thresholds. For

DC0 in all scenarios, the majority of the damage index values fall within the thresholds, confirming the bridge's unaltered healthy state. Similarly, OC-SVM accurately predicts DC0 as the healthy condition of the bridge in all scenarios. As the severity of damage increases from DC1 to DC3, the damage index proportionally rises. These results demonstrate the sensitivity of the proposed damage index to damage severity in all scenarios, unlike OC-SVM, which only functions as an anomaly detector.

The results in Fig. 9 enable also a direct comparison of the method's performance based on various measured load effects. The results indicate that Scenario-1, which employs displacement signals, outperforms the other scenarios (Fig. 9*a*). This is because displacements are more sensitive to structural damage than acceleration or other load effects. Rotation measurements offer also insights into a structure's global behaviour by tracking changes in the overall structural response. However, this load effect is generally less sensitive to minor, localised damage and may not effectively capture higher mode shapes [8]. This is evident in the results presented in Fig. 9*b*, where some events of DC1 are misclassified as healthy bridge conditions. The results (Fig. 9*d*) also highlight that integrating multi-sensor information can improve damage sensitivity across different damage cases. Therefore, regardless of the sensor type, the proposed damage assessment strategy can be effectively applied.

4. KW51 bridge case study

4.1. Introduction

The experimental validation of the proposed method considers the signals recorded on a steel bowstring bridge in Leuven, Belgium, known as KW51 railway bridge. This bridge spans 115m and is 12.4 meters wide, with two separate ballasted tracks, designated as track A and track B, located on the north and south sides respectively. Both tracks have curved horizontal alignment, and a speed limit of 160km/h is enforced for passenger trains.

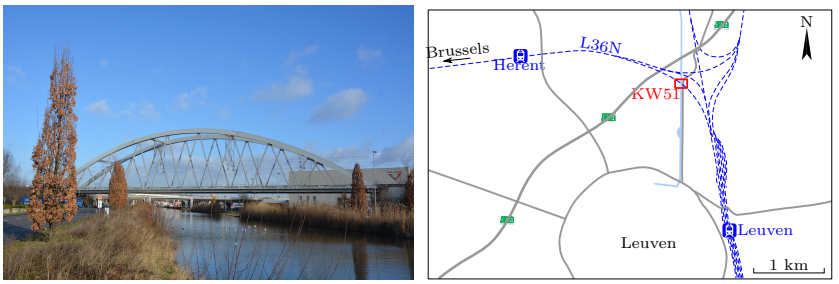

(a) (b)

Figure 10: (a) KW51 Railway bridge in Leuven, Belgium (Image by Kristof Maes) [49]; (b) situation sketch [49]

The monitoring system was installed on the bridge in September 2018 with a configuration as shown in Fig. 11. Various sensing devices were placed on the structure, including accelerometers on the bridge deck in both lateral and vertical directions, as well as accelerometers on the arch in the lateral direction. Additionally, strain sensors were installed on the bridge deck along the longitudinal direction. A National Instruments data acquisition system collected the measurements, which also included temperature and relative humidity measurements taken beneath the bridge deck. This study only considers the acceleration measurements from the bridge deck, because strain signals for multiple train crossing are missing. For a comprehensive description of the monitoring system and data, readers are directed to [50].

During the monitoring period, the bridge underwent retrofitting to address a construction error. This process involved reinforcing the connections between the diagonals, arches, and bridge deck. The retrofitting occurred between 15 May and 27 September. Therefore, there exist measurements from three distinct time periods: the original bridge before the retrofit (7.5 months); during the works of retrofit installation (4.5 months); and for the strengthened bridge with the operational retrofit (3.5 months).

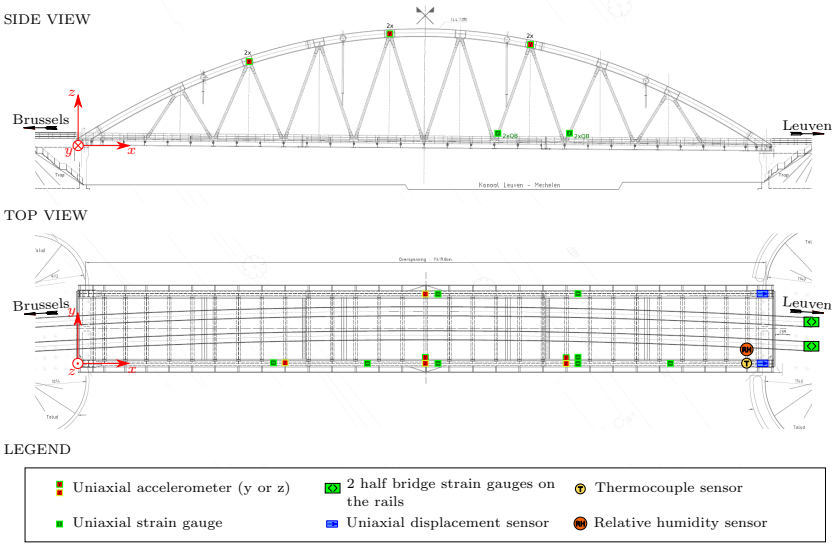

Figure 11: Sketch of KW51 bridge with an overview of the measurement setup. Sensors installed on the diagonals and the arches are shown in the side view and sensors installed on the bridge deck are shown in the top view [49]

.

4.2. Data preparation and training

To validate the proposed method, only acceleration signals during train passages are considered. Each day the bridge was in operation, two train passages were recorded. For each passage, vibration data was collected from 10 seconds before the train entered the bridge until 30 seconds after the train left. To focus on data collected while the train was on the bridge, a 10-second time window was removed. For each sensor, the moving root-mean-square (RMS) value of acceleration was calculated for a 1-second interval, and when that value fell below the 0.05 m/s^2 threshold, the remaining signal was discarded. The acceleration signals had a sampling frequency of 825.8065Hz. In this study, six acceleration sensors were used, including four in the vertical direction and two in the lateral direction, as shown in Fig. 11.

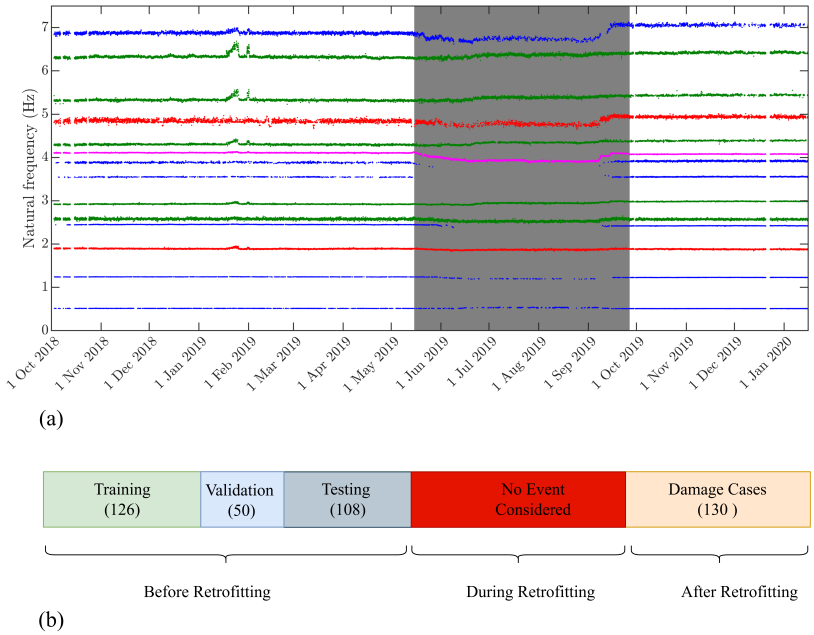

Figure 12: (a) Identified frequencies of the KW51 Bridge, with the shaded area representing the time period during which the installation of the retrofitting was carried out; The color blue corresponds to the lateral modes of the arches, while red represents the lateral modes of the bridge deck. The color green denotes global vertical modes, and magenta indicates global torsional modes; (b) Visualisation of dataset used for assessing bridge conditions. In brackets, number of train crossing events

For the PTAE training, 284 train crossing events were considered before the retrofitting, and 130 train passage events were identified after the retrofitting for damage detection cases. No train passages were taken into account during the retrofitting stage, as Fig. 12a clearly shows significant changes in bridge modal frequencies. Any existing damage detection method would identify the change in structural behaviour. This period of the monitoring campaign is not representative of typical damage. On the other hand, after the bridge is fully strengthened (retrofitted) the structural response can be considered as "positive" damage. a change in the structure. The train crossing events before retrofitting were further divided for training, validation, and testing, as shown in Fig12*b*.

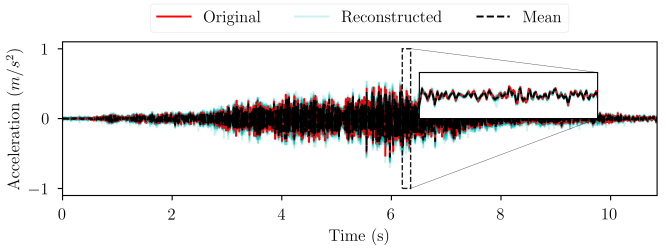

(a)

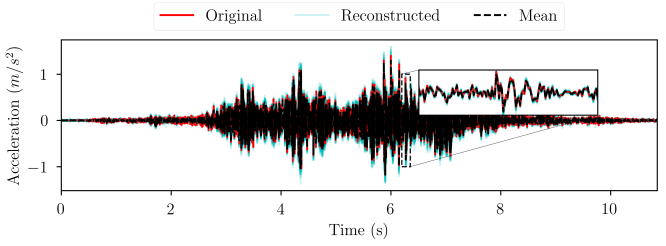

(b)

Figure 13: Comparison between original and reconstructed signals from two sensors; (a)Vertical acceleration signal at mid-span of the bridge (Track A, North side); (b)Vertical acceleration signal at mid-span of the bridge (Track B, South side

A pre-processing step was implemented to slice the signal into fixed window lengths of 128 and 256 samples, using the procedure discussed in Section 2.4. Two separate PTAE models were trained with the same architecture as described in Section 3.4, with $m = 6$ and $z = 1$. For the model using a window size of 256, the input shape became (256 x m), and the architecture's shape was adjusted accordingly. During training and subsequent testing, 50% random connection pruning was performed for each forward pass. The trained PTAE network was tested with 50 simulations for the same input. Fig. 13 displays the reconstructed signals and their respective mean responses of randomly chosen events from the testing dataset. The zoomed-in sections of each signal show that the mean value of multiple passes aligns well with the original input signal. These results were expected since the model was trained and tested with a dataset from the same bridge conditions (before retrofitting).

4.3. Results

This section evaluates the PTAE model's ability to detect changes in the bridge's condition (after retrofitting). The trained PTAE is employed to reconstruct the input frames for training, validation, and testing data. The NRMSE is calculated for each window frame. The distribution of computed NRMSE for the training dataset of all acceleration sensors is utilised to compute the mean ($\boldsymbol{\mu}_1$) and covariance matrices (Σ_1), representing the baseline condition. Likewise, for each subsequent event, the statistics (mean ($\boldsymbol{\mu}_2$) and covariance matrices (Σ_2)) of NRMSE are calculated and used in Eq. 6 to compute the damage feature. Before applying the EWMA-based damage index, outliers are removed from the dataset using the method discussed in Section3.5.1. The EWMA is applied with the value of $\alpha = 0.02$ and $L = 4$ to compute the damage index using Eq. 8. The threshold is calculated using the damage index data computed for the validation events by employing the UCL (Eq. 9) and LCL (Eq. 10) expressions. Similar to the numerical case study, OC-SVM with the same parameters is also trained with the validation dataset and subsequently used to differentiate between the two bridge conditions.

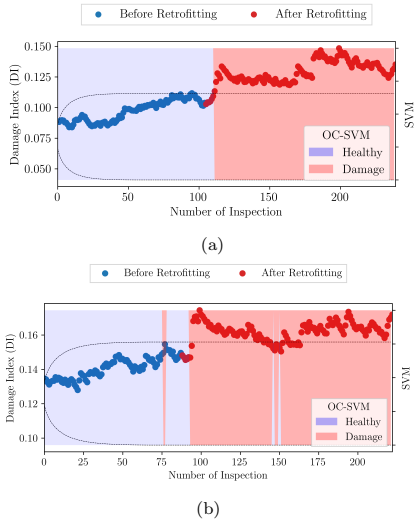

Figure 14: Evolution of damage index over periods of the monitoring campaign. The dashed lines indicate the UCL and LCL threshold values. (a) PTAE is trained with window size 128; (b) PTAE is trained with window size 256.

Fig. 14 demonstrates how to track the bridge condition's evolution using train crossing events. A threshold line is established, and significant deviation from this line indicates a change in the structure's condition. Fig. 14*a* and Fig. 14*b* display the results of the bridge's condition assessment using two different window lengths. The effect of retrofitting is clearly depicted by the jump in the damage index at the end of the time period when no retrofitting had been applied. Likewise, OC-SVM can effectively differentiate between the two bridge conditions, particularly when the model is trained using a length of 128, as depicted in Fig. 14*a*. In instances where the window length was 256, both the proposed method and SVM misclassified a few train crossing events; however, the overall result remains within a satisfactory performance scope.

In summary, the analysis of the results showcases the effectiveness of the proposed PTAE model-based damage index in detecting changes in the bridge's condition, particularly when the extent of damage or alteration in condition is minimal. The method presents a reliable and efficient means for assessing the bridge's condition by solely utilising train-induced responses,

while employing different window lengths and monitoring the damage index. It is important to note that the proposed method exhibits considerable robustness against environmental fluctuations, even without implementing specific data pre-processing methods to eliminate the effects of varying environmental and operational conditions. This study sets the stage for further advancements in structural health monitoring and provides valuable insights for implementing bridge monitoring systems using vehicle-induced responses.

5. Conclusions

This paper presents an innovative methodology for assessing bridge conditions using a probabilistic temporal autoencoder (PTAE). By gathering multi-sensor data during train crossings and employing a PTAE comprising multiple convolutional blocks and an LSTM recurrent neural network, the framework effectively extracts features and captures temporal relationships in the data. Through the computation of the reconstruction loss and KL divergence-based damage features, the methodology enables the detection of potential damage in the bridge structure. The application of an Exponentially Weighted Moving Average (EWMA) filter and a control chart-based threshold mechanism further refines the damage assessment process, allowing for differentiation between healthy and subsequent progressive damage cases. The effectiveness of the proposed method was evaluated using numerically generated data, where a train crossed a simply supported bridge under realistic speed and loading conditions. Similarly, the methodology was validated by applying it to data obtained from the KW51 bridge to detect different bridge conditions. The main findings and advantages of this study can be summarised as follows:

- The proposed methodology accommodates multi-sensor data, such as accelerations, displacements, and rotations, making it adaptable to various monitoring scenarios and sensor configurations. This also allows for the avoidance of manual feature extraction or single sensor level model training for similar tasks.
- The probabilistic nature of the autoencoder enhances robustness for varying operational and environmental conditions and enables the quantification of uncertainty in predictions under these conditions.

- The Exponentially Weighted Moving Average (EWMA) control chart-based threshold mechanism facilitates the identification of subtle changes in the bridge's condition, allowing for early damage detection and timely maintenance interventions.
- The results of this study suggest that detecting and quantifying different types of damage is possible even without employing any pre-processing method to remove the effects of operational and environmental conditions.
- By incorporating model uncertainty and providing accurate damage assessments, the methodology supports better decision-making in maintenance planning and resource allocation.
- The proposed method can be easily integrated with existing monitoring systems and data collection platforms, enabling seamless adoption and implementation in various contexts.

In conclusion, this methodology holds significant potential for the future of bridge health monitoring and maintenance, offering a data-driven solution that can enhance the safety of infrastructure.

Acknowledgement

The authors would like to acknowledge Kristof Maes and Geert Lombaert, members of the Structural Mechanics Section at KU Leuven, for providing the measurement data for the KW51 bridge.

References

[1] B. F. Spencer Jr, V. Hoskere, Y. Narazaki, Advances in computer vision-based civil infrastructure inspection and monitoring, Engineering 5 (2) (2019) 199–222.

[2] H. Nick, A. Aziminejad, Vibration-based damage identification in steel girder bridges using artificial neural network under noisy conditions, Journal of Nondestructive Evaluation 40 (2021) 1–22.

[3] Z. Lingxin, S. Junkai, Z. Baijie, A review of the research and application of deep learning-based computer vision in structural damage detection, Earthquake engineering and engineering vibration 21 (1) (2022) 1–21.

[4] Y. An, E. Chatzi, S.-H. Sim, S. Laflamme, B. Blachowski, J. Ou, Recent progress and future trends on damage identification methods for bridge structures, Structural Control and Health Monitoring 26 (10) (2019) e2416.

[5] Y. Zhang, K.-V. Yuen, Review of artificial intelligence-based bridge damage detection, Advances in Mechanical Engineering 14 (9) (2022) 16878132221122770.

[6] O. Avci, O. Abdeljaber, S. Kiranyaz, M. Hussein, M. Gabbouj, D. J. Inman, A review of vibration-based damage detection in civil structures: From traditional methods to machine learning and deep learning applications, Mechanical systems and signal processing 147 (2021) 107077.

[7] M. M. Alamdari, K. Kildashti, B. Samali, H. V. Goudarzi, Damage diagnosis in bridge structures using rotation influence line: Validation on a cable-stayed bridge, Engineering Structures 185 (2019) 1–14.

[8] F. Huseynov, C. Kim, E. J. Obrien, J. Brownjohn, D. Hester, K. Chang, Bridge damage detection using rotation measurements–experimental validation, Mechanical Systems and Signal Processing 135 (2020) 106380.

[9] E. J. Obrien, J. Brownjohn, D. Hester, F. Huseynov, M. Casero, Identifying damage on a bridge using rotation-based bridge weigh-in-motion, Journal of Civil Structural Health Monitoring 11 (2021) 175–188.

[10] S. Quqa, L. Landi, P. P. Diotallevi, Automatic identification of dense damage-sensitive features in civil infrastructure using sparse sensor networks, Automation in Construction 128 (2021) 103740.

[11] S. Quqa, L. Landi, P. P. Diotallevi, Instantaneous identification of densely instrumented structures using line topology sensor networks, Structural Control and Health Monitoring 29 (3) (2022) e2891.

[12] C. Rainieri, F. Magalhaes, D. Gargaro, G. Fabbrocino, A. Cunha, Predicting the variability of natural frequencies and its causes by second-order blind identification, Structural Health Monitoring 18 (2) (2019) 486–507.

[13] Y. Bao, H. Li, Machine learning paradigm for structural health monitoring, Structural Health Monitoring 20 (4) (2021) 1353–1372.

[14] H. Salehi, R. Burgueño, Emerging artificial intelligence methods in structural engineering, Engineering structures 171 (2018) 170–189.

[15] K. A. Eltouny, X. Liang, Large-scale structural health monitoring using composite recurrent neural networks and grid environments, Computer-Aided Civil and Infrastructure Engineering 38 (3) (2023) 271–287.

[16] M. Z. Sarwar, D. Cantero, Vehicle assisted bridge damage assessment using probabilistic deep learning, Measurement 206 (2023) 112216.

[17] A. I. Ozdagli, X. Koutsoukos, Machine learning based novelty detection using modal analysis, Computer-Aided Civil and Infrastructure Engineering 34 (12) (2019) 1119–1140.

[18] D. Posenato, F. Lanata, D. Inaudi, I. F. Smith, Model-free data interpretation for continuous monitoring of complex structures, Advanced Engineering Informatics 22 (1) (2008) 135–144.

[19] Z. Nie, E. Guo, J. Li, H. Hao, H. Ma, H. Jiang, Bridge condition monitoring using fixed moving principal component analysis, Structural Control and Health Monitoring 27 (6) (2020) e2535.

[20] Z. Ma, C.-B. Yun, H.-P. Wan, Y. Shen, F. Yu, Y. Luo, Probabilistic principal component analysis-based anomaly detection for structures with missing data, Structural Control and Health Monitoring 28 (5) (2021) e2698.

[21] A. Anaissi, M. Makki Alamdari, T. Rakotoarivelo, N. L. D. Khoa, A tensor-based structural damage identification and severity assessment, Sensors 18 (1) (2018) 111.

[22] J. Gu, M. Gul, X. Wu, Damage detection under varying temperature using artificial neural networks, Structural Control and Health Monitoring 24 (11) (2017) e1998.

[23] J. Mao, H. Wang, B. F. Spencer Jr, Toward data anomaly detection for automated structural health monitoring: Exploiting generative adversarial nets and autoencoders, Structural Health Monitoring 20 (4) (2021) 1609–1626.

[24] X. Ma, Y. Lin, Z. Nie, H. Ma, Structural damage identification based on unsupervised feature-extraction via variational auto-encoder, Measurement 160 (2020) 107811.

[25] M. F. Silva, A. Santos, R. Santos, E. Figueiredo, J. C. Costa, Damage-sensitive feature extraction with stacked autoencoders for unsupervised damage detection, Structural Control and Health Monitoring 28 (5) (2021) e2714.

[26] Z. Wang, Y.-J. Cha, Unsupervised deep learning approach using a deep auto-encoder with a one-class support vector machine to detect damage, Structural Health Monitoring 20 (1) (2021) 406–425.

[27] V. Giglioni, I. Venanzi, V. Poggioni, A. Milani, F. Ubertini, Autoencoders for unsupervised real-time bridge health assessment, Computer-Aided Civil and Infrastructure Engineering (2022).

[28] Y. Zhang, Y. Miyamori, S. Mikami, T. Saito, Vibration-based structural state identification by a 1-dimensional convolutional neural network, Computer-Aided Civil and Infrastructure Engineering 34 (9) (2019) 822–839.

[29] M. Z. Sarwar, D. Cantero, Deep autoencoder architecture for bridge damage assessment using responses from several vehicles, Engineering Structures 246 (2021) 113064.

[30] Z. Shang, L. Sun, Y. Xia, W. Zhang, Vibration-based damage detection for bridges by deep convolutional denoising autoencoder, Structural Health Monitoring 20 (4) (2021) 1880–1903.

[31] Y.-W. Wang, Y.-Q. Ni, S.-M. Wang, Structural health monitoring of railway bridges using innovative sensing technologies and machine learning algorithms: a concise review, Intelligent Transportation Infrastructure 1 (2022).

[32] I. Gonzalez, R. Karoumi, Bwim aided damage detection in bridges using machine learning, Journal of Civil Structural Health Monitoring 5 (2015) 715–725.

[33] A. C. Neves, I. González, R. Karoumi, Development and validation of a data-based shm method for railway bridges, Structural Health Monitoring Based on Data Science Techniques (2022) 95–116.

[34] M. R. Azim, M. Gül, Damage detection of steel girder railway bridges utilizing operational vibration response, Structural Control and Health Monitoring 26 (11) (2019) e2447.

[35] A. Meixedo, J. Santos, D. Ribeiro, R. Calçada, M. Todd, Damage detection in railway bridges using traffic-induced dynamic responses, Engineering Structures 238 (2021) 112189.

[36] Y. Gal, Z. Ghahramani, Dropout as a bayesian approximation: Representing model uncertainty in deep learning, in: international conference on machine learning, PMLR, 2016, pp. 1050–1059.

[37] R. Pascanu, T. Mikolov, Y. Bengio, On the difficulty of training recurrent neural networks, in: International conference on machine learning, Pmlr, 2013, pp. 1310–1318.

[38] S. Hochreiter, J. Schmidhuber, Long short-term memory, Neural computation 9 (8) (1997) 1735–1780.

[39] N. S. Madiraju, Deep temporal clustering: Fully unsupervised learning of time-domain features, Ph.D. thesis, Arizona State University (2018).

[40] O. Ibidunmoye, A.-R. Rezaie, E. Elmroth, Adaptive anomaly detection in performance metric streams, IEEE Transactions on Network and Service Management 15 (1) (2017) 217–231.

[41] A. S. Neubauer, The ewma control chart: properties and comparison with other quality-control procedures by computer simulation, Clinical Chemistry 43 (4) (1997) 594–601.

[42] D. Cantero, Ttb-2d: Train–track–bridge interaction simulation tool for matlab, SoftwareX 20 (2022) 101253.

[43] L. Fryba, W. Courage, Dynamics of railway bridges, Meccanica 32 (1) (1997) 95–95.

[44] H. Xia, N. Zhang, G. De Roeck, Dynamic analysis of high speed railway bridge under articulated trains, Computers & structures 81 (26-27) (2003) 2467–2478.

[45] D. Cantero, T. Arvidsson, E. OBrien, R. Karoumi, Train–track–bridge modelling and review of parameters, Structure and Infrastructure Engineering 12 (9) (2016) 1051–1064.

[46] K. N. Gia, J. M. G. Ruigómez, F. G. Castillo, Influence of rail track properties on vehicle–track responses, in: Proceedings of the Institution of Civil Engineers-Transport, Vol. 168, Thomas Telford Ltd, 2015, pp. 499–509.

[47] I. Behmanesh, B. Moaveni, Accounting for environmental variability, modeling errors, and parameter estimation uncertainties in structural identification, Journal of Sound and Vibration 374 (2016) 92–110.

[48] S. Seo, A review and comparison of methods for detecting outliers in univariate data sets, Ph.D. thesis, University of Pittsburgh (2006).

[49] K. Maes, L. Van Meerbeeck, E. Reynders, G. Lombaert, Validation of vibration-based structural health monitoring on retrofitted railway bridge kw51, Mechanical Systems and Signal Processing 165 (2022) 108380.

[50] K. Maes, G. Lombaert, Monitoring railway bridge kw51 before, during, and after retrofitting, Journal of Bridge Engineering 26 (3) (2021) 04721001.

PAPER III

Muhammad Zohaib Sarwar, Daniel Cantero

Vehicle assisted bridge damage assessment using probabilistic deep learning, Measurement 206 (2023) 112216.

III

Measurement 206 (2023) 112216

Contents lists available at ScienceDirect

Measurement

journal homepage: www.elsevier.com/locate/measurement

Vehicle assisted bridge damage assessment using probabilistic deep learning

Muhammad Zohaib Sarwar *, Daniel Cantero

Department of Structural Engineering, Norwegian University of Science & Technology, Trondheim, Norway

ARTICLE INFO

Keywords:
Vehicle assisted monitoring
Damage assessment
Highway bridges
Probabilistic deep learning
Fully connected neural network
Uncertainty quantification

ABSTRACT

Vehicle assisted monitoring has shown promising potential for the condition assessment of existing bridges in a road network, by removing practical complications faced in traditional Structural health monitoring (SHM) methods such as traffic interruption and dense deployment of sensors. However, the combination of different measurement sources during vehicle assisted monitoring has not yet been fully explored. This paper aims to evaluate the potential benefit of considering multiple measured responses from various sources, including fixed sensors on the bridge and on-board vehicle sensors. To this end, this paper proposes a Probabilistic Deep Neural Network, a stochastic data-driven framework for damage assessment. This framework enables the combination of vehicle and bridge responses to extract damage sensitive features for the classification of different damage states. In addition, the proposed method estimates the uncertainty of its predictions, providing an indication of the reliability of the result. The proposed method is validated using two numerical based case studies while considering realistic operational conditions, which include temperature oscillations, additional traffic, and measurement noise. The results from this study indicate that combining multiple sensor information results in lower uncertainties in damage detection and localisation. The results also suggest that the proposed method is robust in handling measurement noise and varying environmental conditions.

1. Introduction

The growing stock of bridges is continuously subjected to deterioration caused by different factors, such as excessive loading, fatigue, corrosion, and environmental impact [1]. A failure to identify these damages at an early stage can lead to catastrophic outcomes in terms of human life and the economy. Currently, for safe and reliable operation of bridges, visual inspection based methods are in practice, which are generally expensive and prone to errors [2]. With recent advancements in sensing technologies and data acquisition systems, vibration-based health monitoring solutions are promising alternatives for effective and accurate tracking of the structural deterioration processes [3]. These methods mainly rely on the detection of damage and potential anomalies by analysing the dynamic response of bridges.

Vibration-based Structural Health Monitoring (SHM) systems can be categorised into fixed or mobile sensing frameworks. In a fixed sensing framework, the sensors are directly installed at a fixed location of the target bridge. There are three main challenges associated to this framework. First, the extensive deployment requirements in terms of cost and labour, that is generally prohibitive for the inspection of short to medium span bridges. Second, the spatial information obtained with a fixed sensing system is mainly confined to certain discrete locations, which adversely affects the outcome of the bridge's assessment. The third main challenge is that often the collected vibration data is obtained during ambient and forced vibration. However, the bridge response induced by ambient vibrations and random traffic loading may not be sufficiently big to excite the stiff bridge properly and the measured responses are often corrupted by measurement noise [4]. While forced vibration responses can be obtained using impact load testing, human-induced loads or by applying hydraulic actuators, which in practice significantly affect the serviceability of the bridge and increase maintenance costs. In recent years Vehicle assisted monitoring is an active research topic. In vehicle assisted monitoring, traversing vehicles are used as the source of excitation. The forced response of the bridge is measured using installed sensors on the bridge or sensors installed inside the moving vehicles. With this framework the process of the bridge's excitation becomes relevantly economical and bridge vibration data is only acquired when the vehicle is on the bridge. Moreover, when vehicles are acting as mobile sensors, the measured responses contain all the spatial information of the target bridge, which significantly improves the condition assessment of bridges [5].

In recent years, many researchers have explored vehicle assisted monitoring systems to perform damage assessment. Shokravi et al. [6] conducted a comprehensive review on conventional vehicle assisted bridge damage assessment techniques. These techniques can be categorised into direct (fixed sensing) or indirect (mobile sensing). Using direct sensing, [5,7] applied Moving Force Identification (MFI)

* Corresponding author.
E-mail addresses: muhammad.z.sarwar@ntnu.no (M.Z. Sarwar), daniel.cantero@ntnu.no (D. Cantero).

https://doi.org/10.1016/j.measurement.2022.112216
Received 19 August 2022; Received in revised form 3 November 2022; Accepted 14 November 2022
Available online 21 November 2022

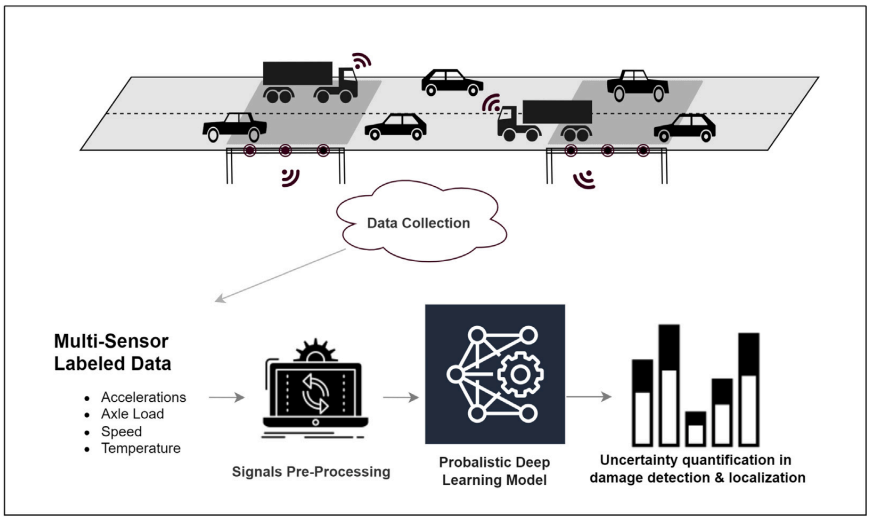

Fig. 1. Main overview of proposed framework.

method for bridge damage assessment. Furthermore, in [8,9] the authors utilised the measured rotational response of a bridge under the influence of moving loads for damage assessment. On the other hand, indirect techniques (or drive-by) have also been studied for bridge damage assessment, of which Wang et al. [10] provide a detailed overview of their application. The reported methods mainly rely on advanced signal processing techniques and machine learning methods for damage detection. For instance, [11,12] used data driven techniques and statistical analysis for damage detection and quantification. While [13,14] estimate the contact point response between vehicle and bridge for damage detection and localisation.

Therefore, it can be concluded that vehicle assisted monitoring systems have great potential to be used for damage assessment. The reported methods have limitations and face unaddressed challenges, which include the influence of vehicle speed, the effect of road profile and additional random traffic, and the requirement of specialised vehicles, among others. However, considering the merits of direct and indirect methods, it is possible that the combination of both strategies could be advantageous and complement each other. The combination of recent advancements in wireless sensing systems to instrument the infrastructure together with the increasing trend of equipping vehicles with multiple sensors, opens the possibility for Vehicle to Infrastructure (V2I) connectivity. This integration has shown potential benefits to improve traffic and resources management [15,16]. However, to the author's best knowledge this interconnectivity between vehicle and bridge sensors has not been fully explored in the context of damage assessment and bridge maintenance.

Traditionally, free and ambient vibration responses have been used for SHM relying on the assumption that the acquired structural responses are linear and stationary. However, this assumption does not hold when the bridge is exited by a moving vehicle, when the structural dynamic properties are time-varying making the response nonstationary. Then, combining multi-variant data (fixed sensors and moving sensors) and extracting damage sensitive features is a challenging task. Recently, Deep Learning (DL) models are getting significant attention in SHM applications. Deep learning models are tools that can be used to find complex non-linear correlations within the datasets. These models have the ability to combine multi-sensor data and perform various tasks, including non-linear feature extraction, classification and regression. For damage assessment, Ni et al. [17] and Zhang et al. [18] used a 1-D Convolutional Neural Network (CNN) to extract damage sensitive features from acceleration responses. Zhang et al. [19] used phase motion estimation and CNN for damage detection application. In [20,21] applied the CNN based method for condition assessment of engine valve and rolling bearings. Similarly, for bridge health monitoring Ma et al. [22] applied a convolutional variational autoencoder to compress the high-dimensional data to a low-dimensional feature space, which was then used to establish a damage index, and validated experimentally. In [23], the authors proposed the idea of the natural excitation technique for data normalisation and then applied 1-D CNN for automated damage detection. Nevertheless, the practical implementation of DL models for SHM is hindered because the collected training data does not contain all operational and loading conditions, which would facilitate the quantification of the uncertainty in decision output of the model. For reliable decision making, the SHM system must be able to handle uncertainty in its predictions.

Therefore, the goal of this study is to develop a damage assessment method for bridges by combining forced response data obtained from fixed and moving sensors, capable of quantifying the uncertainties of the output. This study presents a data-driven method for damage assessment using vehicle assisted monitoring data. The main overview of the proposed framework is shown in Fig. 1, where data from multiple sources is collected. The gathered data is further analysed using advanced data-driven methods for damage assessment. A probabilistic Deep Neural Network (PDNN) based framework is developed in order to extract damage sensitive features and account for uncertainty in predictions. The framework leverages the usage of probabilistic neural layers, which can represent the problem's uncertainties. Monte Carlo analysis is used to sample the weights from trained models to predict different damage states. To evaluate the performance of the proposed approach, ten different information scenarios (signal source combinations) are considered for training each PDNN. The idea is validated numerically for two types of bridges traversed by 5-axle trucks. The study considers a range of vehicle dynamic properties and the presence of road profile and evaluates the effect ambient temperature variations, additional traffic, and measurement noise.

The remainder of the paper is organised as follows. Section 2 provides an overview of the proposed deep learning strategy, including architecture of the model and implementation details. Section 3 presents the details of the vehicle-bridge interaction model used to generate the datasets. Section 4 evaluates the performance of the proposed

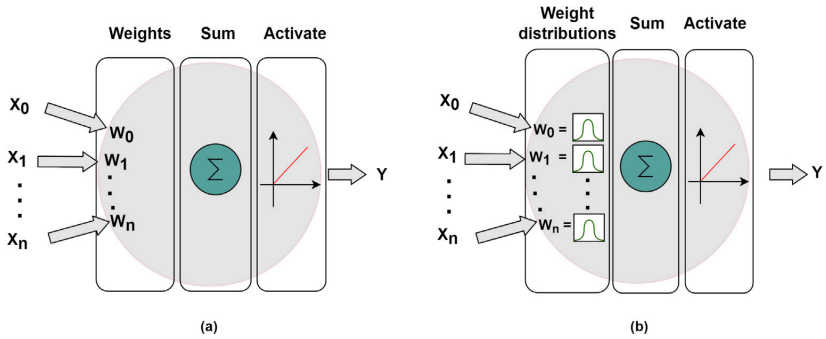

Fig. 2. Basic ANN model; (a) with deterministic weights; (b) with probabilistic weights.

method for two case studies, a simply supported bridge and a multi-span continuous bride. Section 5 provide the discussion on overall finding of the proposed studies. Section 6 summarises the findings of this study.

2. Deep learning model

2.1. Research significance

Deep Learning (DL) based models are widely used in SHM applications, including damage assessment. In that case, these models provide solutions to tackle the problem of differentiating among large number of damage classes [1]. However, DL models are prone to underfitting or overfitting, which affect their generalisation capabilities for the given data [24]. What is more, these models also tend to be overconfident in their predictions and do not account for the inherent uncertainties [25] of the problem. To overcome these issues, probabilistic deep learning based models have been proposed. These models provide the framework to account for the uncertainty in their predictions. Probabilistic Deep Neural Networks (PDNN) are stochastic artificial neural networks that are trained by using a Bayesian approach [26].

2.2. Probabilistic deep neural network

Standard Deep Neural Network (DNN) are built using an input layer $\boldsymbol{l_0}$, multiple hidden layers $\boldsymbol{l}_i$ (for $i = 1, 2, \ldots, n-1$) with non-linear operations, and a final output layer $\boldsymbol{l}_o$. For a simple feedforward network, each layer $\boldsymbol{l}$ is composed of linear transformation and activation function denoted as α. The goal in a simple DNN is to approximate an arbitrary function $\boldsymbol{Y} = \boldsymbol{\Phi}(\boldsymbol{X})$, based on the input $\boldsymbol{X}$. Their architecture can be summarised as follows:

$$\begin{aligned} &\boldsymbol{l_0} = \boldsymbol{X}, \\ &\boldsymbol{l}_i = \alpha(\boldsymbol{W}_i \boldsymbol{l}_{i-1} + \boldsymbol{b}_i) \quad i \in [1, n], \\ &\boldsymbol{Y} = \boldsymbol{l}_n \end{aligned} \tag{1}$$

Here, n is the number of hidden layers while $\boldsymbol{W}$ and $\boldsymbol{b}$ are the weights and biases of the network. These learning parameters $\boldsymbol{\theta} = (\boldsymbol{W}, \boldsymbol{b})$ are optimised as single deterministic estimates for a given data set (Fig. 2a) using backpropagation algorithm.

On the other hand, stochastic neural networks or PDNN are built by introducing stochastic components into the network [27]. The stochastic neural networks are mainly built to account for two types of uncertainties: either the randomness in the input data or the uncertainties in the estimated parameters of the deep learning model. The first one can be handled by using probability distributions in the loss function as discussed in thoroughly in [28]. While the latter can be accounted for by considering weights as stochastic (Fig. 2b) to simulate multiple possible model parameters $\boldsymbol{\theta}$ with their associated probability distribution $p(\boldsymbol{\theta})$. For this study the main goal of PDNN is to capture the associated uncertainty of the underlying processes. This can be achieved by evaluating predictions of multiple parameterised $\boldsymbol{\theta}$ sampled models. If the outputs of multiple models agree, then the uncertainty is considered to be low. While in the case of extended disagreement in predictions, then the uncertainty is considered as high. The process at a high level can be expressed as:

$$\begin{aligned} &\boldsymbol{\theta} \sim p(\boldsymbol{\theta}), \\ &\boldsymbol{Y} = PDNN_{\theta}(\boldsymbol{X}) + \varepsilon \end{aligned} \tag{2}$$

where ε represents a noise to account for the fact that $PDNN_{\theta}$ is only a probabilistic approximation of a function.

In order to design the PDNN, the first step is to select the architecture of the neural network, namely a fully connected network or a convolutional neural network. Then the second step is to include the selection of prior distributions over the possible model parameters $p(\boldsymbol{\theta})$ and their prior confidence over the predictive power of the model $p(\boldsymbol{Y}|\boldsymbol{X}, \boldsymbol{\theta})$. For supervised learning, Bayesian posteriors can be computed as shown in Eq. (3) by applying Bayes's theorem and considering independence between the input data D and the model parameters $\boldsymbol{\theta}$.

$$p(\boldsymbol{\theta}|D) = \frac{p(D_y|D_x, \boldsymbol{\theta})\, p(\boldsymbol{\theta})}{\int p(D_y|D_x, \boldsymbol{\theta}^*)\, p(\boldsymbol{\theta}^*)\, d\boldsymbol{\theta}^*} \tag{3}$$

where D_x and D_y are training inputs and training labels for the dataset D. In complex models such as deep neural networks, Bayesian posteriors become high dimensional probability distributions. This issue makes computing and sampling using the standard method an intractable problem, especially computing the evidence (denominator) in Eq. (3). To mitigate this problem and for practical implementation, variational inference is applied, which learns a variational distribution to approximate the exact posterior. The main idea behind variational inference is to have a prior variational distribution $q_{\phi}(H)$ parameterised by a set of parameters ϕ and then learn those parameters such that it is close to the exact posterior. More details about variational inference can be found in [25]. Therefore, the probabilistic prediction with known posterior can be expressed as:

$$p(\boldsymbol{Y}|\boldsymbol{X}, D) = \int p(Y|X, \boldsymbol{\theta}^*)\, p(\boldsymbol{\theta}^*|\boldsymbol{D})\, d\boldsymbol{\theta}^* \tag{4}$$

Eq. (4) can be interpreted as the predictive distribution of an infinite ensemble of networks. In practice $p(\boldsymbol{Y}|\boldsymbol{X}, D)$ is sampled indirectly from Eq. (2). The final prediction can be computed via a Monte Carlo analysis [29] by using a finite number of randomly sampled weight parameters from the posterior to compute the series of possible outputs as shown in Fig. 3. In order to measure the uncertainty in the classification problem the average model prediction will give the probability of each class, which can be computed as follows:

$$\hat{\boldsymbol{p}} = \frac{1}{N} \sum_{\boldsymbol{\theta}_i \in \boldsymbol{N}} PDNN_{\boldsymbol{\theta}_i}(\boldsymbol{X}) \tag{5}$$

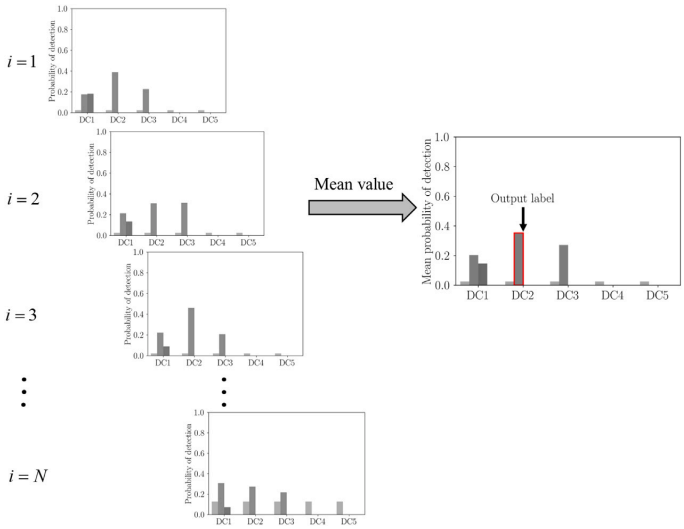

Fig. 3. Illustration to compute final prediction for single input using probabilistic deep neural network.

where N is the number of total samples used for the Monte Carlo analysis. To get the final prediction as shown in Fig. 3, the most likely class can be taken as:

$$\hat{\boldsymbol{Y}} = \arg\max_{i} p_i \in \hat{\boldsymbol{p}} \tag{6}$$

2.3. Network architecture of probabilistic deep neural network

In recent years, Fully Convolutional Neural networks (FCN) have shown the state of the art performance in classifying time series datasets for a wide range of fields, including SHM [1,30]. FCN has been mainly developed to avoid the demanding pre-processing and feature extraction task on raw data in classification problems. However, they are mainly limited to univariate time series [31]. Karim et al. [32] proposed the augmentation of FCN with Long Short-Term Memory (LSTM) recurrent neural network. This significantly enhances the performance of FCN with a nominal increase in computational cost and has also shown satisfactory performance on various multivariate time series datasets [33]. The network architecture proposed in this paper is mainly inspired by [33] with some modifications according to the problem at hand.

For vehicle assisted damage assessment, the input dataset would include information from multiple sensors (vehicle speed, axle loads, acceleration responses and temperature). The proposed neural network is designed to utilise all (or parts) of this information. The proposed model is mainly divided into two modules, as shown in Fig. 4. The first module takes the time series measurements as input. The architecture of this module is similar to what is proposed in [33]. This module includes three temporal convolutional blocks used as a feature extractor. Each convolutional block includes convolutional layers with filter sizes 128, 256 and 128, strides value as 2 and a kernel size of 7, 5 and 3 respectively. Each convolutional layer is followed by a non-linear activation function (ReLU). In addition to that, it is assumed that the bias and kernel in the convolutional layers are drawn from distributions. Finally, the extracted features are fed into global average pooling layers, which substantially reduces the number of weights of the model, as opposed to feeding the dataset directly to a fully connected layer.

In parallel, the time series input is passed through the dimension shuffle layer. The transformed input is then passed to the LSTM block followed by the activation function and dropout layer. The main goal of this block is to learn the global temporal information of each variable at each time step. The multivariate time series has T time steps (length of signal) and K variables (number of different sensors). Each variable K is defined as a channel of the FCN block. However, if the same data is passed through the LSTM block, then the LSTM would require T time steps to process K variables per time step, which significantly increases the computational cost and adversely affects the efficiency of the model. Instead, the dimension shuffle layer is applied, which effectively transposes the temporal dimension of the input data. After this operation, the input of LSTM now receives the entire time history T of each variable K at each time step. As a result, the LSTM block has global temporal information of each variable at the same time, which significantly helps in improving the overall performance of the model and also reduces the time of training.

In addition, the input data can also have some discrete valued information. In the case of vehicle assisted monitoring, vehicle speed, axle weights and temperature information can be combined to see the overall effect of these features in damage assessment. In order to add these features, the second module is designed using 4 fully connected layers, with layer sizes (32, 64, 64 and 32), followed by the ReLU activation function. Here it is assumed that the bias and kernel in the fully connected layers are also drawn from distributions, as done in the convolutional layers. The output of the last fully connected layer, the global average pooling layer of FCN, and the LSTM block are concatenated and fed into a fully connected layer with Softmax as an activation function for the classification task.

2.4. Implementation

The proposed model is implemented using TensorFlow's probability module and Keras [34]. The FCN convolutional layers are implemented using the convolutional1DFlipout, while DenseFlipout layer is used for the fully connected layers. These layers implement the Bayesian inference by assuming that the bias and kernel are drawn from distributions, which are approximated with the Flipout Monte Carlo estimator [35]. The implementation of each layer assumes the prior for weight $\boldsymbol{W}$ as Gaussian distribution with zero mean μ and unit variance σ^2. For the approximation of the posterior distribution and the classification task,

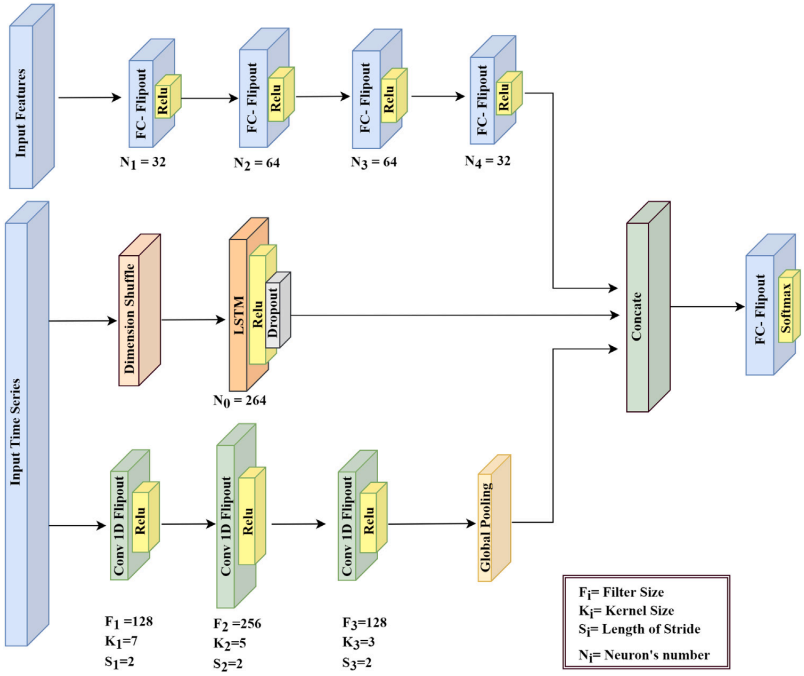

Fig. 4. Architecture of probabilistic deep neural network (PDNN).

Flipout gradient estimator is used to minimise the loss function, called as negative Evidence Lower Bound (ELBO) which is expressed as:

$$\boldsymbol{L}(\boldsymbol{W}_{(\mu,\sigma^2)}) = \underset{\mu,\sigma^2}{\arg\min} \sum_{(\boldsymbol{X},\boldsymbol{Y})\in\boldsymbol{D}} log[p(D_y|D_x,\boldsymbol{\theta})] + D_{\mathrm{KL}}(q_{\boldsymbol{\phi}} \,||\, P) \tag{7}$$

The loss term shown in Eq. (7) is the sum of the negative log-likelihood and the approximated Kullback–Leibler (KL) divergence, which measures the distance between variational and posterior distributions. The KL term here acts as a regularisation term to prevent overfitting on the training dataset.

3. Numerical modelling

This section presents the vehicle-bridge interaction model used to simulate the vehicle responses while traversing a bridge. Fig. 5 shows the schematic representation of the vehicle-bridge coupled system. This numerical model can simulate multiple vehicle crossing events at different speeds, while including the effect of road irregularities. The generated vehicle responses constitute the signals used to evaluate the performance of the proposed PDNN model for damage detection and quantification.

The vehicle model used in this study represents an articulated 5-axle truck with a tractor-trailer configuration. The tractor has two axles and the trailer has three axles at the back. The main bodies of tractor and trailer are modelled as rigid bodies, while the axles are represented as lumped masses. The main bodies are connected to the axle masses by spring and dashpot systems, while the axle masses are connected to the road profile using single springs representing the tyres. The vehicle model has a total of 8 independent Degrees Of Freedom (DOFs) and 1 dependent DOF because of the articulation between tractor and trailer [36,37]. The generic equation of motion of such a vehicle model can be represented as:

$$\boldsymbol{M_v}\ddot{u}_v + \boldsymbol{C_v}\dot{u}_v + \boldsymbol{K_v}u_v = \boldsymbol{F_v} \tag{8}$$

In Eq. (8), $\boldsymbol{M_v}$, $\boldsymbol{C_v}$, and $\boldsymbol{K_v}$ are the mass, damping and stiffness matrices, while u_v contains the displacements of all DOFs of the vehicle model. The vehicle parameters and their variability are taken from [12], for the realisation of Monte Carlo simulations. The values of the vehicle parameters are mainly based on European 5-axles trucks and adopted from [38,39]. This study utilises the 5-axle truck model because it is arguably the most frequent heavy vehicle found on European roads.

The bridge is simulated using a Finite Element Model (FEM) representation, consisting of beam elements with 2 nodes and 2 DOFs per node. The bridge has length L, second moment of area I, mass per unit length ρ, and modulus of elasticity E. Eq. (9) represents the equation of motion of the bridge model:

$$\boldsymbol{M_b}\ddot{u}_{br} + \boldsymbol{C_b}\dot{u}_{br} + \boldsymbol{K_b}u_{br} = \boldsymbol{F_{br}} \tag{9}$$

where $\boldsymbol{M_b}$, $\boldsymbol{C_b}$, and $\boldsymbol{K_b}$ are the mass, damping and stiffness matrices, while $\ddot{u}_{br}$, $\dot{u}_{br}$ and u_{br} are the vectors of accelerations, velocities and displacements for each node. To consider the effect of pavement irregularities on the vehicle and bridge responses, the road profile is represented as ISO class A [40]. Fig. 6 shows the road profile generated for the two bridges studied in Section 4. In each figure, the black lines indicate the span of the bridges. In addition, the road profiles have a 100 m approach distance to allow the traversing vehicle to achieve dynamic equilibrium before entering the bridge. In order to represent the contact surface of the truck tyres, a moving average filter of 0.24 m is applied to the profile as suggested in [41].

Finally, to simulate the vehicle-bridge interaction, the equations of motion of the vehicle and bridge models are coupled together into the system of second order differential equations shown in Eq. (10).

$$\boldsymbol{M_c}\ddot{u}_c + \boldsymbol{C_c}\dot{u}_c + \boldsymbol{K_v}u_v = \boldsymbol{F} \tag{10}$$

where in $\boldsymbol{M_c}$, $\boldsymbol{C_c}$, and $\boldsymbol{K_c}$ are the time varying mass, damping and stiffness matrices respectively. The vectors $\ddot{u}_c$, $\dot{u}_c$, and u_c contain the

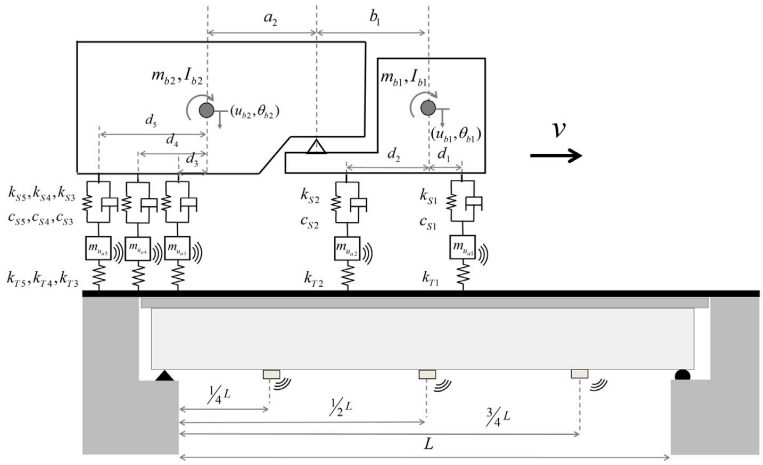

Fig. 5. Vehicle-bridge interaction model for a 5-axle truck traversing a simply supported bridge.

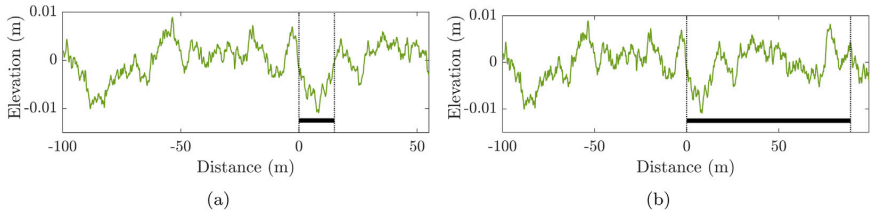

Fig. 6. Road profile of class A and location of bridges (black lines); (a) for study with 15 m simply supported bridge; (b) for study with multi-span continuous bridge.

responses (accelerations, velocities and displacements) of all DOFs of vehicle and bridge. The VBI analysis is carried out by integrating the equations of motion using Newmark-β scheme and implemented in MATLAB [42]. For more details about the coupling procedure and the solution method, the reader is referred to [43].

4. Validation of proposed method

This section applies the proposed damage detection method to 2 separate case studies. Each case study is investigated for a range of damage cases, information scenarios and simulation modes. Fig. 7 provides a schematic overview of all the possibilities considered in this study. The case study A is based on a relatively short simply supported reinforced concrete bridge. It is used to investigate the performance of the proposed method for different damage cases and information scenarios for simulation mode 1 only. At the same time, this case study is used as an example to explain in detail several aspects of the proposed method. In case study B, the method is applied to a multi-span continuous bridge to evaluate the influence of environmental (temperature) and operational effects (additional traffic) by considering different simulation modes (Fig. 7). For both case studies, the crossing vehicles are modelled as fleet of similar vehicles. To model the fleet of the vehicle the variation in vehicles properties is applied to account for normal fluctuations in payload and the inherent uncertainties of the mechanical properties of each vehicle.

4.1. Case study A: Simply supported bridge

4.1.1. Data generation

In this case study, 5-axle trucks travelling over a class A road profile traversing a simply supported bridge, as shown in Fig. 5, are simulated with the vehicle-bridge interaction model presented in Section 3. The FEM of the bridge consists of 30 elements for a total span length L of 15 m. The corresponding section and material properties are: second moment of area $I = 0.5273$ m^4, mass per unit length $\rho = 28\,125$ kg/m, modulus of elasticity $E = 3.5{\times}10^{10}$ N/m^2, and 2% damping. To simulate bridge damage, a localised stiffness reduction in a beam element is considered. In particular, 5 different locations along the beam length are studied with 3 different damage magnitude levels $(15\%, 30\%, 45\%)$ for each location. Therefore, the list of all different damage cases is:

- Healthy case
- Section $L/4$ and stiffness reductions of: 15%, 30%, 45%
- Section $3L/8$ and stiffness reductions of: 15%, 30%, 45%
- Section $L/2$ and stiffness reductions of: 15%, 30%, 45%
- Section $5L/8$ and stiffness reductions of: 15%, 30%, 45%
- Section $3L/4$ and stiffness reductions of: 15%, 30%, 45%

The dataset is generated considering the variation in vehicle properties in such a way that it mimics a fleet of similar vehicles crossing the bridge. The vehicle properties are randomly sampled considering the statistical variability presented in Table A.1. For each of the 16 damage cases, 1000 vehicle passages are simulated, which results a in total 16 000 crossing events. Each event in the dataset contains the information from both, vehicle and bridge. For the 5-axle truck, acceleration measurements from all five axles $\ddot{u}_{a_i}$ is available with a sampling rate of 1000 Hz, as well as, the vehicle speed v, the static axle loads and the ambient temperature. As for the bridge, acceleration readings $\ddot{a}_{br_i}$ are available from 3 assumed sensors installed on the bridge, as indicated in Fig. 8.

The length of the acceleration signals is not the same for all events because the vehicle speed v was randomly sampled for each vehicle

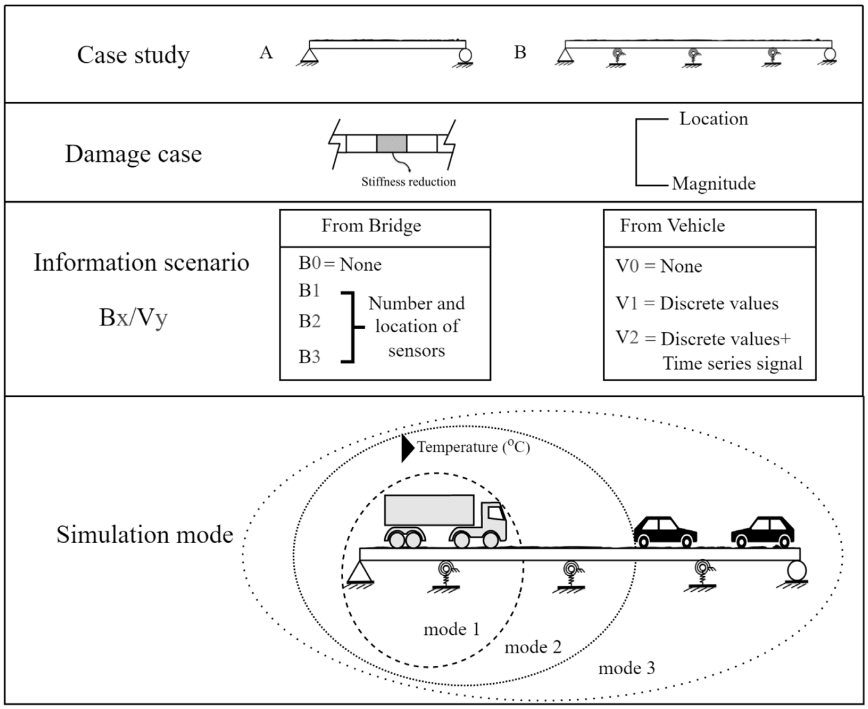

Fig. 7. Overview the possibilities considered in the numerical studies to evaluate the proposed damage detection method.

passage. For the PDNN input, equal length accelerations signals are obtained by zero padding the signals. The length of the required signals depends on the minimum vehicle speed v in the dataset. For this study, the input to the time series module is fixed to $T = 3072$. Therefore, the input size for the time series module of dataset X is $(N, 3072, K)$, for N number of events and K number of variables (number of sensors). On the other hand, the size of the input dataset for the discrete feature module is (N, M), where M is number of input features and M is equal to 3. The dataset has a total 16 output labels, namely the healthy case and 15 different damage scenarios.

4.1.2. Pre-processing

It is well known that the road profile has significant impact on vehicle vibrations. Any measured acceleration within a vehicle is dominated by the excitation produced by the road profile. These road induced vibrations generally mask the component directly related to the bridge response. In previous studies, researchers have applied different techniques to remove the effect of the road profile in vehicle accelerations signals. For instance, in [44], the authors compute the residual response of two connected vehicles, which poses the practical limitation of requiring 2 identical vehicles. Then [45] applied a narrow band pass filter to remove the dynamic effect of the road profile. However, this approach requires to have prior knowledge of the bridge's fundamental frequency. It is safe to say that there is a need for a reliable method that can be used to automatically extract the bridge dynamic response from sensors in passing vehicles.

To address this challenge, in the present study the authors employed the Maximal Overlap Discrete Wavelet Packet Transforms (MODWPT) proposed in [46]. A filter bank based on MODWPT is used here to suppress the road profile component from the vehicle's vertical acceleration signals. MODWPT decomposes the signal $x(t)$ into wavelet components of narrow band frequencies using a wavelet filter [46]. The main advantage of MODWPT over the traditional Discrete Wavelet Transform (DWT) is that it can decompose the signal in both low-frequency and high-frequency signals at each level, whereas DWT can only decompose the signal in low frequency signals [47]. For a given signal $x(t)$, MODWPT produces 2^n equivalent wavelet components W_j, where each has a passband range of $F_s/2^{n+1}$, for a sampling frequency F_s and level number n. Then, the sum of all wavelet components is equal to the approximation of the original signal, as shown in Eq. (11). Similarly, the MODWPT partition of the energy at each wavelet component and the sum of the energy over all the wavelet components is equals the total energy of the input signal [48].

$$x(t) = \sum_{j=1}^{n} W_j(t) \tag{11}$$

In the case of a single vehicle passage, when the truck enters the bridge, the response of the first axle $\ddot{u}_{a_1}$ measures the transient response of the bridge as well as the excitation from the road profile. Then, subsequent axles also cross the same locations on the bridge exposed to the same road profile. Therefore, the dynamic response of all axles should contain the same (or similar) contributions from the road profile. Thus, if the component containing the frequency content of the road profile can be identified in the measured dynamic response, then the contribution of the road profile can be eliminated.

To remove the effect of the road profile from the responses of a vehicle travelling with speed v, the MODWPT with $n = 8$ levels is applied to the axle accelerations $\ddot{u}_{a_i}$. Fig. 9(a) shows the energy level of the first 25 wavelet components (out of 256) for axles 1 and 2. The wavelet components 2 and 3 for axle 1 show significant high energy in comparison to the other components. The additional energy in axle 1 at those particular components can be attributed to the transient response of the bridge. Therefore, it is possible to argue that the sum of certain wavelet components (2 and 3 in this case) from all axle signals $\ddot{u}_{a_i}$ contains predominantly the dynamic response of the bridge.

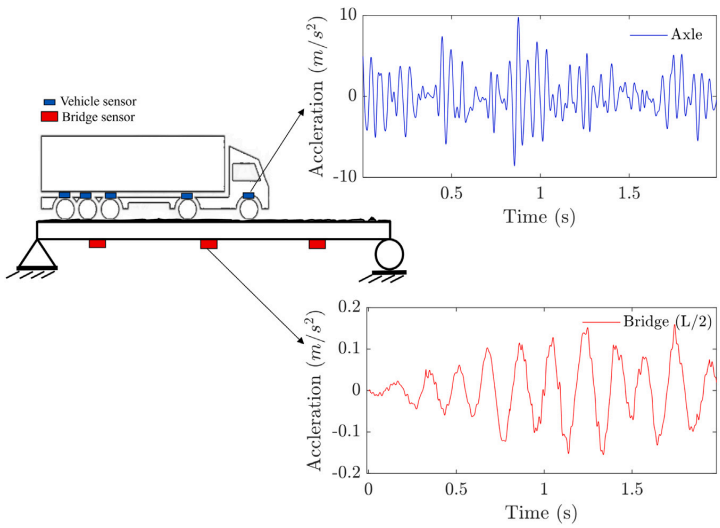

Fig. 8. Samples of signals for case study A.

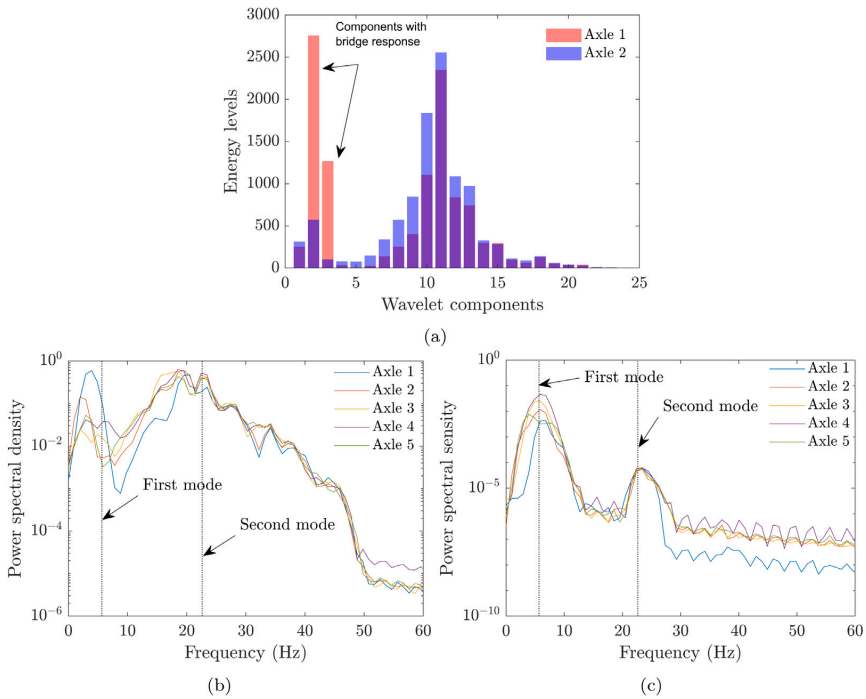

Fig. 9. Pre-processing example; (a) Energy of the wavelet components for axles 1 and 2; (b) Power spectral density of axle responses before applying MODWPT; (c) Power spectral density of axle responses after applying MODWPT.

Fig. 9(b) and (c) show the Power Spectral Density (PSD) of the 5 axle acceleration signals before and after applying MODWPT. The PSD of the raw signals (Fig. 9(b)) shows that the peaks for the first two bridge modes are not distinguishable. However, when the PSD is computed for the sum of the 2nd and 3rd wavelet components, the peaks of first two modes of the bridge are clearly distinguishable (Fig. 9(c)). The advantage of applying MODWPT is clear because it isolates, to a large extent, the contribution of the bridge response in the vehicle acceleration signals. Therefore, the use of filtered vehicle responses via MODWPT is advantageous for structural condition assessment using

drive-by measurements. In this study all vehicle acceleration signals are pre-processed following the procedure discussed in this section.

4.1.3. Evaluation method

In order to demonstrate the performance of the proposed damage detection method, this study considers a range of different information scenarios. Each scenario is defined in terms of the available information for each vehicle crossing event. In some scenarios, the bridge might be instrumented with one or more accelerometers at different sections. In other scenarios, the vehicle might provide no information, discrete values about the event (speed, static axle loads, and temperature), or continuous axle acceleration signals. Thus, several possible scenario exist, which are defined by the amount of information available from both, the vehicle and the bridge. To clearly characterise a given scenario, the following notation has been used:

- B0: No measurement available of the bridge
- B1: Bridge acceleration measurement at section $L/2$
- B2: Bridge acceleration measurement at sections $L/4$ and $3L/4$
- B3: Bridge acceleration measurement at sections $L/4$, $L/2$, and $3L/4$
- V0: No information or measurement available from the vehicle
- V1: Vehicle speed, static axle loads and ambient temperature
- V2: As V1 plus measured axle accelerations

For example, the scenario B1/V2 corresponds to the situation where mid-span bridge accelerations are measured (B1), and the vertical accelerations of all axles of the 5-axle truck are also recorded (V2). Therefore, there exist 10 possible valid scenarios to consider for structural assessment, (since scenarios B0/V0 and B0/V1 do not provide any information about the structure).

The proposed method is applied to these 10 different scenarios, together with a comparative study of the method's performance. Separate PDNN models are created for every information scenario. Fig. 10 shows the flow diagram for training and validation of the PDNN models. More in particular, the datasets are divided into 70–30 splits, for training and validation respectively. For training of the PDNN, a batch size of 128 events is considered, while learning and decay rates are set to $1 \cdot 10^{-4}$ and $1 \cdot 10^{-6}$ respectively, and adaptive moment estimation (Adam) is used as an optimiser. All models are trained using Intel Core i9–10 900 K CPUs with 64 GB RAM and NVIDIA GTX 2080Ti graphic card. Once the model is trained, the single input dataset is evaluated by Monte Carlo based weight sampling from the trained model. The mean value of each prediction by Monte Carlo simulation is computed using Eq. (5). The outcome of the model is the label with the maximum mean probability, and computed using equation Eq. (6).

4.1.4. Results

For the case study A (simply supported beam), the 10 different information scenarios discussed in previous section are studied separately. For each scenario a separate model is trained. The performance of the proposed method for each scenario is evaluated on the basis of overall accuracy of the trained model. The overall accuracy for damage assessment for different combinations of bridge/vehicle information sources is shown in Table 1. It shows that the accuracy of the trained model for scenario B0/V2 (where only vehicle information is available) is equal to 84.2%, which is significantly less compared to the other scenarios. On the other hand, the accuracy of proposed method raises to 91.0% when only using the measurement from a single sensor on the bridge (B1/V0). Then again, the performance of the trained model improves by 4.5 percentage point when including also vehicle axle responses (B1/V2). In addition, the results show that there is no significant performance improvement, in terms of accuracy for damage assessment, when discrete valued vehicle information (V1) is combined with bridge sensors. This can be attributed to the fact that the bridge signals indirectly contain the information (speed and axle loads) of the passing vehicle. Furthermore, accuracy improvements are only marginal in scenarios with multiple bridge signals (B2 and B3) combined with full vehicle information availability (V2). Therefore, the results indicate that a PDNN model can differentiate multiple damage cases with sufficient accuracy solely by extracting damage sensitive features from the bridge signals.

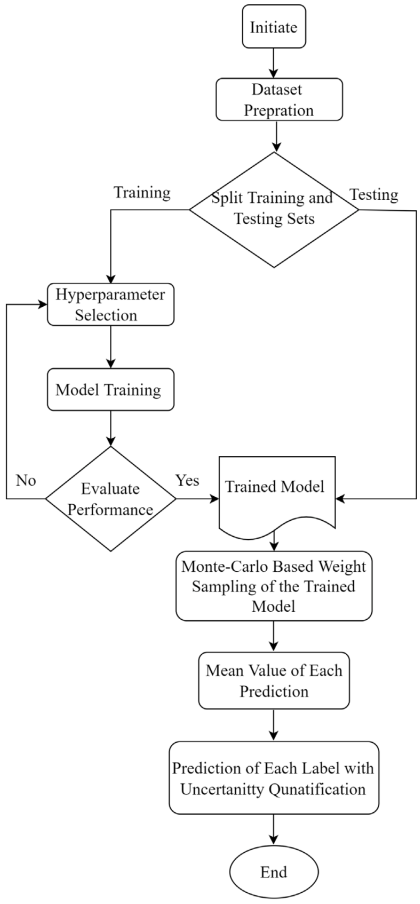

Fig. 10. Flow diagram of probabilistic deep learning model (PDNN).

Table 1
Performance comparison for case study A.

Scenario	V0	V1	V2
B0	NA	NA	84.2%
B1	91.0%	91.2%	95.7%
B2	98.7%	98.9%	99.1%
B3	99.6%	99.2%	99.5%

The performance comparison of the trained models on the validation data provides an indication of the potential use of different information scenarios for damage assessment. But in addition, the use of the PDNN architecture allows us to quantify the uncertainty in the predictions. This is best illustrated with an example. Consider the analysis of a single randomly chosen event crossing a bridge with a 15% damage at section $L/2$. Fig. 11 shows the outputs obtained for different information scenarios in terms of the mean probability of detection of the trained models for different damage labels, computed

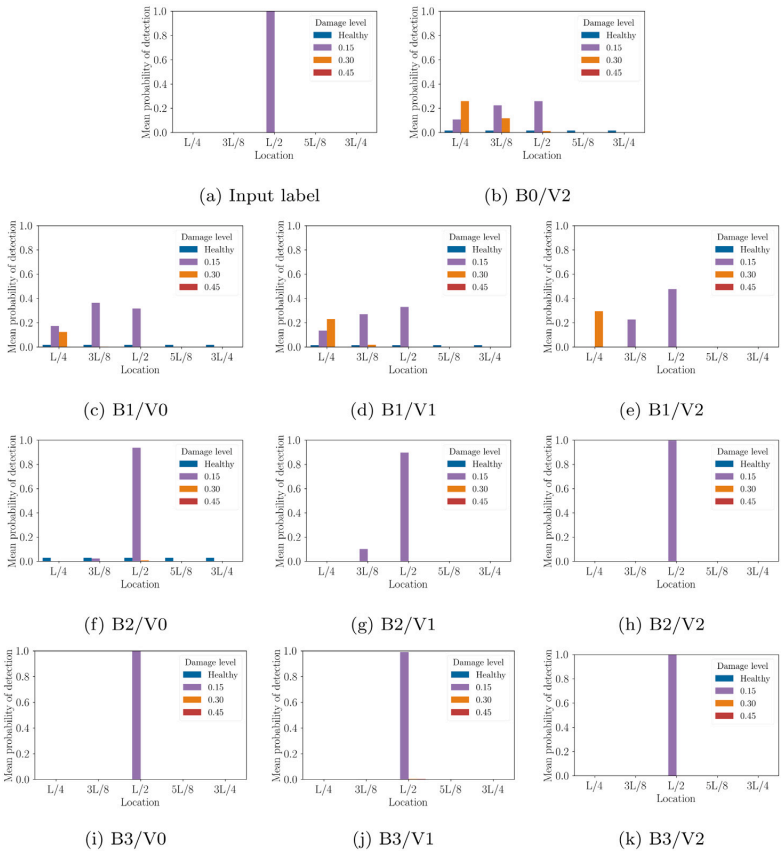

Fig. 11. Damage localisation and quantification, for a single vehicle crossing event in case study A with a 15% damage at L/2 section, for different information scenarios.

using Eq. (6). From the results it can be observed that some scenarios show large uncertainties in damage detection. This is evident, especially in Fig. 11(b), where only vehicle signals are available (B0/V2). The analysis assigns similar mean probabilities to a series of damage cases. There is no clear predominant label. Similarly, when only signals from a single bridge sensor are considered (as in scenarios B1/V0 and B1/V1) the models have difficulties differentiating the exact location and magnitude of the damage, as shown in Fig. 11(c) and (d). However, when the measurement information from the bridge is combined with vehicle sensors (B1/V2), the uncertainty in the decision decreases. Then, the correct label is more prominent (Fig. 11(e)), which indicates that the model in such scenario would be able to locate and quantify the damage. The remaining information scenarios show high and very high certainties providing the correct damage case label.

It is important to stress that the final output decision is solely based on the maximum of the mean probability of detection. Therefore, based on the results in Fig. 11, all the models are able to detect the correct label. From these results, it can be concluded that the PDNN has some difficulty in differentiating damage location and magnitude when only vehicle information is considered. However, by combining sources of information, the damage assessment reliability increases drastically.

4.1.5. Effect of measurement noise

Measurement noise is arguably the most important factor that can affect the performance of the proposed damage assessment procedure. In order to study the effect of noise, white Gaussian noise is added to the acceleration signals by using Eq. (12).

$$\ddot{u}_{polluted} = \ddot{u} + \sigma\, \mathcal{N}(0,\, 1) \tag{12}$$

where $\ddot{u}_{polluted}$ is the noise polluted signal, ü is the clean signal, and $\mathcal{N}(0,\, 1)$ is a noise vector with zero mean and unit standard deviation. The standard deviation of the noise component σ is computed using the definition of Signal to Noise Ratio (SNR) as follows:

$$SNR = \frac{P_{\ddot{u}}}{\sigma^2} \tag{13}$$

where $P_{\ddot{u}}$ is the power of the noise-free signal. By using predefined SNR values, the corresponding standard deviation σ of the noise signal can be computed. Often, SNR is given in decibels (dB) and so Eq. (13) can be rewritten as follows:

$$SNR_{dB} = 10\, log_{10}\left(\frac{P_{\ddot{u}}}{\sigma^2}\right) \tag{14}$$

To evaluate the performance of the proposed damage assessment method in the presence of measurement noise, a single random vehicle crossing is studied in detail. The randomly chosen event corresponds to a B0/V2 scenario, i.e., only vehicle information and signals are available. Four different levels of signal to noise ratios (20 dB, 15 dB, 10 dB, and 5 dB) are added to the axle acceleration signals using Eq. (12).

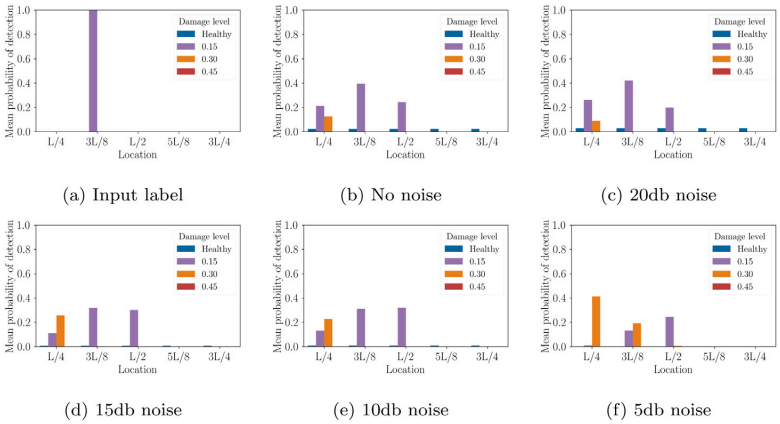

Fig. 12. Effect of measurement noise on damage localisation and quantification for a single crossing event in a B0/V2 scenario.

Fig. 12 shows the results of the sensitivity analysis of measurement noise for damage assessment. The input label shows that the considered event has damage at section $3L/8$ with a 15% stiffness reduction. Fig. 12(b), (c), and (d), show the output prediction of the PDNN models with no noise, 20 dB and 15 dB respectively. For these cases, the trained models are able to localise and quantify the damage with similar levels of uncertainty in the output. However, for larger levels of noise, the performance reduces. For the case of 10 dB SNR (Fig. 12(e)), the output of the model is not able to identify the correct label of damage and instead shows almost equal probabilities for three different damage cases. In the case of very high noise (5 dB SNR), as reported in Fig. 12(f), the PDNN mode failed to quantify and localise the damage case completely. The results from this analysis highlight that the proposed PDNN-based procedure is capable of compensating for normal operational levels of noise, but ceases to work for large noise levels.

4.2. Case study B: Multi-span continuous bridge

4.2.1. Data generation

This section evaluates the proposed damage detection method applied to the case of an existing multi-span continuous bridge. The Voigt Drive I-5 bridge, shown in Fig. 13, is a reinforced concrete box girder bridge with 4 spans and a total length of 89 m [49]. The bridge is simulated as an updated FEM with 0.5 m long beam elements. The section properties have been computed using the actual material properties and cross section dimensions shown in Fig. 13(b). The column supports of the continuous beam model are represented using vertical and rotational springs, of stiffness K_v and K_r respectively. The values for these stiffness have been tuned to match the first three measured frequencies of the original bridge [49]. The final list of the updated bridge properties is presented in Table 2. In addition, and similar to case study A, a road profile of class A is considered with a 100 m approach distance shown in Fig. 6(b).

In line with case study A, damage is modelled as local stiffness reductions also in case study B. But because it is a different bridge, different damage cases have been defined to evaluate the performance the PDNN-based procedure. The Damage Cases (DC) considered in case study B are:

- DC0: Healthy case
- DC1-DC2: Damage at mid-span of span 2 with stiffness reductions of: 30%, 45%
- DC3-DC4: Damage at mid-span of span 3 with stiffness reductions of: 30%, 45%

Table 2
Multi-span bridge model properties.

Description	Symbol	Value
Total span length (m)	L	89
Young's modulus (N/m^2)	E	$3.5 \cdot 10^{10}$
Second moment of area (m^4)	I	1.3427
Cross-section area (m^2)	A	5.6180
Mass per unit length (kg/m)	ρ	2500
Rotational stiffness (N m/rad)	$K_{r,(1,2,3)}$	$4.5 \cdot 10^9$
Vertical stiffness (N/m)	$K_{v,(1,2,3)}$	$3.5 \cdot 10^{10}$
First three modal frequencies (Hz)	$f_{(1,2,3)}$	[4.91, 6.54, 13.45]

- DC5-DC6: Stiffness reduction of 30% at supports 1 and 2

The dataset for this case study is generated by solving the vehicle-bridge interaction model presented in Section 3. To examine the sensitivity of the PDNN method in realistic situations, three simulation modes are examined. Mode 1 considers events with individual 5-axle trucks crossing the multi-span bridge. In addition, simulation mode 2 includes the environmental effect of daily and seasonal temperature variations. Finally, in mode 3, the simulation includes random traffic on the bridge, in addition to the individual 5-axle trucks and temperature oscillations. The dataset for all these three simulation modes is generated considering the statistical variability of the 5-axle truck parameters, by means of Monte Carlo analysis. For Modes 2 and 3, the environmental effect is included by modelling the temperature dependency of concrete's elastic modulus, which is discussed in greater detail in the following subsection. The additional random traffic in mode 3, is modelled including 2-axle vehicles with randomly sampled entry times, speeds, travelling directions and mechanical properties. Additional information about the 2-axle vehicle model and its corresponding parameter values are included in Appendix.

For each simulation mode, separate datasets are generated for different information scenarios. As in the analysis for case study A, these scenarios are defined in terms of the available information from the bridge and the passing vehicles. For the latter, the same definitions for V0, V1 and V2 are used as in Section 4.1.3. However, because the modelled bridge is different now, the information scenarios regarding the available bridge information is different. Case study B defines the possible bridge instrumentation with four accelerometers $\ddot{a}_{b_j}$ as shown in Fig. 13(a). The corresponding bridge information scenarios considered now are listed below.

- B0: No measurement available of the bridge

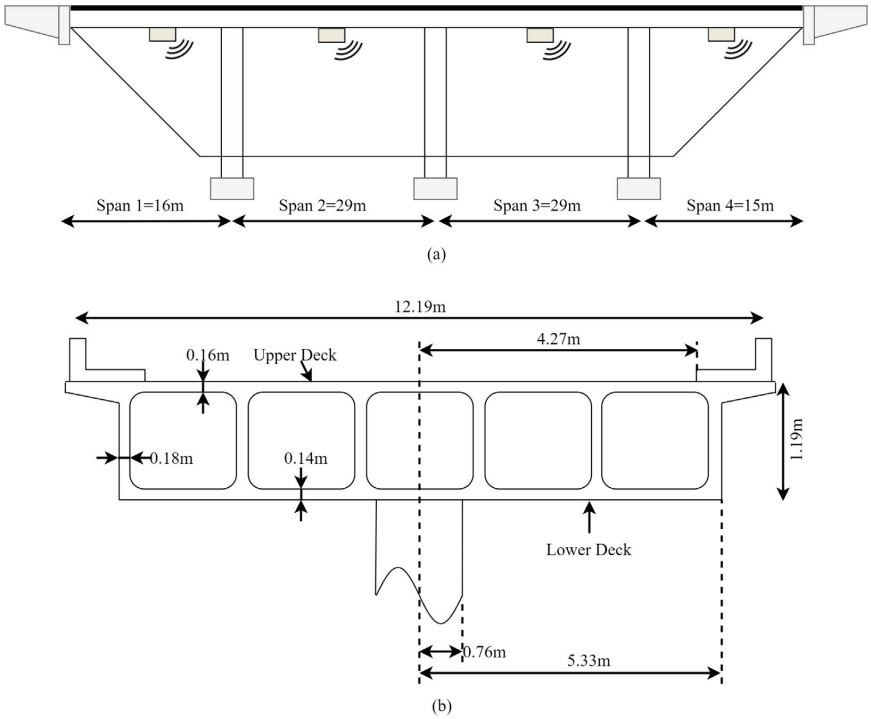

Fig. 13. Voigt Drive/I-5 Bridge; (a) Multi-span bridge model; (b) Cross-section.

- B1: Bridge acceleration measurements at mid-span of spans 1 and 4
- B2: Bridge acceleration measurements at mid-span of spans 2 and 3
- B3: Bridge acceleration measurements at mid-span of all spans

Therefore, this section considers 7 different bridge conditions for each of the 10 valid information scenarios, for each of the 3 simulation modes. Each of the 21 datasets consist of batches of 1000 vehicle crossing events with randomly sampled configurations and properties. These datasets are pre-processed as in Section 4.1.2 to remove the contribution of the road profile from the vehicle signals. The PDNN models are trained using the same hyperparameters, and the datasets are divided in 70–30 splits for training and validation respectively.

4.2.2. Modelling the effect of temperature

In long-term bridge monitoring, variation in temperature plays an important role because it directly influences the material properties of the bridge. As a result the structure experiences changes of its modal properties, that ultimately lead to different dynamic behaviour for the same load. Temperature dependent material properties have been included in the VBI model in order to evaluate the performance of the proposed PDNN model in the presence of oscillating temperatures. This subsection explains how the effect of temperature variation has been modelled.

Concrete's elastic modulus depends on the material's temperature, and this relationship can be linearised for typical ambient temperature ranges [50,51]. It is also known that this linear relationship is different for temperatures below the freezing point [52]. Such bi-linear relationships have been reported, for instance, at the Dowling Hall Foot bridge [53]. Nevertheless, modelling the relationship between temperature and elastic modulus is not a straightforward task and depends on structure's type, location, and environmental conditions. To solve this, empirical models from bridge measurements can be leveraged to establish the relationship between temperature and changes in bridge properties. One such model was developed in [53], where the authors proposed the bi-linear equation for bridge elastic modulus as given in Eq. (15).

$$E_T = E_0 \left[Q + S\,T + R\left(1 - erf\left(\frac{T-\kappa}{\tau}\right)\right)\right] \tag{15}$$

In Eq. (15), E_T is the temperature dependent elastic modulus and E_0 is its value for a reference temperature. The linear relationship is defined in terms of the parameters Q and S, while the term $R\left(1 - erf\left(\frac{T-\kappa}{\tau}\right)\right)$ modifies the relationship for temperatures below zero. In Eq. (15), T is the temperature in degrees Celsius, while κ and τ are the parameters that govern the transition around the freezing point. More details about the temperature dependency of concrete and the model parameters can be found in [54].

In the present study, the influence of temperature has been simulated considering a 2 year temperature record obtained from a weather station in Trondheim (Norway), shown in Fig. 14. For simulation modes 2 and 3, temperature for each crossing event was randomly sampled from these records. Then, the elastic modulus of the concrete was adjusted accordingly using Eq. (15). The parameters in this relationship are also sampled randomly to account for possible uncertainties, as suggested in [54], based on the mean and standard deviation values given in Table 3.

4.2.3. Results

This section reports the results of the proposed damage detection method applied to the case of the multi-span bridge considering the damage cases discussed in Section 4.2.1. The results are presented in a similar format as for case study A. The performance test results for

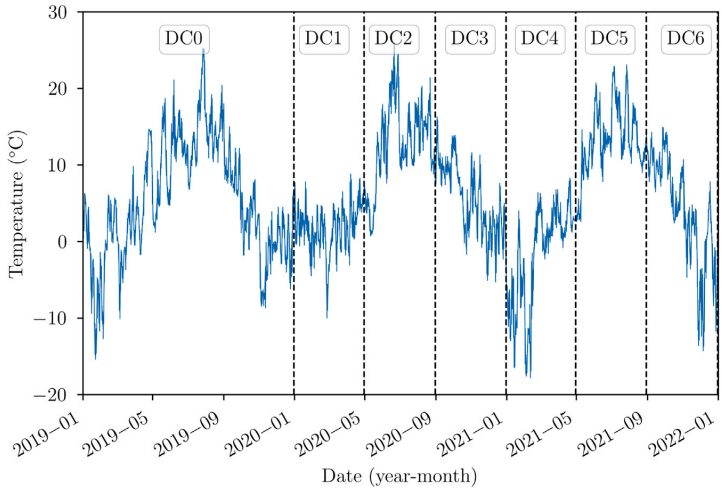

Fig. 14. Daily average temperature record of Trondheim (Norway), and corresponding damage case considered on the bridge.

Table 3
Mean and standard deviation of parameters modelling the effect of temperature on concrete's elastic modulus.

	Q	S	κ	τ	R
μ	1.0129	−0.0048	0.1977	3.1466	0.1977
σ	0.003	0.0001	0.0027	0.0861	0.0027

Table 4
Performance comparison for multi-span bridge case and simulation mode 1.

Scenario	V0	V1	V2
B0	NA	NA	96.1%
B1	97.2%	97.4%	97.4%
B2	98.1%	98.3%	99.0%
B3	98.2%	98.7%	99.2%

Table 5
Performance comparison for multi-span bridge case and simulation mode 2.

Scenario	V0	V1	V2
B0	NA	NA	74.6%
B1	89.2%	90.4%	81.4%
B2	93.9%	94.3%	92.8%
B3	94.2%	94.7%	95.6%

each information scenario, are presented in a table format, indicating the overall accuracy of the trained models. However, in case study B, the analysis is repeated for 3 simulation modes, namely mode 1 (single 5-axle events), mode 2 (with additional temperature variations) and mode 3 (with additional random 2-axle traffic), as discussed in Section 4.2.1.

The results for mode 1 are reported in Table 4. It shows that the PDNN-based approach exhibits comparatively high accuracy in damage assessment for all scenarios. This is even the case for the B0/V2 scenario, where only vehicle sensor information is used. The overall accuracy in this scenario is good (96.1%), and much better that the corresponding result in case study A (see Table 1), which was 84.2%. This improvement is attributed to the duration of the crossing event. Vehicles traversing a longer bridge, spend more time interacting with the structure, which results in longer signals for the proposed method. In addition, the vehicle to mass ratio decreases drastically, ensuring that there is practically no variation of the bridge's modal properties during the crossing event. It is also worth noting that the damage cases considered in case study B are more distinct, as opposed to those considered in case study A. This makes each label (damage case) more distinctive, which facilitates the classification task. The combination of these reasons allow the PDNN model to generalise more precisely the damage sensitive features, leading to the improved accuracy observed in case study B for simulation mode 1.

Table 5 presents the overall performance results for simulation mode 2. In this mode the temperature variations have been included in the simulation, affecting directly the elastic modulus of the bridge model, as discussed in Section 4.2.2. In the simulated information scenarios the temperature is provided by the passing vehicles, and therefore only available in scenarios with V1 and V2. In this setup, it is possible to study what is the effect of that additional information on the performance of the PDNN-based models. By direct comparison of the results between V0 and V1 scenarios, it can be seen that adding the temperature information as input has little impact on the overall accuracy of the models. In addition, the accuracy improvements are of similar magnitude as those reported for mode 1 (where no temperature variations were considered). However, there is an overall decrease in accuracy compared to mode 1 results. This is because the varying temperature creates fluctuations in bridge modal properties (especially first and second mode), which mask the variations associated to small damage cases. This temperature effect is particularly relevant in scenarios using vehicle information (V2). The pre-processing of the vehicle signals effectively isolates the first and second frequencies of the bridge, as shown in Fig. 9(c). As a result of this pre-processing, the PDNN model is not able to properly classify the less severe damage cases, which contributes to the decrease in overall accuracy for scenario B0/V2 reported in Table 5. Compared to bridge only scenarios, where the signals contain the full spectrum, the proposed model can successfully generalise the feature space and thus classify different damage cases more accurately. Furthermore, the results show that when V2 information is combined with B1 and B2 the accuracy of the model decreases. This decrease in accuracy is attributed to the relative weight given by the model to the actual input signals. In B1/V2 and B2/V2 the inputs to the model are 5 vehicle signals and 2 bridge responses. The model gives more weight to the vehicle signals, which are affected more by the effect of temperature variations, resulting in a decrease in accuracy.

Simulation mode 3 imitates the actual operational conditions found in a real case. The bridge vibrations captured by the passing 5-axle

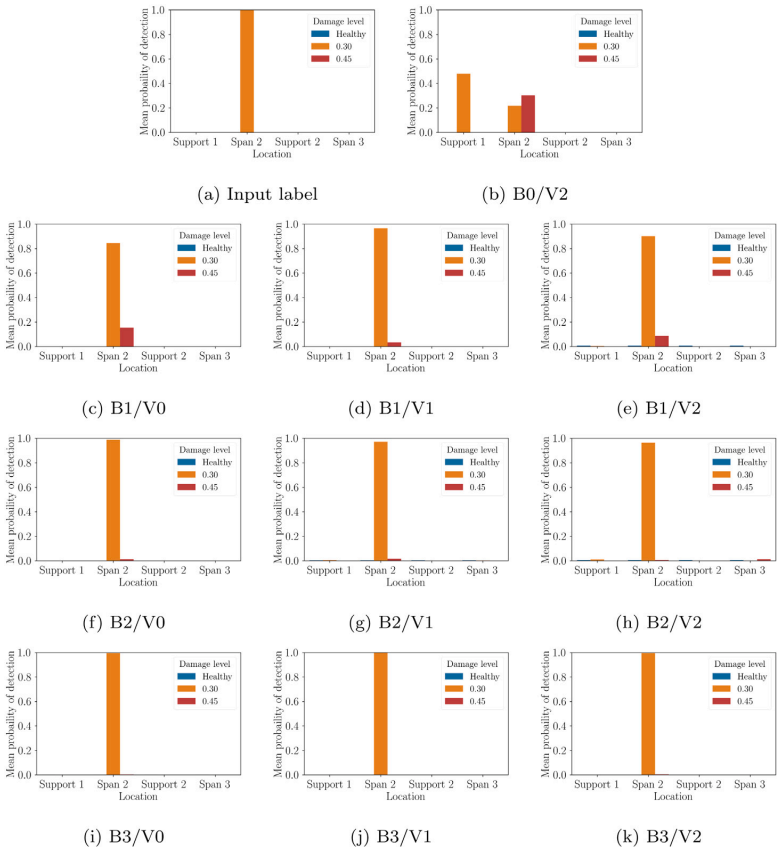

Fig. 15. Effect of measurement information scenario on the accuracy for damage localisation and quantification, for case study B and simulation mode 3.

trucks are affected by the continuous oscillations in ambient temperature and the disturbances induced by additional traffic. The performance results for mode 3 (see Table 6) indicate overall performance reduction but similar trends as those reported for mode 2. Vehicle responses are highly influenced by temperature and by the presence of random traffic compared to bridge response. This is clearly seen in overall decrease of accuracy for all scenarios when V2 information is combined with bridge sensors as discussed in previous section for mode 2.

However, when compared to the other simulation modes, the performances for mode 3 are significantly lower for all scenarios. This is expected because of the additional random traffic, which is unknown to the models. The PDNN models do not get any information about this extra traffic, because these vehicles are not instrumented. The added mass of these additional vehicles affect the bridge dynamic response. The PDNN-based models achieve a suboptimal generalisation of the feature space, and thus have more difficulties classifying the event among the different damage case labels. This is then reflected in overall poorer accuracy, as reported in Table 6.

Taking advantage of the PDNN architecture, it is possible to explore the uncertainty in the model prediction. The analysis of one single crossing event can be presented in terms of mean probability of detection, as explained in Section 2.2. Here, the analysis is repeated for all information scenarios considering one random event under simulation mode 3, and presented in Fig. 15. In particular, in this event the bridge had a damage at the mid-span section of the second span with a severity

Table 6
Performance comparison for multi-span bridge case and simulation mode 3.

Scenario	V0	V1	V2
B0	NA	NA	44.1%
B1	79.2%	82.0%	60.1%
B2	81.1%	82.3%	76.8%
B3	82.4%	84.1%	82.1%

of 30% stiffness reduction. The analysis shows that in scenario B0/V2, when only vehicle measurements are available, the PDNN-based model is not able to correctly identify the damage label. The model distributes the probability among 3 different labels, including the correct one (see Fig. 15(b)). The final outcome of the model is selected as the label with greatest mean probability, which in this case is the wrong answer. However, for the rest of information scenarios, the PDNN models are able to correctly identify the damage with very low uncertainty in the output.

Therefore, from these results it can be concluded that random traffic on the bridge adversely effects the damage detection capability of the proposed PDNN-based method. This negative influence is particularly evident for damage assessment using exclusively the signals from passing vehicles. Therefore, the recommendation for drive-by methods in general is to utilise signals from instrumented vehicles that traverse the target bridge without the presence of additional traffic. Furthermore, the presented results also indicate that to reduce the uncertainties in

damage assessment, it is beneficial to combine the vehicles' responses with the signals from a limited number of sensors mounted on the bridge.

5. Discussion

The results presented here provide the proof of concept for the applicability of vehicle assisted bridge monitoring. The study demonstrates the merits of combining multiple sensory information, including fixed sensor as well as moving sensors (vehicle mounted). The strengths of the proposed PDNN model approach are: (1) scalability, because the proposed method can easily incorporate different types of measurements for damage assessment tasks; (2) robustness, because of the inherit probabilistic nature of proposed method, the effect of noise and different loading conditions do not alter the overall accuracy; (3) implementable, because it does not require heavy pre-processing of the measurements since it can work with raw signals; and (4) enhanced performance of damage detection and localisation in comparison to the similar methods reported in literature [23,45], because the proposed method does not only provide the damage detection results but also quantifies the uncertainty in the output decision.

Furthermore, the novelty of the proposed method can be summarised in three points. First, the proposed PDNN model can combine multiple sensors and extract the damage sensitive features without any pre-processing of the input signals, even when considering realistic operational conditions. The accuracies of damage assessment results for different sensor combinations highlight the ability of the proposed model to distinguish small changes in structural dynamic characteristics. Secondly, compared to other commonly used data driven methods, the proposed PDNN model provides additional insights, since it can quantify the reliability of the model's decision. In previous studies reported in literature, the deep learning models have been trained with fixed weights. This makes their generalisation ability highly susceptible to changing operational and environmental conditions. The proposed PDNN model addresses this issue by replacing fixed weights by probabilistic distributions of weights. This, not only enhances the generalisation ability of the PDNN model, but also quantifies the reliability of the decision making. Lastly, this study can be used as a guideline for future planning of bridge health monitoring systems in practice. The study comprehensively discussed multiple bridge health monitoring scenarios for different levels of damage. Bridge owners can greatly benefit from this study while considering their needs for a monitoring campaign for a particular bridge.

However, there are still some limitations for the implementation of the proposed method. Arguably, the main limitation is related to the requirement of damage labels while training the proposed PDNN model. At present, this can be addressed by combining hybrid approaches and transfer learning techniques, as discussed in [55]. In a hybrid approach, the target bridge labels can be acquired from numerical simulations from Finite element model (FEM) of the bridge and then further combined with real measurements of the bridge for further damage assessment. Nevertheless, this line of work still requires more studies to properly demonstrate the ability for damage assessment in a real life implementation. The other minor limitation is the requirement of synchronised signals from multiple sensors. This can be addressed by adequately utilising existing technologies.

6. Conclusions

This paper has explored the feasibility of vehicle assisted monitoring for damage assessment. The study had two main objectives; (1) to develop a damage assessment method by combining direct and indirect measurement response; (2) to study and quantify the influence of different sensor information combinations. To that end, a probabilistic deep neural network (PDNN) based method was proposed, which is capable of quantifying the uncertainty of its predictions under varying operational and environmental conditions. The effectiveness of the proposed method was evaluated with two case studies, which consisted of 5-axle trucks traversing a simply supported beam and a multi-span continuous bridge. These studies considered several damage cases and investigated the effect of measurement noise, temperature variations, and random traffic. The main findings of this study can be summarised as follows:

- The overall results suggest that vehicle assisted monitoring has the potential to detect small and realistic damage cases under the influence of varying operational and environmental conditions.
- By employing the wavelet transform based filter bank the contribution of the road profile can be removed from vehicle responses which is one of the main hinders in deployment of on-board vehicle sensors for structural damage assessment.
- The combination of sensor information from vehicle and bridge enables a more reliable damage assessment with lower uncertainty in the decision making.
- Random traffic on the bridge adversely affects the ability of the proposed method to detect and localise the damage, when only vehicle sensors are used. Thus, is drive-by or indirect monitoring strategies, it is recommended to use only vehicle responses with no additional traffic present on the bridge.
- Road authorities and bridge owners can use the proposed probabilistic deep neural network based method as a reliable decision making tool for damage assessment.

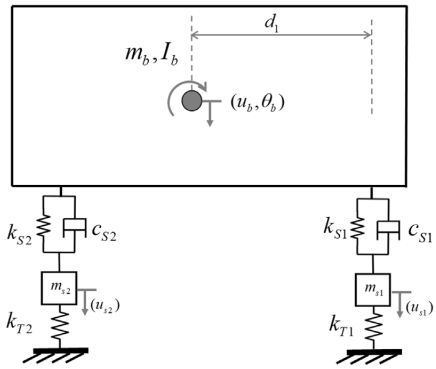

Fig. A.1. 2-axle vehicle model.

CRediT authorship contribution statement

Muhammad Zohaib Sarwar: Conceptualization, Methodology, Software, Investigation, Formal analysis, Writing – original draft. **Daniel Cantero:** Conceptualization, Software, Writing – review & editing, Resources, Supervision.

Declaration of competing interest

The authors declare that they have no known competing financial interests or personal relationships that could have appeared to influence the work reported in this paper.

Data availability

Data will be made available on request.

Table A.1
5-axle truck model parameters.

Parameters	Min.	Max.	Mean	SD
Mass (kg)				
Tractor body m_{b1}	2800	3400	3100	80
Trailer body m_{b2}	15 000	25 000	20 000	1000
Tractor axles m_{u1}, m_{u2}	500	1000	750	30
Trailer axles m_{u3}, m_{u4}, m_{u5}	800	1400	1100	50
Moment of inertia (kg m^2)				
Tractor body I_{b1}	4250	5500	4875	50
Trailer body I_{b2}	112 000	135 000	123 000	2500
Spring stiffness (N/m)				
Tractor suspension k_{S1}, k_{S2}	$4.0 \cdot 10^6$	$8.0 \cdot 10^6$	$6.0 \cdot 10^6$	$0.5 \cdot 10^6$
Trailer suspension k_{S3}, k_{S4}, k_{S5}	$5.0 \cdot 10^6$	$15.0 \cdot 10^6$	$10.0 \cdot 10^6$	$0.5 \cdot 10^6$
Tractor tyre k_{T1}, k_{T2}	$1.3 \cdot 10^6$	$2.3 \cdot 10^6$	$1.8 \cdot 10^6$	$0.2 \cdot 10^6$
Trailer tyre k_{T3}, k_{T4}, k_{T5}	$2.8 \cdot 10^6$	$4.8 \cdot 10^6$	$3.5 \cdot 10^6$	$0.2 \cdot 10^6$
Viscous damping (N s/m)				
Tractor suspension c_{S1}, c_{S2}	$1.0 \cdot 10^4$	$8.0 \cdot 10^4$	$4.0 \cdot 10^4$	$0.5 \cdot 10^4$
Trailer suspension c_{S3}, c_{S4}, c_{S5}	$2.0 \cdot 10^4$	$16.0 \cdot 10^4$	$8.0 \cdot 10^4$	$1.0 \cdot 10^5$
Geometry (m)				
b_1	3.50	6.50	5.00	0.10
a_2	3.00	5.00	4.00	0.02
d_1	−0.50	−1.20	−1.09	−0.01
d_2	3.00	4.00	3.50	0.05
d_3	–	–	1.20	–
d_4	–	–	2.20	–
d_5	–	–	3.20	–
Velocity (km/h)				
Velocity	36	72	54	8

Table A.2
2-axle truck model parameters.

Parameters	Min.	Max.	Mean	SD
Mass (kg)				
Body mass m_{b1}	5000	16 000	10 500	500
Tractor axles m_{u1}, m_{u2}	600	1200	900	100
Moment of inertia (kg m^2)				
Body I_b	45 000	65 000	53 651	2000
Spring stiffness (N/m)				
Suspension k_{S1}, k_{S2}	$4.0 \cdot 10^6$	$8.0 \cdot 10^6$	$6.0 \cdot 10^6$	$0.5 \cdot 10^6$
Tyre K_{T3}, K_{T4}	$1.25 \cdot 10^6$	$2.25 \cdot 10^6$	$1.75 \cdot 10^6$	$0.20 \cdot 10^6$
Viscous damping (N s/m)				
Suspension c_{S1}, c_{S2}	$0.5 \cdot 10^4$	$1.5 \cdot 10^4$	$1.0 \cdot 10^4$	$0.2 \cdot 10^4$
Geometry (m)				
d_1	4	6	–	–
Velocity (km/h)				
Velocity	36	72	54	8

Appendix

Table A.1 provides the numerical values of the parameters for the 5-axle truck model, together with their statistical variability, used for the Monte Carlo simulations. Similarly, Table A.2 provides the model parameter for the 2-axle vehicle model (shown in Fig. A.1), which is used to simulate the additional random traffic in case study B (Section 4.2).

References

[1] O. Avci, O. Abdeljaber, S. Kiranyaz, M. Hussein, M. Gabbouj, D.J. Inman, A review of vibration-based damage detection in civil structures: From traditional methods to Machine Learning and Deep Learning applications, Mech. Syst. Signal Process. 147 (2021) 107077.

[2] L. Quirk, J. Matos, J. Murphy, V. Pakrashi, Visual inspection and bridge management, Struct. Infrastruct. Eng. 14 (3) (2018) 320–332.

[3] Y. An, E. Chatzi, S.-H. Sim, S. Laflamme, B. Blachowski, J. Ou, Recent progress and future trends on damage identification methods for bridge structures, Struct. Control Health Monit. 26 (10) (2019) e2416.

[4] P. Singh, A. Sadhu, Limited sensor-based bridge condition assessment using vehicle-induced nonstationary measurements, in: Structures, Vol. 32, Elsevier, 2021, pp. 1207–1220.

[5] S. Wang, E.J. OBrien, D.P. McCrum, A novel acceleration-based moving force identification algorithm to detect global bridge damage, Appl. Sci. 11 (16) (2021) 7271.

[6] H. Shokravi, H. Shokravi, N. Bakhary, M. Heidarrezaei, S.S. Rahimian Koloor, M. Petr, Vehicle-assisted techniques for health monitoring of bridges, Sensors 20 (12) (2020) 3460.

[7] E. OBrien, C. Carey, J. Keenahan, Bridge damage detection using ambient traffic and moving force identification, Struct. Control Health Monit. 22 (12) (2015) 1396–1407.

[8] C. McGeown, F. Huseynov, D. Hester, P. McGetrick, E.J. Obrien, V. Pakrashi, Using measured rotation on a beam to detect changes in its structural condition, J. Struct. Integr. Maint. 6 (3) (2021) 159–166, http://dx.doi.org/10.1080/24705314.2021.1906092, arXiv:https://doi.org/10.1080/24705314.2021.1906092.

[9] E.J. Obrien, J. Brownjohn, D. Hester, F. Huseynov, M. Casero, Identifying damage on a bridge using rotation-based Bridge Weigh-In-Motion, J. Civ. Struct. Health Monit. 11 (1) (2021) 175–188.

[10] Z. Wang, J.P. Yang, K. Shi, H. Xu, F. Qiu, Y. Yang, Recent advances in researches on vehicle scanning method for bridges, Int. J. Struct. Stab. Dyn. (2022).

[11] R. Corbally, A. Malekjafarian, A data-driven approach for drive-by damage detection in bridges considering the influence of temperature change, Eng. Struct. 253 (2022) 113783.

[12] M.Z. Sarwar, D. Cantero, Deep autoencoder architecture for bridge damage assessment using responses from several vehicles, Eng. Struct. 246 (2021) 113064.

[13] R. Corbally, A. Malekjafarian, Examining changes in bridge frequency due to damage using the contact-point response of a passing vehicle, J. Struct. Integr. Maint. 6 (3) (2021) 148–158.

[14] Y. Yang, Y. Li, K.C. Chang, Constructing the mode shapes of a bridge from a passing vehicle: a theoretical study, Smart Struct. Syst. 13 (5) (2014) 797–819.

[15] A. Sumalee, H.W. Ho, Smarter and more connected: Future intelligent transportation system, Iatss Res. 42 (2) (2018) 67–71.

[16] J. Guerrero-Ibáñez, S. Zeadally, J. Contreras-Castillo, Sensor technologies for intelligent transportation systems, Sensors 18 (4) (2018) 1212.

[17] F. Ni, J. Zhang, M.N. Noori, Deep learning for data anomaly detection and data compression of a long-span suspension bridge, Comput.-Aided Civ. Infrastruct. Eng. 35 (7) (2020) 685–700.

[18] Y. Zhang, Y. Miyamori, S. Mikami, T. Saito, Vibration-based structural state identification by a 1-dimensional convolutional neural network, Comput.-Aided Civ. Infrastruct. Eng. 34 (9) (2019) 822–839.

[19] T. Zhang, D. Shi, Z. Wang, P. Zhang, S. Wang, X. Ding, Vibration-based structural damage detection via phase-based motion estimation using convolutional neural networks, Mech. Syst. Signal Process. 178 (2022) 109320.

[20] M. Tabaszewski, G.M. Szymański, T. Nowakowski, Vibration-based identification of engine valve clearance using a convolutional neural network, Arch. Transp. 61 (1) (2022) 117–131.

[21] B. Zhao, X. Zhang, Z. Zhan, Q. Wu, A robust construction of normalized CNN for online intelligent condition monitoring of rolling bearings considering variable working conditions and sources, Measurement 174 (2021) 108973.

[22] X. Ma, Y. Lin, Z. Nie, H. Ma, Structural damage identification based on unsupervised feature-extraction via Variational Auto-encoder, Measurement 160 (2020) 107811.

[23] J. Won, J.-W. Park, S. Jang, K. Jin, Y. Kim, Automated structural damage identification using data normalization and 1-dimensional convolutional neural network, Appl. Sci. 11 (6) (2021) 2610.

[24] C. Szegedy, W. Zaremba, I. Sutskever, J. Bruna, D. Erhan, I. Goodfellow, R. Fergus, Intriguing properties of neural networks, 2013, arXiv preprint arXiv:1312.6199.

[25] L.V. Jospin, H. Laga, F. Boussaid, W. Buntine, M. Bennamoun, Hands-on Bayesian neural networks—A tutorial for deep learning users, IEEE Comput. Intell. Mag. 17 (2) (2022) 29–48.

[26] E. Goan, C. Fookes, Bayesian neural networks: An introduction and survey, in: Case Studies in Applied Bayesian Data Science, Springer, 2020, pp. 45–87.

[27] N.G. Polson, V. Sokolov, Deep learning: A Bayesian perspective, Bayesian Anal. 12 (4) (2017) 1275–1304.

[28] T. Kim, J. Song, O.-S. Kwon, Probabilistic evaluation of seismic responses using deep learning method, Struct. Saf. 84 (2020) 101913.

[29] C. Andrieu, N. De Freitas, A. Doucet, M.I. Jordan, An introduction to MCMC for machine learning, Mach. Learn. 50 (1) (2003) 5–43.

[30] O. Abdeljaber, O. Avci, S. Kiranyaz, M. Gabbouj, D.J. Inman, Real-time vibration-based structural damage detection using one-dimensional convolutional neural networks, J. Sound Vib. 388 (2017) 154–170.

[31] Z. Wang, W. Yan, T. Oates, Time series classification from scratch with deep neural networks: A strong baseline, in: 2017 International Joint Conference on Neural Networks (IJCNN), IEEE, 2017, pp. 1578–1585.

[32] F. Karim, S. Majumdar, H. Darabi, S. Chen, LSTM fully convolutional networks for time series classification, IEEE Access 6 (2017) 1662–1669.

[33] F. Karim, S. Majumdar, H. Darabi, S. Harford, Multivariate LSTM-FCNs for time series classification, Neural Netw. 116 (2019) 237–245.
[34] TensorFlow Probability. URL https://www.tensorflow.org/probability.
[35] Y. Wen, P. Vicol, J. Ba, D. Tran, R. Grosse, Flipout: Efficient pseudo-independent weight perturbations on mini-batches, in: International Conference on Learning Representations, 2018.
[36] D. Cantero, A. González, Bridge damage detection using weigh-in-motion technology, J. Bridge Eng. 20 (5) (2015) 04014078.
[37] D. Cantero, VEqMon2D—Equations of motion generation tool of 2D vehicles with Matlab, SoftwareX 19 (2022) 101103.
[38] N.K. Harris, E.J. OBrien, A. González, Reduction of bridge dynamic amplification through adjustment of vehicle suspension damping, J. Sound Vib. 302 (3) (2007) 471–485.
[39] A. González, O. Mohammed, Dynamic amplification factor of continuous versus simply supported bridges due to the action of a moving vehicle, Infrastructures 3 (2) (2018) 12.
[40] I.M. Vibration, Road Surface Profiles–Reporting of Measured Data; ISO 8608, International Standards Organisation, Geneve, 2016.
[41] X.-Y. Zhou, M. Treacy, F. Schmidt, E. Brühwiler, F. Toutlemonde, B. Jacob, Effect on bridge load effects of vehicle transverse in-lane position: A case study, J. Bridge Eng. 20 (12) (2015) 04015020.
[42] MATLAB, Version 9.10.0 (r2020a), 2022.
[43] D. Cantero, A. González, E.J. O'Brien, Comparison of bridge dynamic amplification due to articulated 5-axle trucks and large cranes, Balt. J. Road Bridge Eng. 6 (1) (2011) 39–47.
[44] Y. Yang, Y. Li, K. Chang, Using two connected vehicles to measure the frequencies of bridges with rough surface: a theoretical study, Acta Mech. 223 (8) (2012) 1851–1861.
[45] W. Locke, J. Sybrandt, L. Redmond, I. Safro, S. Atamturktur, Using drive-by health monitoring to detect bridge damage considering environmental and operational effects, J. Sound Vib. 468 (2020) 115088.
[46] D.B. Percival, A.T. Walden, Wavelet Methods for Time Series Analysis, Vol. 4, Cambridge University Press, 2000.
[47] A.T. Walden, A.C. Cristan, The phase–corrected undecimated discrete wavelet packet transform and its application to interpreting the timing of events, Proc. R. Soc. Lond. Ser. A Math. Phys. Eng. Sci. 454 (1976) (1998) 2243–2266.
[48] P.-W. Shan, M. Li, Nonlinear time-varying spectral analysis: HHT and MODWPT, Math. Probl. Eng. 2010 (2010).
[49] M. Fraser, A. Elgamal, X. He, J.P. Conte, Sensor network for structural health monitoring of a highway bridge, J. Comput. Civ. Eng. 24 (1) (2010) 11–24.
[50] H. Liu, X. Wang, Y. Jiao, Effect of temperature variation on modal frequency of reinforced concrete slab and beam in cold regions, Shock Vib. 2016 (2016).
[51] Y. Xia, H. Hao, G. Zanardo, A. Deeks, Long term vibration monitoring of an RC slab: temperature and humidity effect, Eng. Struct. 28 (3) (2006) 441–452.
[52] B. Peeters, J. Maeck, G. De Roeck, Vibration-based damage detection in civil engineering: excitation sources and temperature effects, Smart Mater. Struct. 10 (3) (2001) 518.
[53] P. Moser, B. Moaveni, Environmental effects on the identified natural frequencies of the Dowling Hall Footbridge, Mech. Syst. Signal Process. 25 (7) (2011) 2336–2357.
[54] I. Behmanesh, B. Moaveni, Accounting for environmental variability, modeling errors, and parameter estimation uncertainties in structural identification, J. Sound Vib. 374 (2016) 92–110.
[55] B.T. Svendsen, O. Øiseth, G.T. Frøseth, A. Rønnquist, A hybrid structural health monitoring approach for damage detection in steel bridges under simulated environmental conditions using numerical and experimental data, Struct. Health Monit. (2022) 14759217221098998.

ISBN 978-82-326-7119-9 (printed ver.)
ISBN 978-82-326-7120-5 (electronic ver.)
ISSN 1503-8181 (printed ver.)
ISSN 2703-8084 (online ver.)

NTNU
Norwegian University of
Science and Technology